U.S. Department
of Transportation
**Federal Railroad
Administration**

Documentation of Deformation from Passenger Rail Two-Car Impact Test

Office of Research
and Development
Washington, DC 20590

DOT/FRA/ORD-03/08

Final Report
November 2003

This document is available to the public through the National Technical Information Service, Springfield, VA 22161. This document is also available on the FRA web site at www.fra.dot.gov

REPORT DOCUMENTATION PAGE

Form Approved
OMB No. 0704-0188

1. AGENCY USE ONLY (Leave blank)	2. REPORT DATE	3. REPORT TYPE AND DATES COVERED
	November 2003	Final Report April 2000 – February 2002

4. TITLE AND SUBTITLE Documentation of Deformation from Passenger Rail Two-Car Impact Test	5. FUNDING NUMBERS RR228/R2067
6. AUTHOR(S) Robert A. MacNeill and Steven W. Kirkpatrick	
7. PERFORMING ORGANIZATION NAME(S) AND ADDRESS(ES) Applied Research Associates* 2672 Bayshore Parkway, Suite 1035 Mountain View, CA 94043	8. PERFORMING ORGANIZATION REPORT NUMBER DOT-VNTSC-FRA-03-09
9. SPONSORING/MONITORING AGENCY NAME(S) AND ADDRESS(ES) U.S. Department of Transportation Federal Railroad Administration Office of Research and Development 1120 Vermont Avenue, NW - Mail Stop 20 Washington, DC 20590	10. SPONSORING/MONITORING AGENCY REPORT NUMBER DOT/FRA/ORD-03/08

11. SUPPLEMENTARY NOTES

*Under contract to: U.S. Department of Transportation
Research and Special Programs Administration
John A. Volpe National Transportation Systems Center
55 Broadway
Cambridge, MA 02142-0193

12a. DISTRIBUTION/AVAILABILITY STATEMENT This document is available to the public through the National Technical Information Service, Springfield VA 22161 This document is also available on the FRA web site at www.fra.dot.gov.	12b. DISTRIBUTION CODE

13. ABSTRACT (Maximum 200 words)

The Volpe Center has been conducting research into rail equipment crashworthiness in support of the Federal Railroad Administration's (FRA) Office of Research and Development. As part of this research, full-scale crash tests of passenger cars have been performed. Subsequent detailed post-test examinations develop an improved understanding of the collapse mechanisms of the dominant structural elements as well as overall dynamic crash behavior. This knowledge can be used for interpreting test data, estimating energy dissipation during the test, developing detailed finite element models, and designing safer passenger cars.

This report documents a detailed post-test inspection performed on the lead car from a full-scale test featuring two coupled passenger coach cars impacting a fixed wall at 26 mph, which was conducted on April 4, 2000. Damages to primary structural members including the draft sill, side sills, and cant rails were documented including modes and magnitude of deformation. Other secondary structural components such as the superstructure skin, belt rails, and floor were also documented.

14. SUBJECT TERMS Transportation, safety, crashworthiness, occupant protection, passenger rail vehicles	15. NUMBER OF PAGES 120
	16. PRICE CODE

17. SECURITY CLASSIFICATION OF REPORT	18. SECURITY CLASSIFICATION OF THIS PAGE	19. SECURITY CLASSIFICATION OF ABSTRACT	20. LIMITATION OF ABSTRACT
Unclassified	Unclassified	Unclassified	

NSN 7540-01-280-5500

Standard Form 298 (Rev. 2-89)
Prescribed by ANSI Std. 239-18
298-102

PREFACE

The work described in this report was performed under contract to the Volpe National Transportation Systems Center (Volpe Center), as part of the Equipment Safety Research Program sponsored by the Federal Railroad Administration (FRA). The contract was initiated and monitored by David Tyrell and Kristine Severson, Senior Engineers, Structures and Dynamics Division, Volpe Center. Tom Tsai, Program Manager, Equipment and Operating Practices Research Division, FRA, manages the passenger rail equipment crashworthiness research.

METRIC/ENGLISH CONVERSION FACTORS

ENGLISH TO METRIC

LENGTH (APPROXIMATE)

1 inch (in)	=	2.5 centimeters (cm)
1 foot (ft)	=	30 centimeters (cm)
1 yard (yd)	=	0.9 meter (m)
1 mile (mi)	=	1.6 kilometers (km)

AREA (APPROXIMATE)

1 square inch (sq in, in^2)	=	6.5 square centimeters (cm^2)
1 square foot (sq ft, ft^2)	=	0.09 square meter (m^2)
1 square yard (sq yd, yd^2)	=	0.8 square meter (m^2)
1 square mile (sq mi, mi^2)	=	2.6 square kilometers (km^2)
1 acre = 0.4 hectare (he)	=	4,000 square meters (m^2)

MASS - WEIGHT (APPROXIMATE)

1 ounce (oz)	=	28 grams (gm)
1 pound (lb)	=	0.45 kilogram (kg)
1 short ton = 2,000 pounds (lb)	=	0.9 tonne (t)

VOLUME (APPROXIMATE)

1 teaspoon (tsp)	=	5 milliliters (ml)
1 tablespoon (tbsp)	=	15 milliliters (ml)
1 fluid ounce (fl oz)	=	30 milliliters (ml)
1 cup (c)	=	0.24 liter (l)
1 pint (pt)	=	0.47 liter (l)
1 quart (qt)	=	0.96 liter (l)
1 gallon (gal)	=	3.8 liters (l)
1 cubic foot (cu ft, ft^3)	=	0.03 cubic meter (m^3)
1 cubic yard (cu yd, yd^3)	=	0.76 cubic meter (m^3)

TEMPERATURE (EXACT)

[(x-32)(5/9)] °F = y °C

METRIC TO ENGLISH

LENGTH (APPROXIMATE)

1 millimeter (mm)	=	0.04 inch (in)
1 centimeter (cm)	=	0.4 inch (in)
1 meter (m)	=	3.3 feet (ft)
1 meter (m)	=	1.1 yards (yd)
1 kilometer (km)	=	0.6 mile (mi)

AREA (APPROXIMATE)

1 square centimeter (cm^2)	=	0.16 square inch (sq in, in^2)
1 square meter (m^2)	=	1.2 square yards (sq yd, yd^2)
1 square kilometer (km^2)	=	0.4 square mile (sq mi, mi^2)
10,000 square meters (m^2)	=	1 hectare (ha) = 2.5 acres

MASS - WEIGHT (APPROXIMATE)

1 gram (gm)	=	0.036 ounce (oz)
1 kilogram (kg)	=	2.2 pounds (lb)
1 tonne (t)	=	1,000 kilograms (kg)
	=	1.1 short tons

VOLUME (APPROXIMATE)

1 milliliter (ml)	=	0.03 fluid ounce (fl oz)
1 liter (l)	=	2.1 pints (pt)
1 liter (l)	=	1.06 quarts (qt)
1 liter (l)	=	0.26 gallon (gal)
1 cubic meter (m^3)	=	36 cubic feet (cu ft, ft^3)
1 cubic meter (m^3)	=	1.3 cubic yards (cu yd, yd^3)

TEMPERATURE (EXACT)

[(9/5) y + 32] °C = x °F

QUICK INCH - CENTIMETER LENGTH CONVERSION

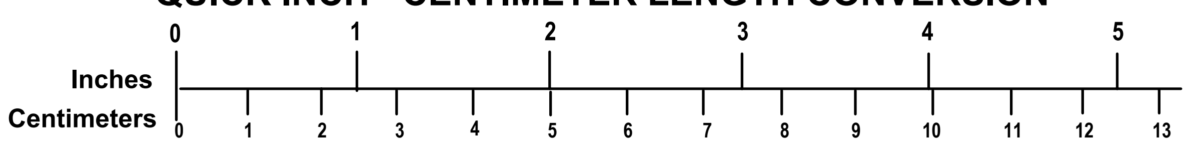

QUICK FAHRENHEIT - CELSIUS TEMPERATURE CONVERSION

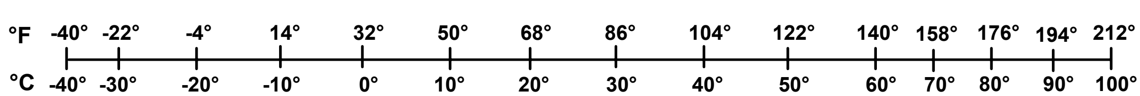

For more exact and or other conversion factors, see NIST Miscellaneous Publication 286, Units of Weights and Measures. Price $2.50 SD Catalog No. C13 10286

Updated 6/17/98

TABLE OF CONTENTS

LIST OF FIGURES

LIST OF FIGURES

EXECUTIVE SUMMARY

A full-scale test featuring two coupled passenger coach cars impacting a fixed wall at 26.25 mph (11.7 m/s) was conducted at the Transportation Technology Center (TTC) in Pueblo, Colorado on April 4, 2000. This report documents a detailed post-test inspection performed on the lead car from the two-car crash test. Damages to primary structural members, including the draft sill, side sills, and cant rails, were documented.* The modes and magnitude of deformation are described. Other secondary structural components such as the superstructure skin, belt rails, and floor in the vicinity of the impact were also discussed. B-end damage was documented, though the lack of knowledge of pretest vehicle condition made it difficult to determine whether some of the damage was a result of the crash test or was preexisting. Other details such as concrete ballast distribution and strain gage location were documented for the benefit of future analysis.

Many similarities exist between the observed damage from this two-car test and the previously conducted single car crash test. Collapse of the draft sill, the primary structural element in the car, was largely the same, though the two-car test draft sill collapse was more extensive, likely the result of higher test energy. Also the draft sill collapse in the two-car test was slightly more symmetric than in single car test. Like the single car test, the origination of the draft sill collapse was due to the failure of the welds surrounding the buff stop as the draft gear was driven back. This initiated the collapse of the draft sill between the buff stop and body bolster.

One major difference was caused by the absence of a pilot in the two-car test. (A pilot is a fixture that is usually mounted on the carbody that is intended to sweep any light debris on the track away from the front of the train. In the case of the Pioneer cars, the pilot was added by SEPTA to keep highway vehicles from getting under the cab car in grade crossing accidents and subsequently causing a derailment.) In the single car test, the loads transmitted from the pilot weakened the connections of the attachment hardware mounted under the draft sill just forward of the buff stop. This allowed the forward part of the draft sill to collapse asymmetrically. Since a pilot was not mounted in the two-car test, the attachment hardware remained well connected to the draft sill, thus preventing the collapse of the forward draft sill.

Superstructure collapse was also similar to the single car test but again the two-car test was more symmetric. Due to the larger longitudinal collapse of the draft sill, the superstructure collapse behind the bulkhead wall was more extensive in the two-car test. As a result, other primary longitudinal structural members such as the side sills, cant rails, and belt rails experienced more crush than in the single car test.

* The cant rail is a longitudinal structural member running the length of the car at or near where the roof and the sidewall meet. The belt rail is a longitudinal sidewall member, situated just below the bottom of the side windows.

1. INTRODUCTION

The Volpe Center has been conducting research into rail equipment crashworthiness in support of the Federal Railroad Administration's (FRA) Office of Research and Development. As part of this research, full-scale crash tests of passenger cars have been performed. Subsequent detailed post-test examinations develop an improved understanding of the collapse mechanisms of the dominant structural elements as well as overall dynamic crash behavior. This knowledge can be used for interpreting test data, estimating energy dissipation during the test, developing detailed finite element models, and designing safer passenger cars.

The second full-scale test was conducted at the Transportation Technology Center (TTC) in Pueblo, Colorado on April 4, 2000. The test featured two coupled passenger coach cars impacting a fixed wall at 26.25 mph (11.7 m/s) [1,2]. The test vehicles used were Pioneer passenger coach cars. The condition of the impact end of the lead test vehicle both before and after the collision is shown in Figure 1. The measured vehicle crash response featured approximately 65 inches (1.65 m) of crush after the structure had relaxed. Inspection of the vehicle showed that, as expected, the draft sill was the dominant structural component and dissipated a significant fraction of the collision energy.

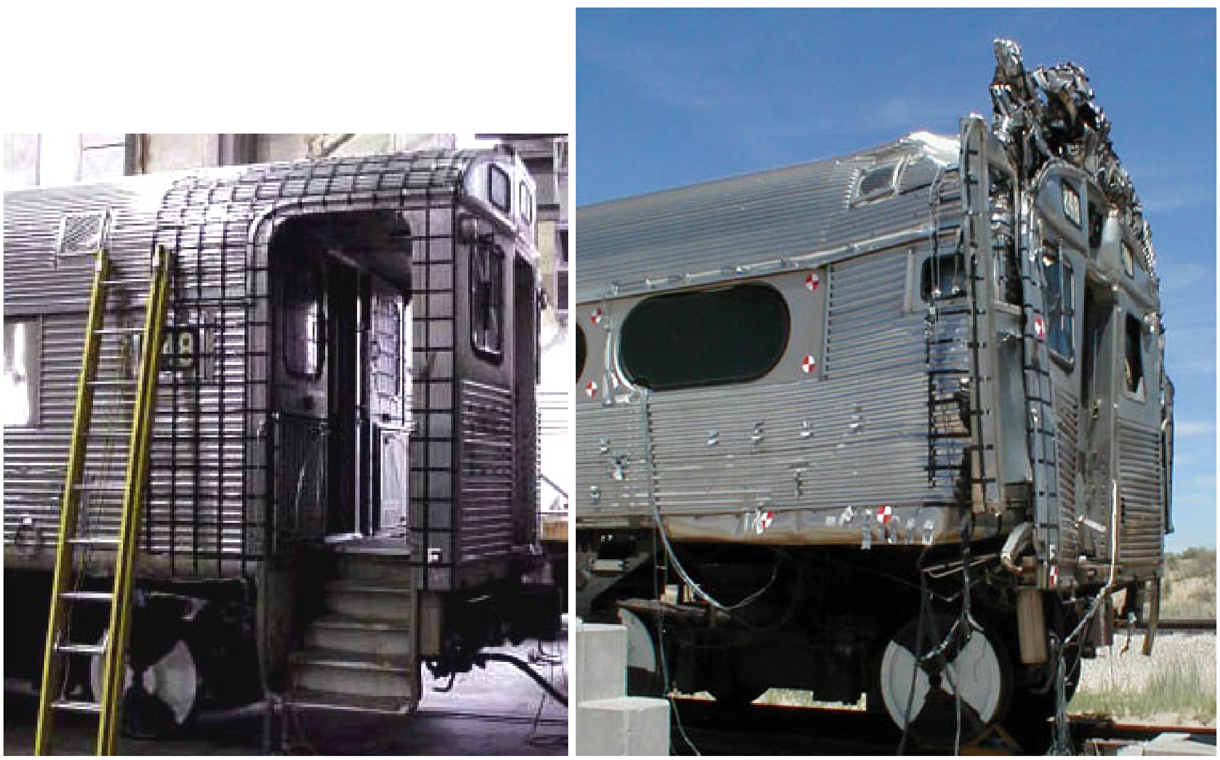

Figure 1. Photographs of the Lead Passenger Car Before and After Impact

The principal objectives of this study were to perform a post-test inspection of the lead car in the two-car consist. Primary attention was given to the principal longitudinal structural members—the draft sill, the side sills, and the cant rails—that absorb the largest share of the crash energy. (The cant rail is a longitudinal structural member running the length of the car at or near where the roof and the sidewall meet. The belt rail is a longitudinal sidewall member, situated just below the bottom of the side windows.) Secondary attention was given to other important structural members such as the vehicle outer sheathing, the belt rails, and other details important to documenting the crush behavior. Primary means of documentation was through photographs and hand drawn sketches.

1.1 SUMMARY OF PRINCIPAL RESULTS

The Pioneer car design has a strong underframe structure with the draft sill and center sill as the dominant member to withstand buff loads. Consequently, the draft sill is a dominant structure in the crash response of the vehicle. Weldment and other material failures were documented, since they contribute to the collapse of the draft sill.

The draft sill collapsed in a manner similar to that seen in the single car test: the draft gear was driven back by the collision forces and failed the connection between the buff stop to the draft sill [3]. This initiated a collapse in the draft sill side immediately aft of the buff stop position. The forward section of the draft sill was driven back and downward as the front of the vehicle continued to crush. As this proceeded, the lower plate was torn free from the draft sill by a failure along the weldments, and the side of the draft sill folded back on them.

In its relaxed state, the longitudinal draft sill crush distance measured 64 5/8 inches (1.64 m) compared to 54 inches (1.37 m) in the single car test. The discrepancy is probably due to the two-car test being a higher energy test (kinetic energy for the two-car test was approximately 3.5×10^6 ft-lb_f (4.7 MJ) while the single car test kinetic energy was approximately 3.0×10^6 ft-lb_f (4.1 MJ)). Also, the longitudinal crush of two-car test appears to have relaxed less than the single-test vehicle. The single car vehicle relaxed from 66 inches (1.68 m) of peak crush to 54 inches (1.37 m) (12 inch (0.30 m) difference), while the two-car test relaxed from approximately 73 inches (1.85 m) of peak crush to 64 5/8 inches (1.64 m) (8 3/8 inch (0.21 m) difference).

Secondary structural members, such as the side sills, cant rails, and the vehicle skin, sustained more damage in the two-car test, than in the single car test and, therefore, absorbed more crash energy than those from the first test. Longitudinal crush extended farther behind the bulkhead wall as a result of the higher energy in the two-car collision.

Little damage was produced on either the trailing end (B-end) of the lead vehicle or on the trailing vehicle. Some minor damage on the B-end was noted during the post-test inspection, some of which was there before the test occurred (e.g., draft sill flange). It was not clear if other damage such as the distorted right-side vestibule doorframe and the end damage above the gutter rail were present on the vehicle before or as a result of the test. Damage in the draft pocket and on the buffer beam damage on the B-end of the lead car was almost certainly a result of interaction between coupled cars during the test.

1.2 REPORT ORGANIZATION

The remainder of this report summarizes the test and equipment postmortem. Section 2 briefly describes the test setup. Section 3 describes the lead car documentation with relevant findings. Summary and conclusions are in Section 4. Finally, a series of appendices are included which contain all the photographs taken and all the full-size sketches made during the postmortem. Many of the sketches are included in the main body of the report in a reduced format. As such, annotations may be difficult to read or the sketches might be slightly light. Refer to the sketches in Appendix A for larger and higher quality images, if necessary.

2. TEST DESCRIPTION

A schematic of the two-car collision test appears in Figure 2. The test was performed to quantify the crash response of a conventional design car and to study the interaction between the two coupled cars. This test was performed with the cars traveling at 26.25 mph (11.7 m/s) when they impacted the wall. The overall test setup is similar to the single car test performed at TTC in November 1999 [3], without the additional car.

The objectives of this test were to observe the failure modes of the major structural components, to measure the gross motions of the car, to measure the force/crush characteristic, and to evaluate selected occupant protection strategies. Data were collected from varying sources, such as high-speed video/film, strain gauges, accelerometers, and string potentiometers to achieve the test objectives. This study is focused on damage documentation only. See References 1 and 2 for discussion and analysis of the collected data.

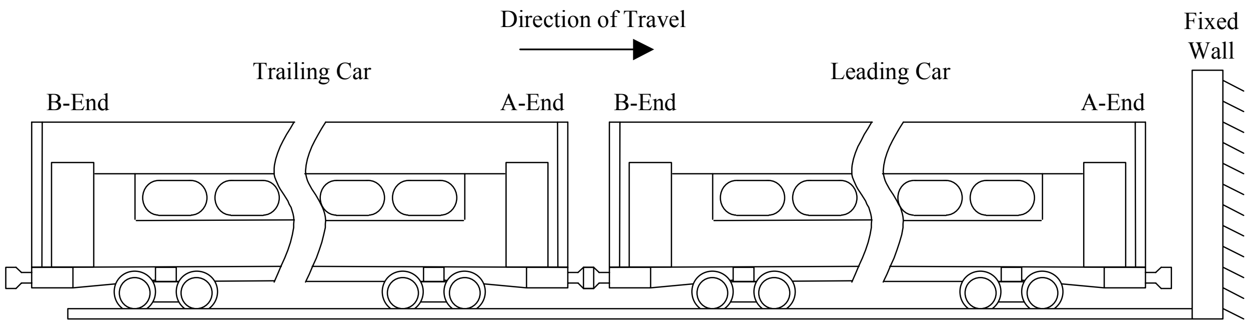

Figure 2. Schematic of Two-Car Test

Budd Company Pioneer-type commuter passenger cars, provided by the Southeastern Pennsylvania Transportation Authority (SEPTA), were used in the two-car test. A photograph of a car similar to those tested is shown in Figure 3. The Pioneer car was designed by the Budd Company to be a low-cost, lightweight passenger car. These cars include a stainless-steel body shell with a high-strength low-alloy steel underframe. The cars were designed in the later half of the 1950s and built through the 1960s. The underframe design of the car is similar to the underframe design of most single-level passenger coach and cab cars used in North America, including the Amtrak Amfleet cars.

The carbody structures of the vehicle prior to the test were intact, with the exception of the original seats and some auxiliary equipment removed from the vehicle. A few prototype seats and crash dummies were added to the vehicle interior to study occupant protection strategies [2]. To account for the mass difference of the removed equipment approximately 10,000 lb_m ($4.5x10^3$ kg) of concrete was added to the test vehicle as ballast to increase the test mass to that of typical in-service vehicles.

Figure 3. Budd Pioneer Car Similar to Those Used During the Two-Car Test

3. EQUIPMENT POSTMORTEM

A postmortem inspection was performed on the lead Pioneer car used in the crash test. The objective of the inspection was to document the deformation modes of the principal structural members—the draft sill, the side sills, and the cant rails. In addition to the principal structural members, other components were documented such as the vehicle superstructure and the vehicle B-end damage. As part of the equipment postmortem, photographs were taken and sketches were drawn of the vehicle. These included both photographs and sketches of the damaged structural components on the impact A-end and the B-end. A complete collection of photographs and sketches from the postmortem inspection of the vehicle appears in Appendices A and B, respectively.

3.1 PRINCIPAL STRUCTURAL MEMBERS

As specified in the program Statement of Work (SOW), the main structural elements investigated were the draft sill, the side sills, and the cant rails. These components tend to absorb the most energy from longitudinal impacts. Documentation of the belt rails is also included in this section since they too provide significant longitudinal support in the superstructure.

3.1.1 Draft Sill

The draft sill suffered the most significant collapse of all major structural components. This is expected since most of the other longitudinal structural components are not continuous through the vestibule region. As such, the draft sill would absorb the most crash energy of any single component. The collapse mode was similar to that seen in the single car test: the coupler was forced back as it impacted the wall, pushing the draft gear aft, which subsequently failed the connection of the buff stop to the draft sill—this was the primary initiation point for the gross failure of the draft sill. The portion of the draft sill forward of the buff stop acted mostly like a rigid body driven down and back while the aft part of the draft sill collapsed. The front portion of the draft sill was pushed to the right side by about 2.5 inches (0.0635 m), which promoted an asymmetric collapse of the aft portion of the draft sill (see Figure 4).

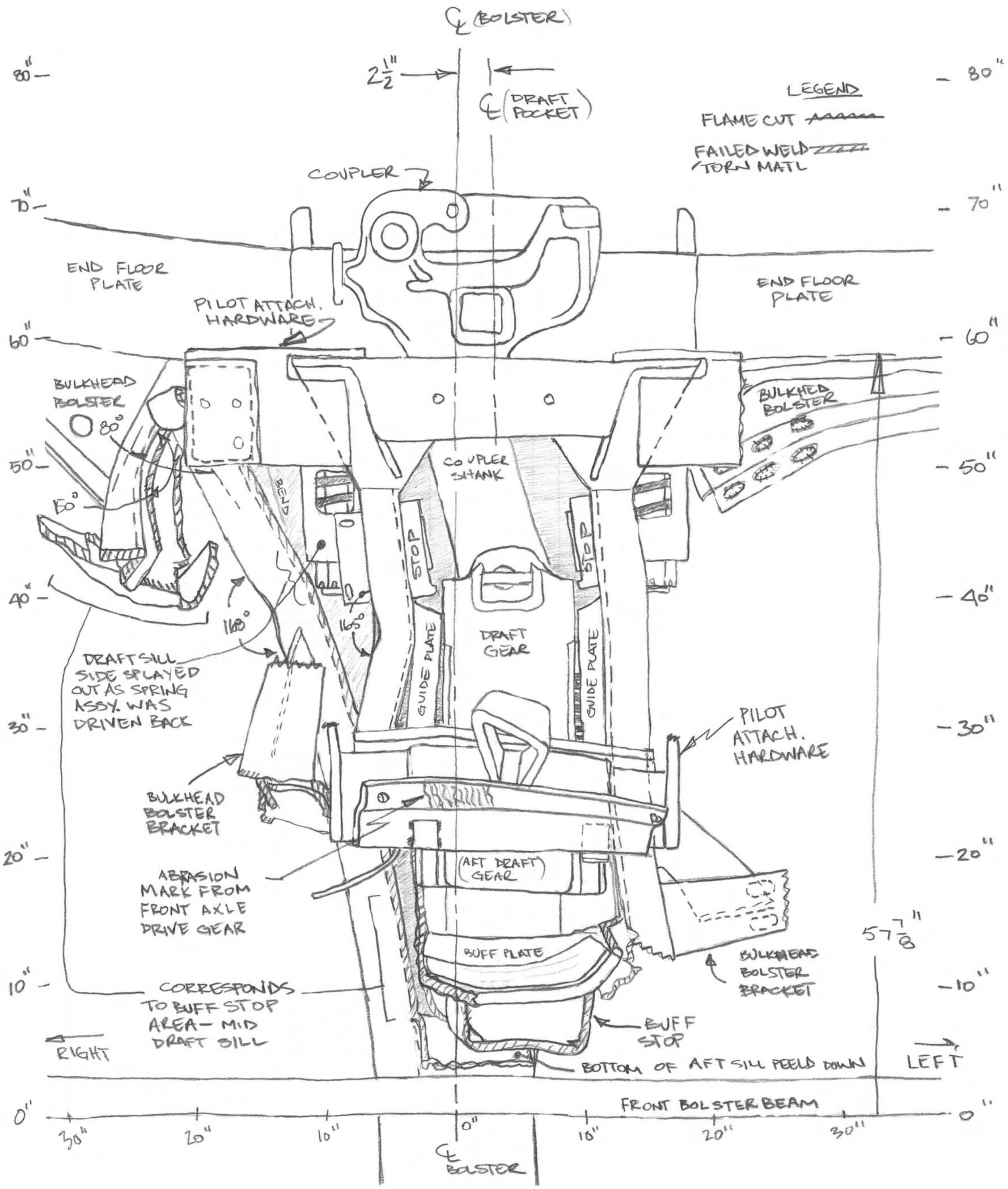

Figure 4. Sketch from Below Draft Sill Collapse

The right side of the aft draft sill folded back on itself and fractured off from the forward section, as the forward part was driven down and back. This fractured section is noted in Figure 4 above (note the right side is shown on the left side of the sketch since it is viewed from below) and may also be seen in Figure 5. The fractured welds and torn steel surfaces in Figure 5 appear as light gray lines, in contrast to the otherwise rust-colored steel.

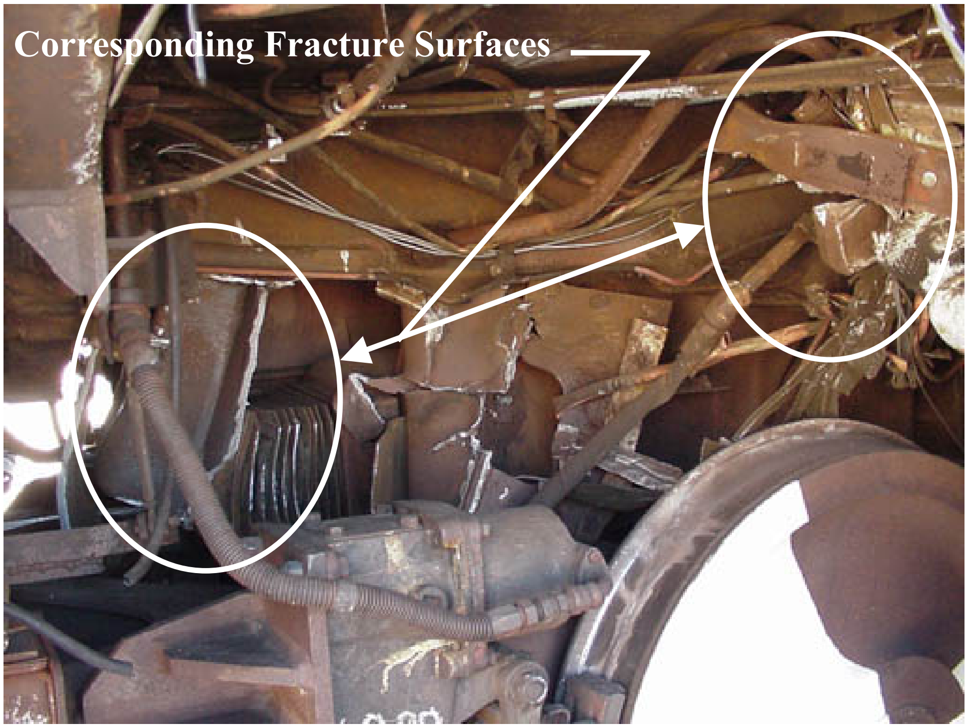

Figure 5. Right-side Draft Sill Collapse, Just After Test

The left sidewall of the aft draft sill was cut by the forward part of the draft sill and folded like a ribbon along the side of the collapsed draft sill. A picture of the folded sidewall is shown in Figure 6, which was taken before the material was removed so that the car could be moved away from the test site.

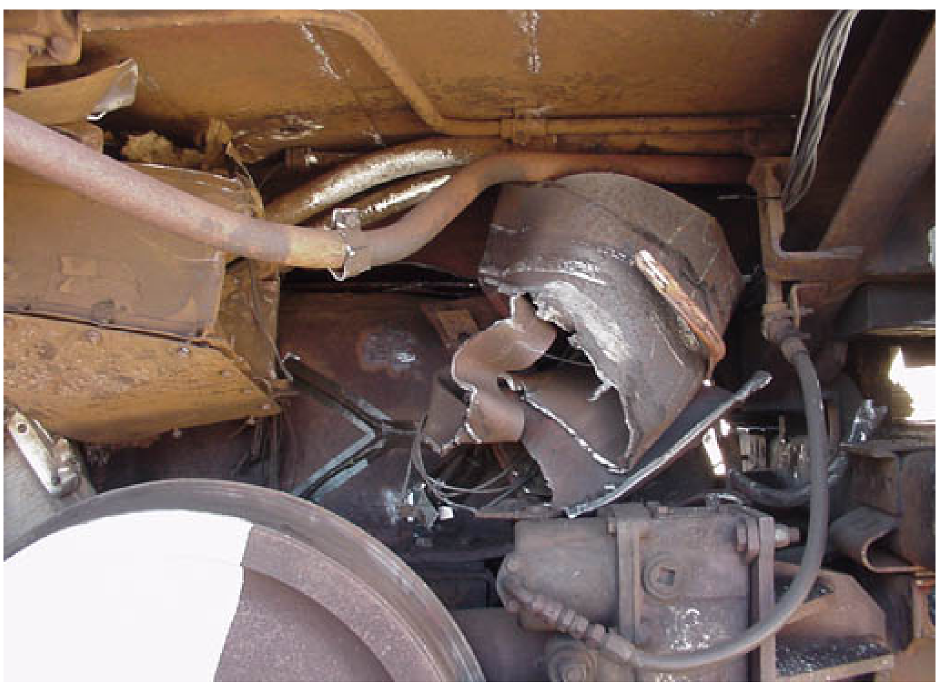

Figure 6. Left-side Draft Sill Collapse, Just After Test

Some of the material seen in Figures 5 and 6 was removed after the test to facilitate moving the damaged car from the test site. The right side of the draft sill had only minor amounts of material removed but large sections such as the left side and bottom aft plate were removed and not retained for later inspection. As a result, these pieces were not available to be studied and documented in this program. It is fairly clear what occurred to the left sidewall from Figure 6 above and by inspection of the remainder of the draft sill. Though the bottom plate of the draft sill that runs from the buff stop to the bolster beam was not retained, it appears to have failed in a manner similar to the single car test. The welds connecting the bottom plate and sidewalls failed as the buff stop was driven back and the plate was driven down below the truck. There is evidence of the bottom plate being thrust downward in Figure 7 below. Also shown in Figure 7 is the left side of the draft sill after the deformed sidewall had been cut away.

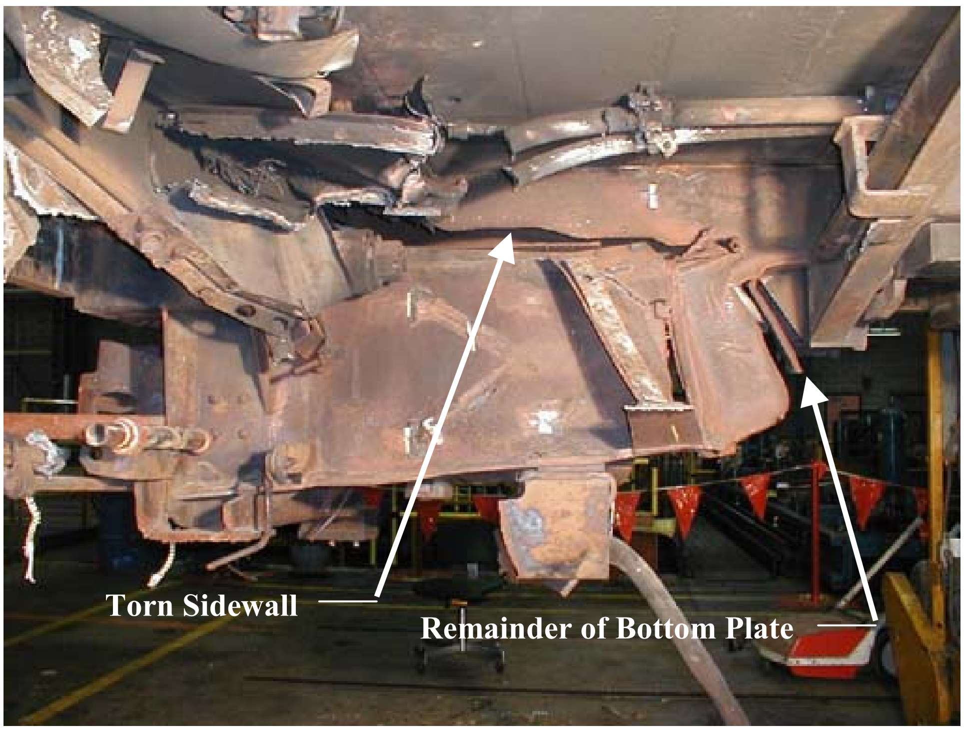

Figure 7. Left Side of Draft Sill During Postmortem Inspection (After Truck Removal)

A corresponding sketch of the left-side draft sill is shown in Figure 8.

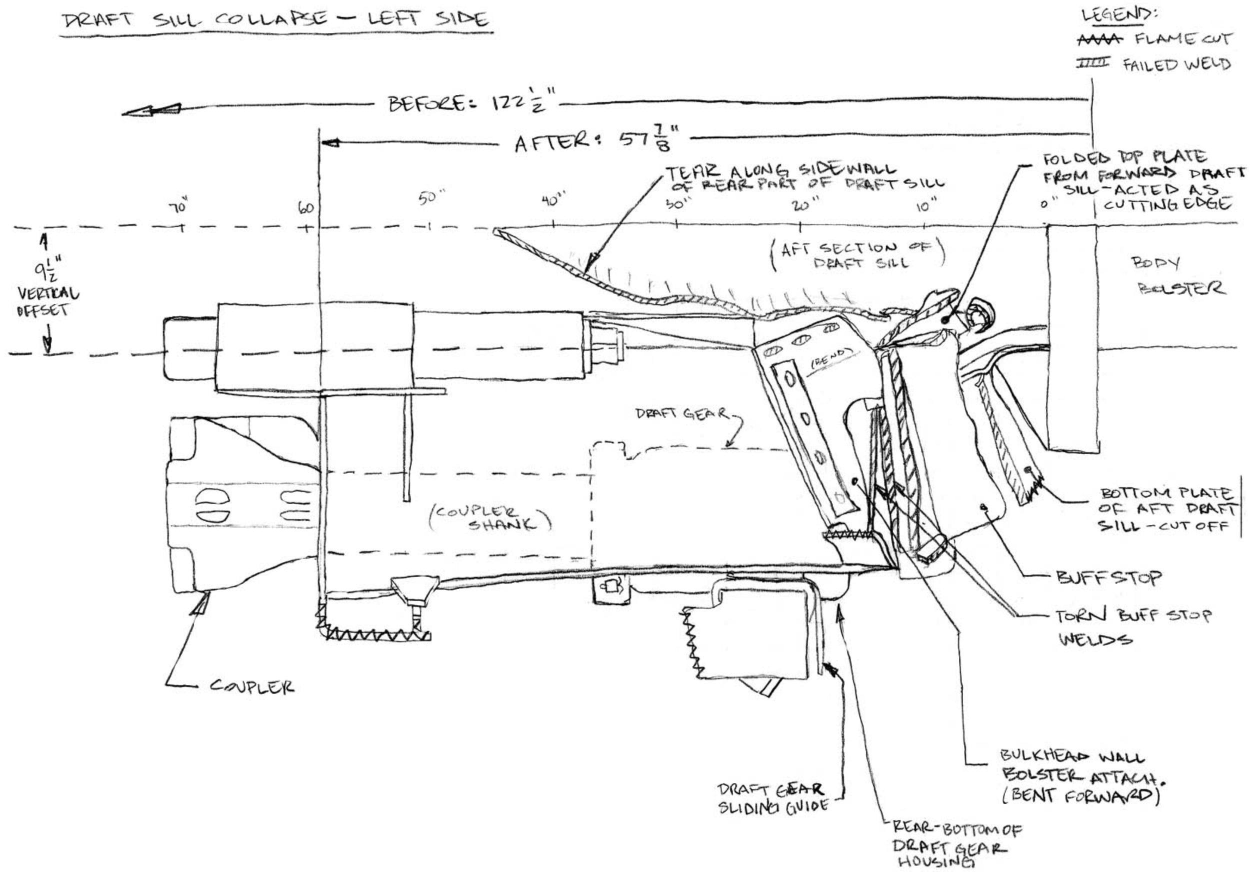

Figure 8. Sketch of Left Side of Draft Sill

The sketch in Figure 8 shows that the overall reduction in length of the draft sill, measured from the front of the draft pocket to the bolster beam, is 64 5/8 inches (1.64 m). A similar sketch of the draft sill right side, shown in Figure 9, indicates the same reduction in length.

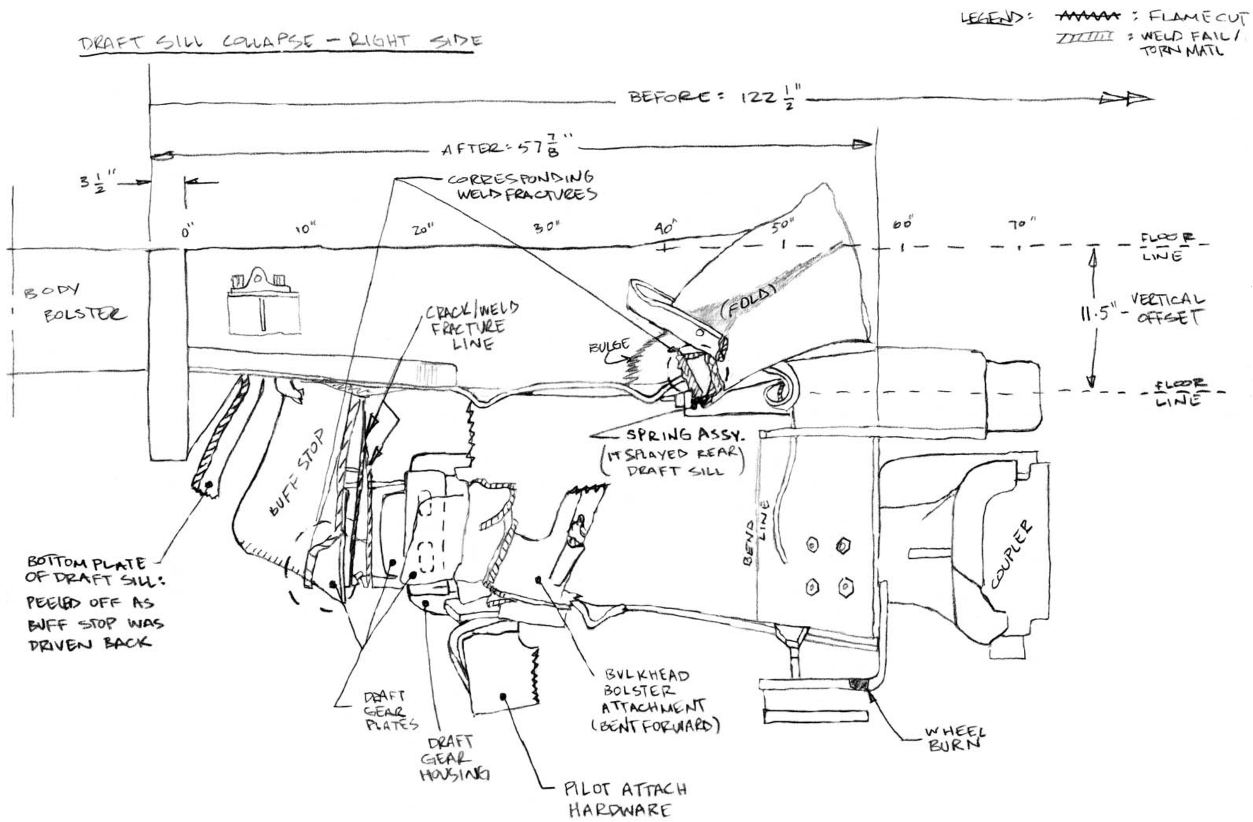

Figure 9. Sketch of Right Side of Draft Sill

A corresponding photograph of the right side of the draft sill is shown in Figure 10. In this figure, the truck had been removed and some nonstructural equipment surrounding the draft sill had been removed to gain better views of the draft sill collapse. Compared to Figure 5, one can see some material was cut away on the side of the draft sill just forward of the opening where the rear of the draft gear is positioned. This material was cut after the test and was not available for inspection during this investigation.

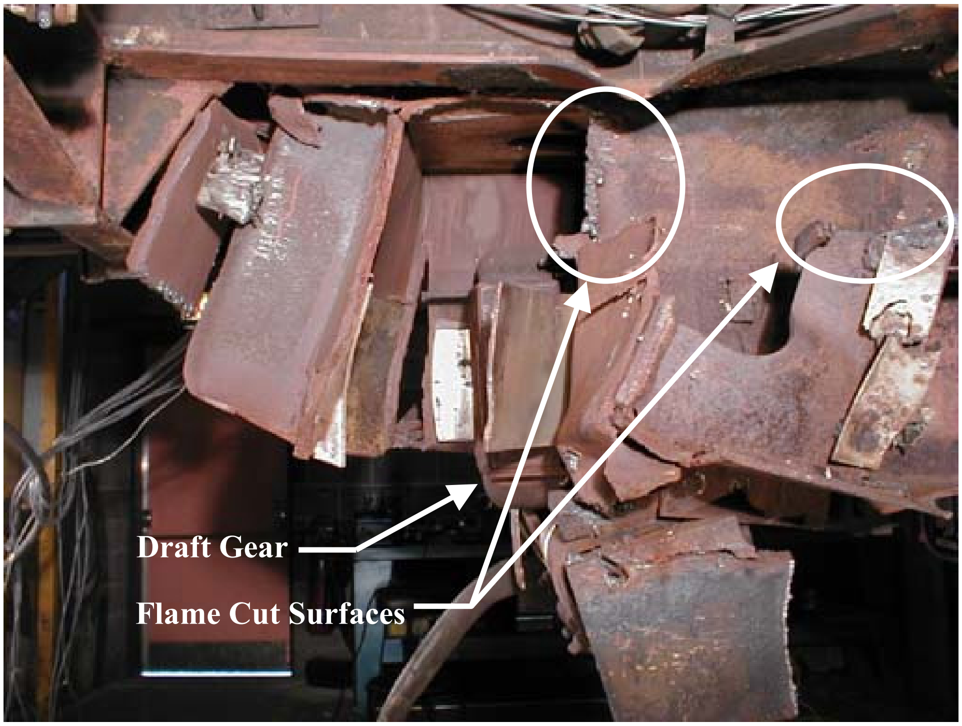

Figure 10. Right-side Draft Sill

Also seen in the figures and sketches is the bent pilot attachment hardware, attached to the bottom of the draft sill below the draft gear. Prior to the detailed postmortem some material was cut away from this component as well and was not available for inspection. The post-test inspection of the pilot attachment hardware found evidence of interaction with the front axle on the forward truck. Normally, this hardware would sit well above and forward of the axle but, as the draft sill collapsed, it was driven down and rode over and behind the axle. Figure 11 shows a detailed photograph of the mark made on the pilot attachment hardware by a drive gear on the most forward truck axle.

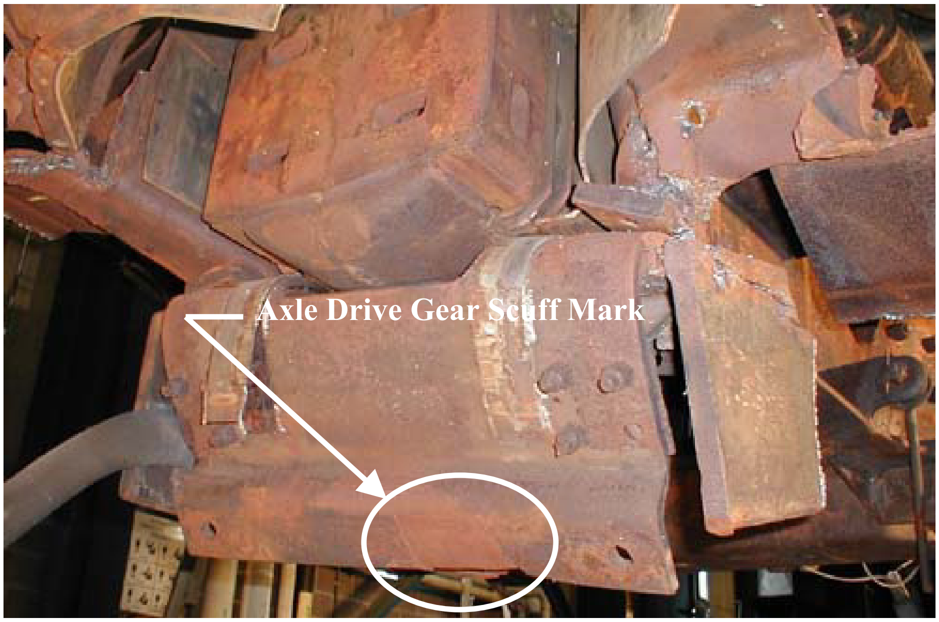

Figure 11. Pilot Attachment Hardware Detail—Axle Interaction

Evidence was found of an impact between the truck bolster beam and the forward body bolster beam. It is not clear at what time during the collision event the truck beam contacted the body beam. One possibility is that the contact occurred early in the crash as the truck continued forward while the underframe decelerated rapidly during the initial crash pulse. The initial deceleration of the truck is produced only by the loads transmitted through the traction rods until the bolster beam contacts the body bolster. The other possibility is that the contact damage occurred late in the collision event as the buff stop contacted the body bolster, creating a load path to the collision wall and more rapid deceleration of the forward bolster structure. The first scenario seams more likely. Accelerometer data could probably be scrutinized to determine the sequence of events. Figure 12 and Figure 13 shows details of the dents left on the truck beam and the forward body bolster beam, respectively, as a result of their impact.

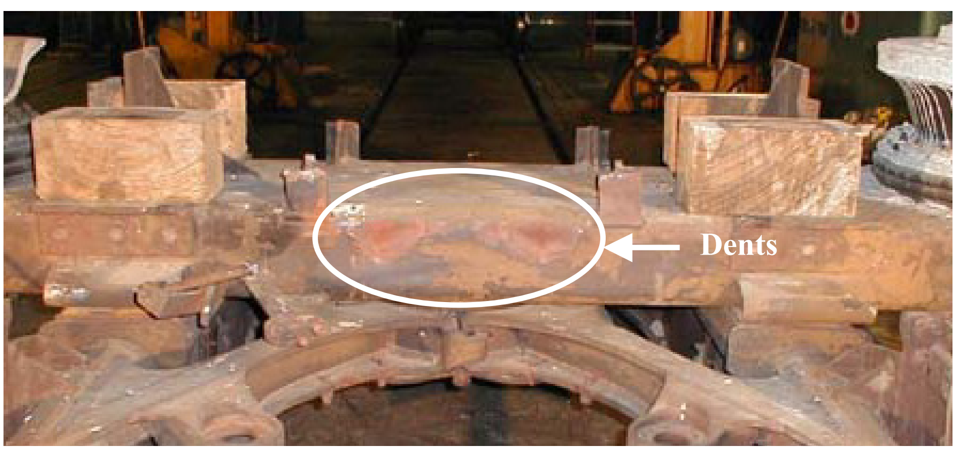

Figure 12. Dents on Truck Beam from Impact with Body Bolster

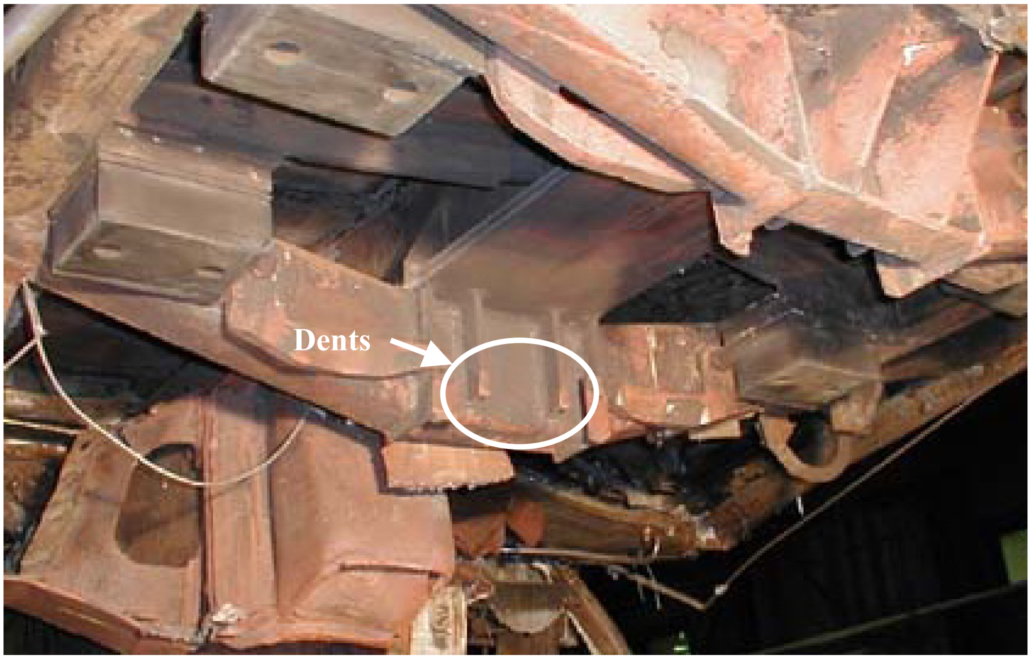

Figure 13. Evidence of Impact with Truck Beam on Body Bolster

As a result of the deformation of the draft sill, the right-side pilot forward attachment block below the draft pocket came into contact with the right forward wheel. As shown in Figure 14, there is a wheel burn on the pilot block from the right forward wheel. There was a corresponding polish mark on the inside of the right front wheel. This occurred due to the downward and lateral shift of the forward draft sill section during the vehicle collapse. Though this would place the front wheels very near the front of the impact face, review of high-speed film from the test suggests the wheels did not impact the wall.

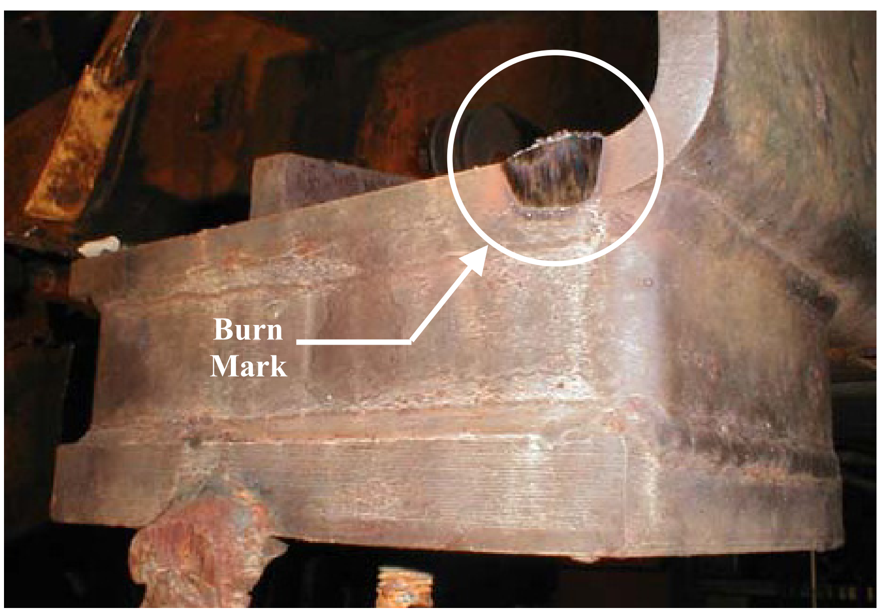

Figure 14. Evidence of Contact Between Draft Sill Pilot Mount and Front Right Wheel

3.1.2 Side Sills

In the previous single car collision test, the side sills suffered little damage. In contrast, the side sills on the lead car from the two-car test suffered significantly more damage. The side sills terminate at the vestibule door opening in the vicinity of the bulkhead wall. Side sill damage was limited in the single car test because underframe and superstructure damage aft of the bulkhead wall was minimal. For the two-car test, superstructure and underframe damage extended farther behind the bulkhead wall, which was probably due to the slightly higher collision energy of the two-car test.

The response of the side sills was asymmetric. As seen in Figure 15, the left side sill mostly crushed straight back, with the lower part of the side sill shearing off and bending inward. The collapse response of the crushed side sill section featured relatively short wavelength buckling. Overall reduction in length of the left side sill was 14 3/8 inches (0.365 m).

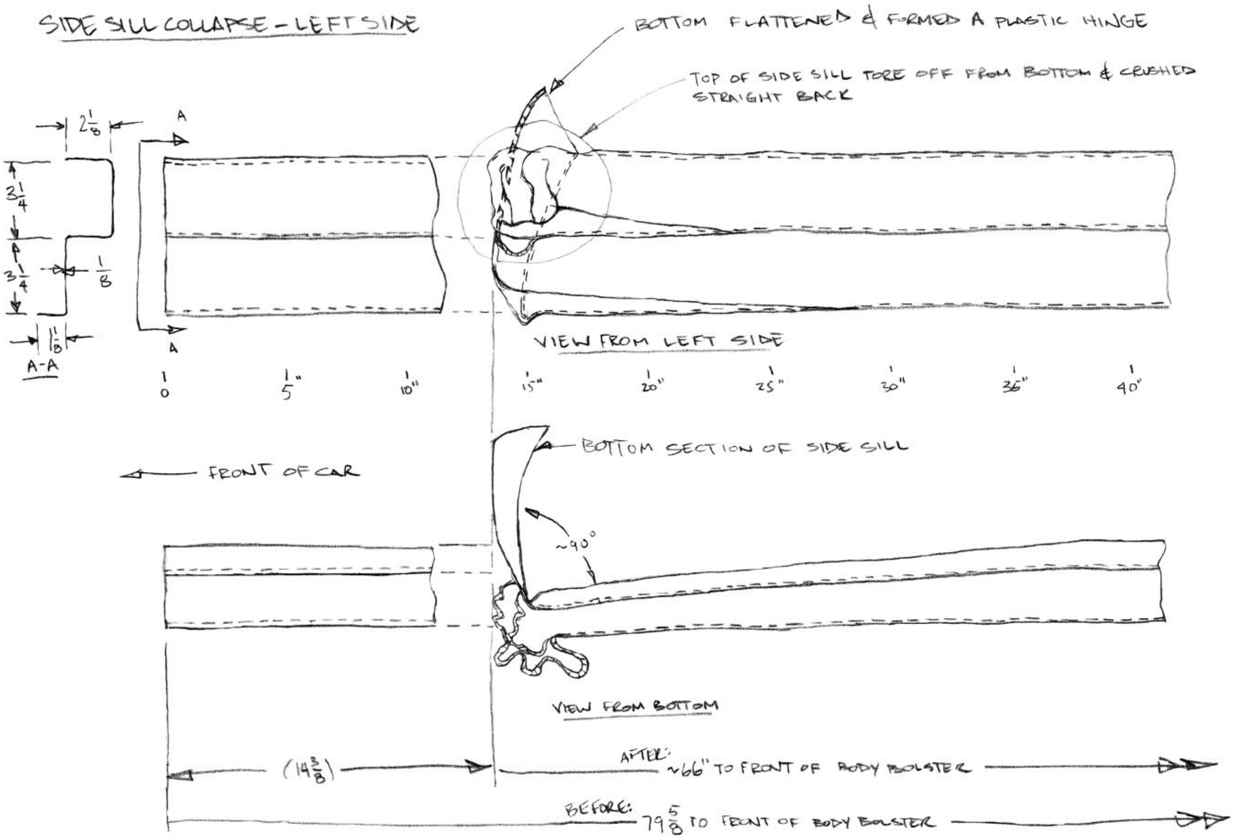

Figure 15. Sketch of Left-side Sill Collapse

The right-side sill buckled outward, forming a primary plastic hinge at one point about 20 inches (0.508 m) aft of the leading edge, as shown in Figure 16. The side sill separated from the floor rails along this buckled area, which opened a gap between the sidewall and the floor. The buckle pushed the side sill and the sidewall outward 17½ inches (0.445 m). The longitudinal displacement of the leading edge was 11 1/8 inches (0.283 m). A photograph of the right-side sill from below is shown in Figure 17, which also shows the gap between the wall and floor.

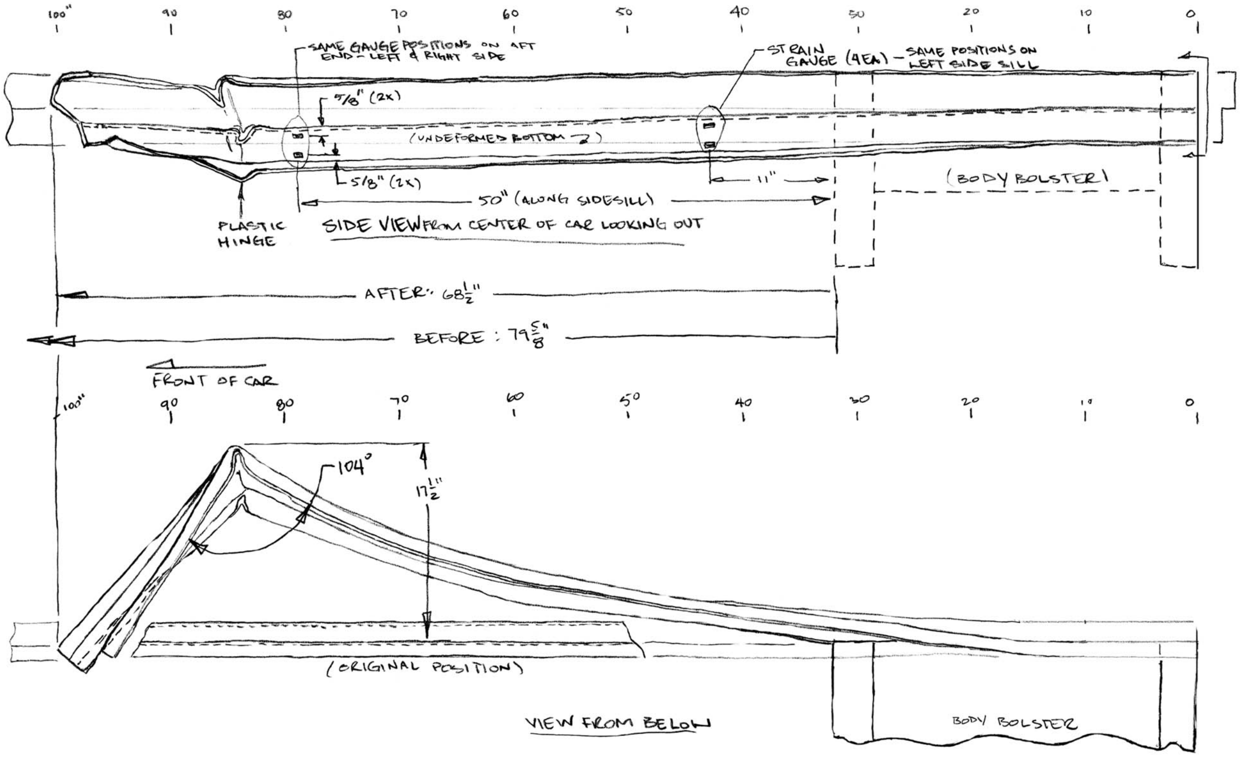

Figure 16. Sketch of Right-side Sill Collapse
(Note: view from below was mistakenly drawn as the mirror image of what it should be).

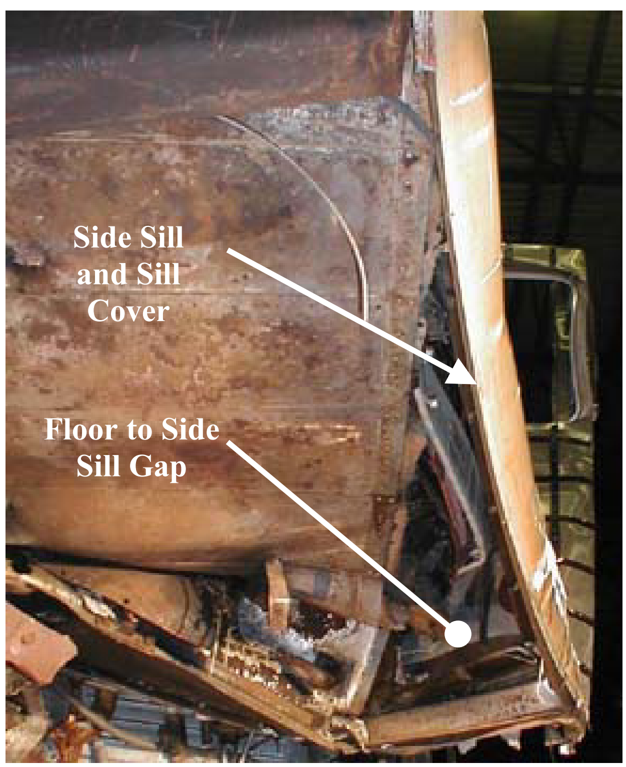

Figure 17. Right-side Sill (From Below Looking Forward)

3.1.3 Cant Rails

Like the side sills, the cant rails of the two-car test suffered more damage than in the single car test. However, unlike the side sills, the response of both sides was largely symmetric. As shown in Figure 18, the left side cant rail buckled out about 12 inches (0.305 m), which reduced the length by 13 inches (0.330 m). Similarly, Figure 19 shows that the right-side cant rail buckled outward 8 inches (0.203 m), reducing the length by 13 inches (0.330 m) as well. The right-side cant rail exhibited more longitudinal crush than the left and, therefore, buckled out slightly less. The corresponding inside view photographs of the left and right-side cant rails are shown below in Figure 20 and Figure 21, respectively.

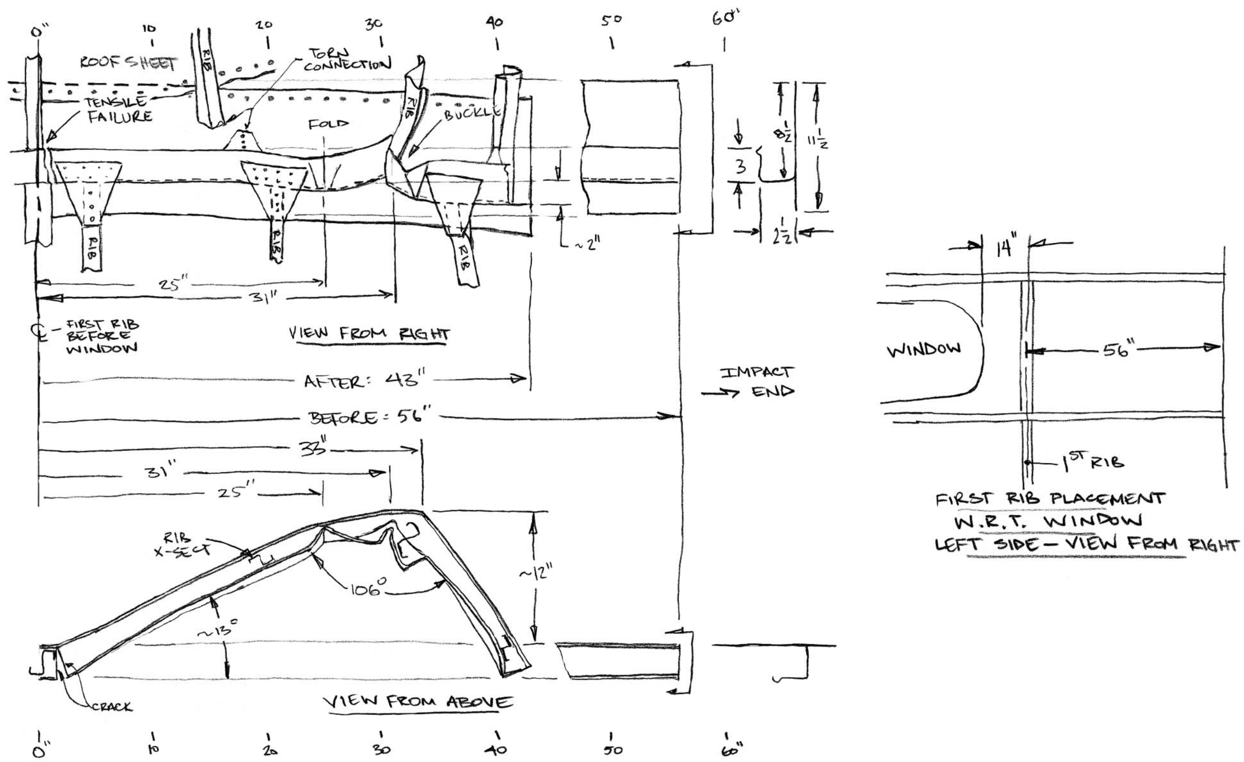

Figure 18. Sketch of Left Cant Rail Damage

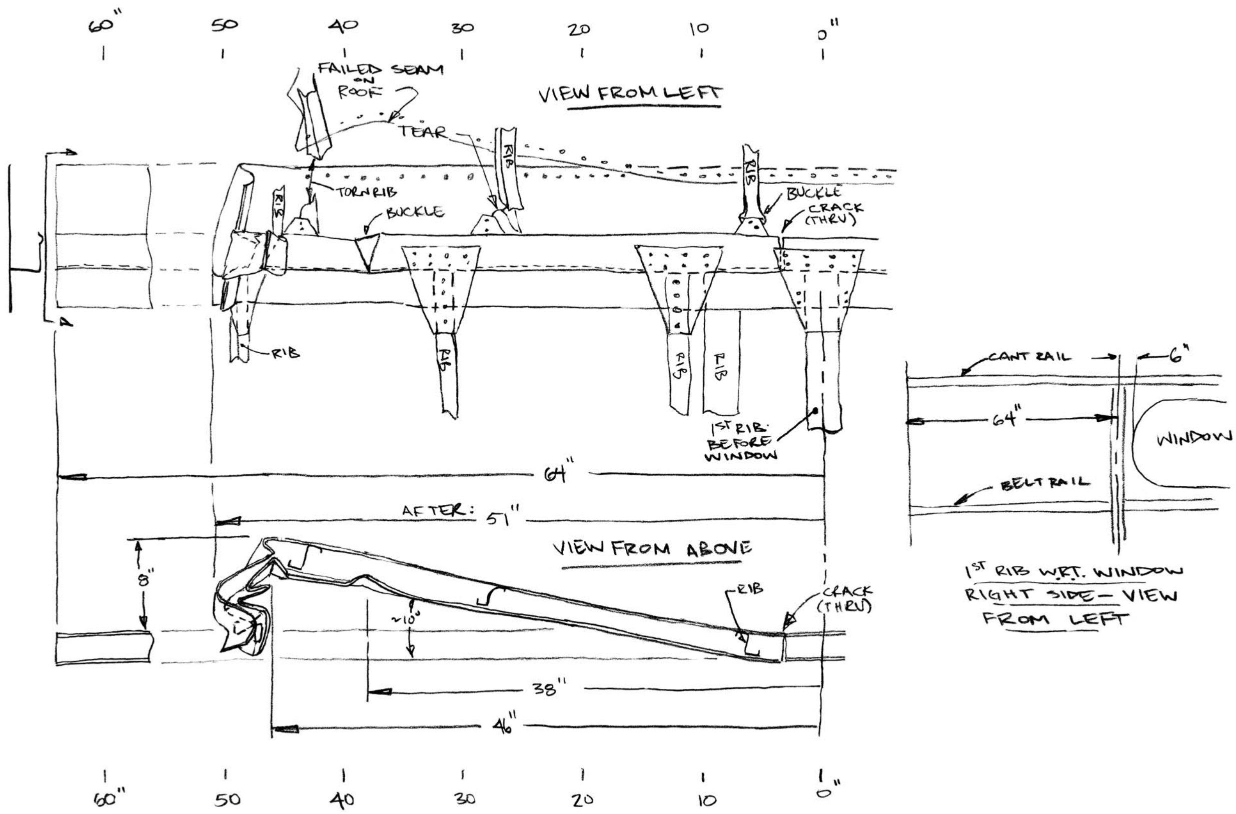

Figure 19. Sketch of Right Cant Rail Damage

Figure 20. Left-side Cant Rail Between Window Frame (left) and Bulkhead Wall (right)

Figure 21. Right-side Cant Rail Between Window Frame (right) and Bulkhead Wall (left)

Figure 18 and Figure 19 show that both right and left side cant rails developed fractures just forward of the window frame. The fractures developed at a point of high bending stress as the sidewalls aft of the bulkhead buckled out and the stiffer window frame sections remained straight. A close-up photograph of the fracture on the right-side cant rail is shown in Figure 22. It appears that the crack runs through a spot weld, at which there was probably a stress concentration that initiated the failure. The fracture on the left side cant rail was nearly identical in character and location.

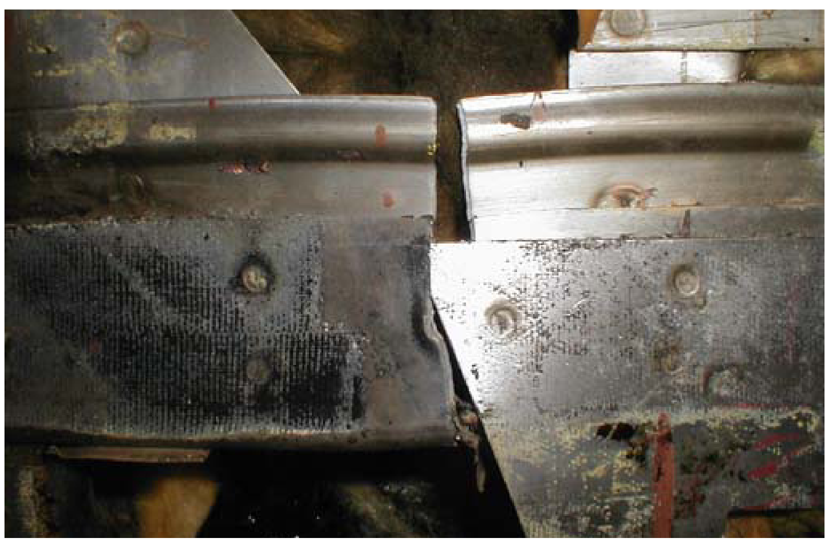

Figure 22. Right-side Cant Rail—Crack Detail Just Forward of Window Frame

3.1.4 Belt Rails

The belt rails were documented because they are another major longitudinal structural component in the superstructure, much like the cant rails. The behavior of the belt rails was largely similar to the cant rails. Symmetric collapse was seen comparing the left and right sides and the amount of longitudinal deflection was similar to the cant rails. Figure 23 shows that the left-side belt rail buckled outward 16 inches (0.406 m), which displaced the leading end 14 inches (0.356 m) in the longitudinal direction.

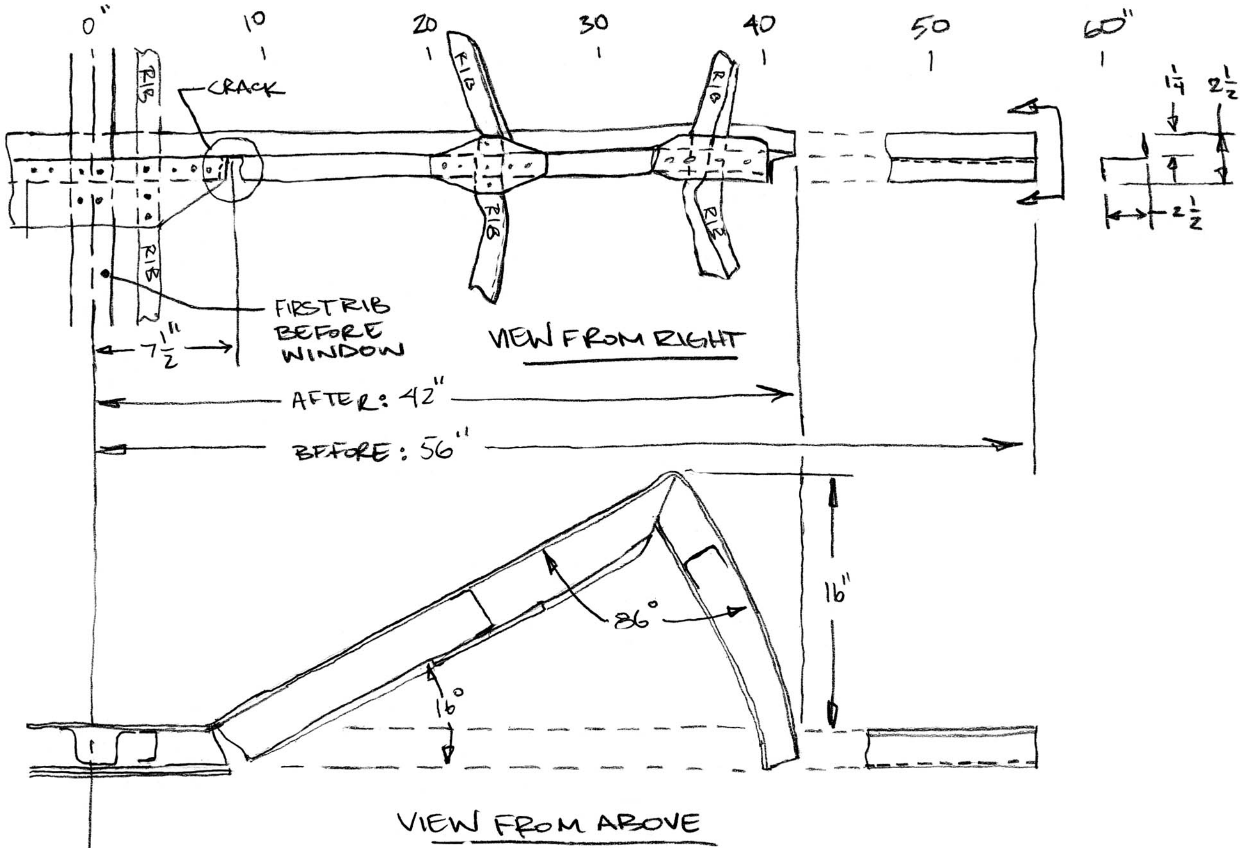

Figure 23. Sketch of Left-side Belt Rail

Similarly, Figure 24 shows that the right-side belt rail buckled out 15 inches (0.381 m) and was deflected back 12½ (0.318 m) inches. One major difference between the two belt rails is that the point of outward deflection was located farther aft on the right side than on the left side. This is because the right-side sill detached from the floor rails and allowed deflection of the sidewall to extend farther back than on the left side, whose side sill remained attached to the floor structure and crushed longitudinally.

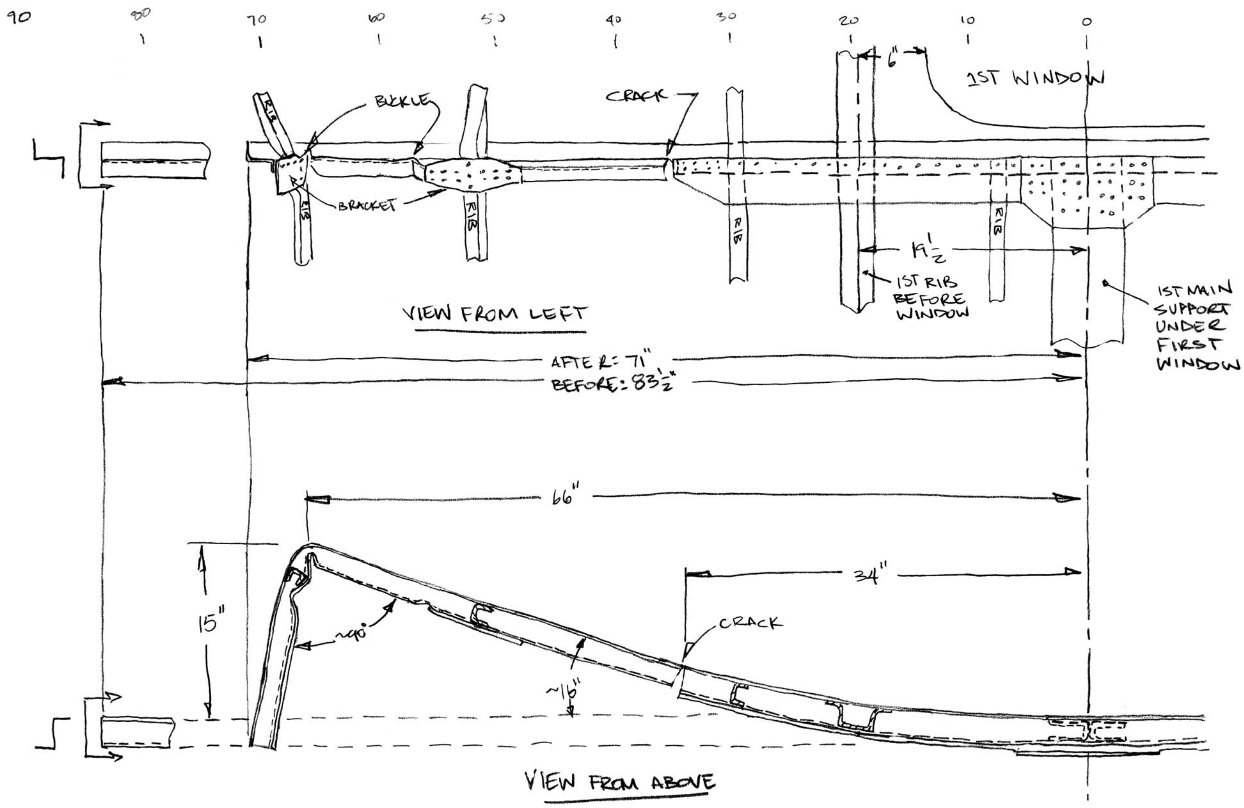

Figure 24. Sketch of Right-side Belt Rail

Cracks in both belt rails were seen like those in the cant rails. The locations of the fractures are nominally the same as those in the cant rails. Figure 25 shows a close-up of the cracked left-side belt rail. Note that the fracture runs through two spot welds, which were probably the initiation points of the failure.

Figure 25. Left-side Belt Rail—Crack Detail Just Forward of Window Frame

3.2 OVERALL SUPERSTRUCTURE DAMAGE

The superstructure collapse in the two-car test was similar to that seen in the single car test. The relatively weak vestibule crushed completely, leaving no available occupant room between the end structure and the bulkhead wall. The collapse of the superstructure was mostly symmetric about the car centerline. Both vestibule doors folded in half and outward. Both weakly connected trap doors were pushed straight back under the floor structure and remained largely intact. The vestibule roof structure buckled into a collapsed length of approximately 12 inches (0.305 m) from about 50 inches (1.27 m). Aft of the bulkhead wall, the sidewalls buckled outward in a mostly symmetric manner. Damage extended back to approximately the first window frame. Figure 26 through Figure 32 below show sketches and photographs of the superstructure damage, both internally and externally.

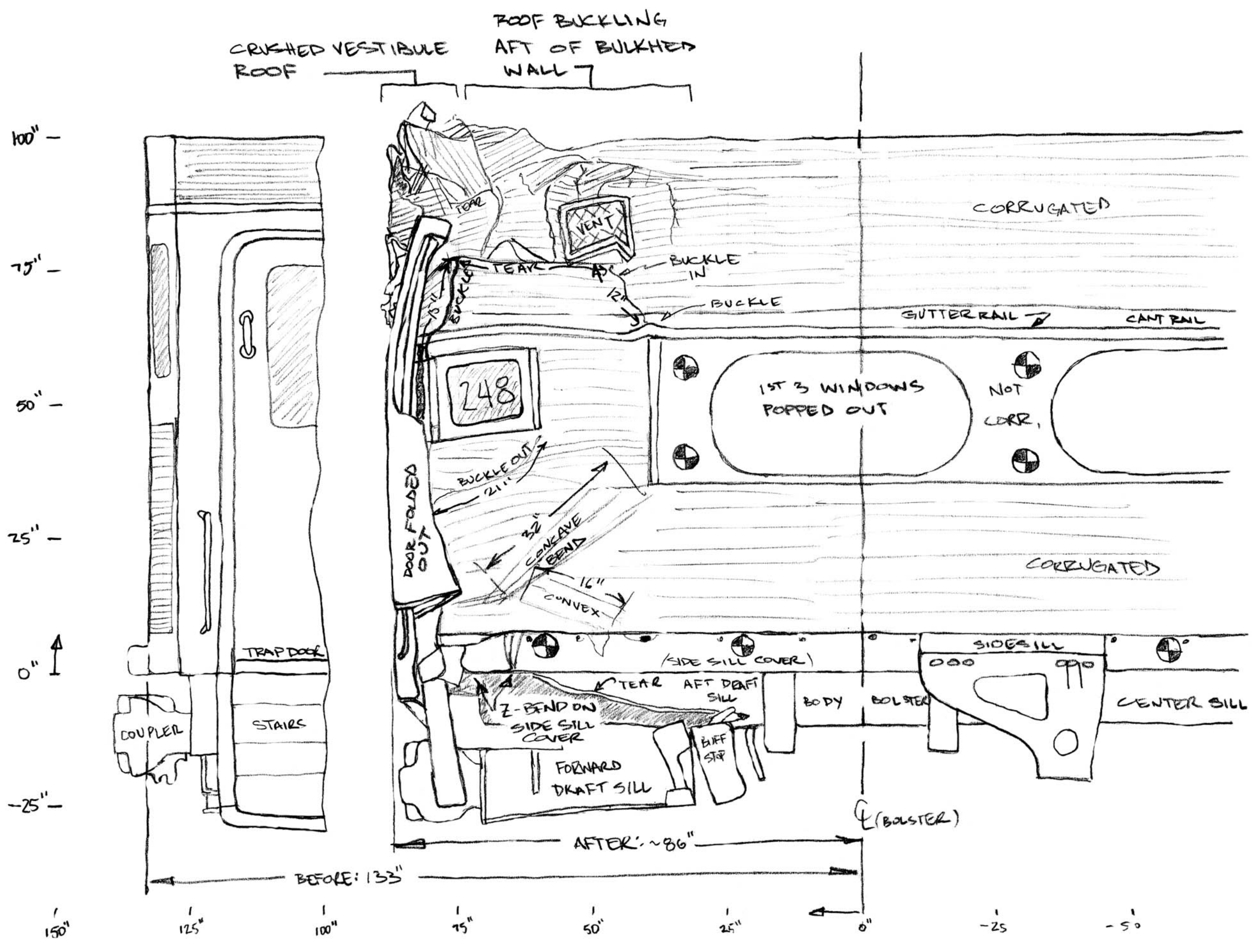

Figure 26. Sketch of Superstructure Crush in Impact Zone—Left Side

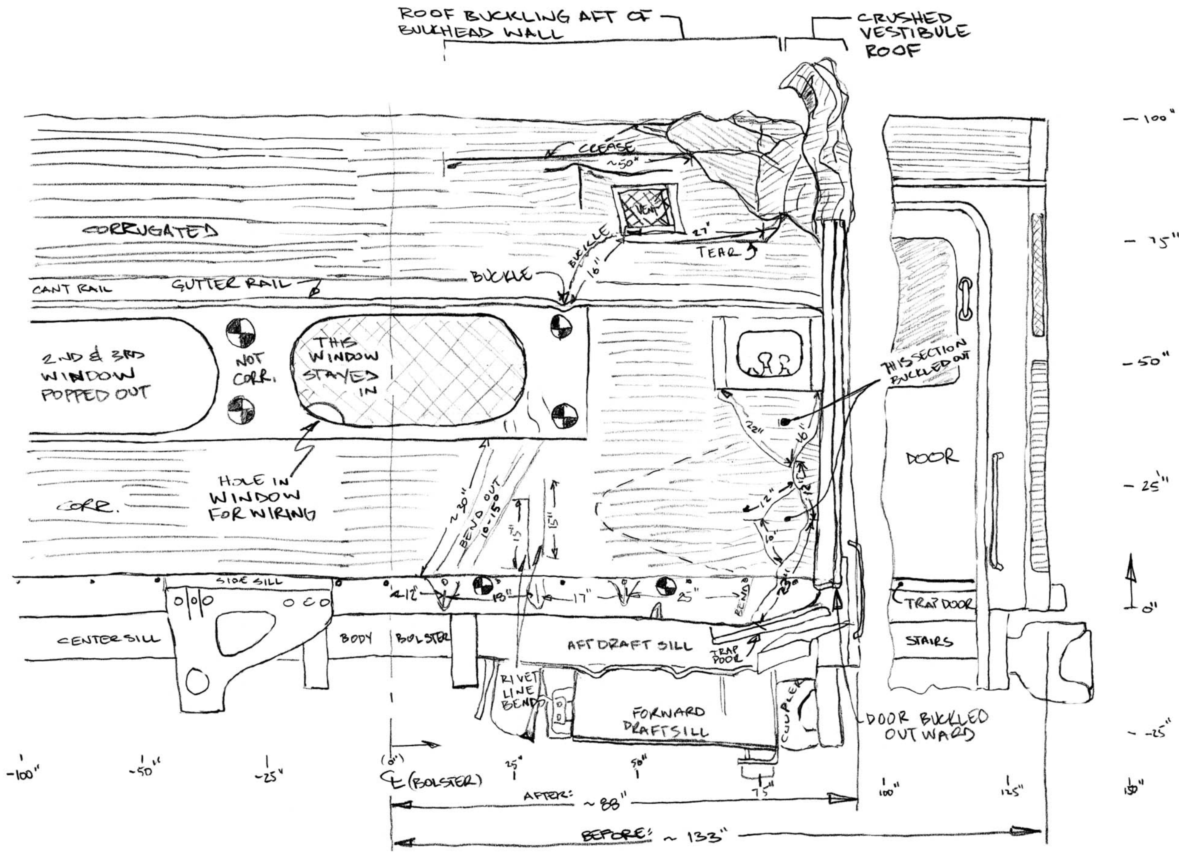

Figure 27. Sketch of Superstructure Crush in Impact Zone—Right Side

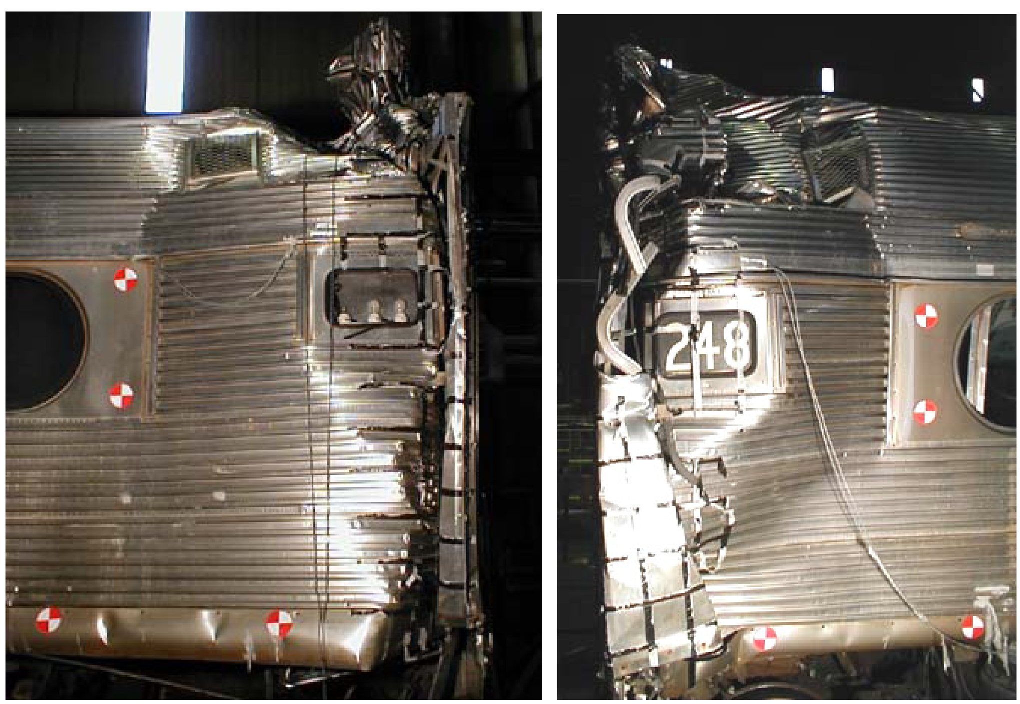

(a) Right Side **(b) Left Side**

Figure 28. Superstructure Crush in Impact Zone

Figure 29 shows a top view of the vehicle crush in the impact zone. The deformations shown in the sketch correspond to those at the carbody floor line. The sketch shows how the impact surface was deformed into a nearly planar surface to conform to the impacted wall. Floor buckling is also noted.

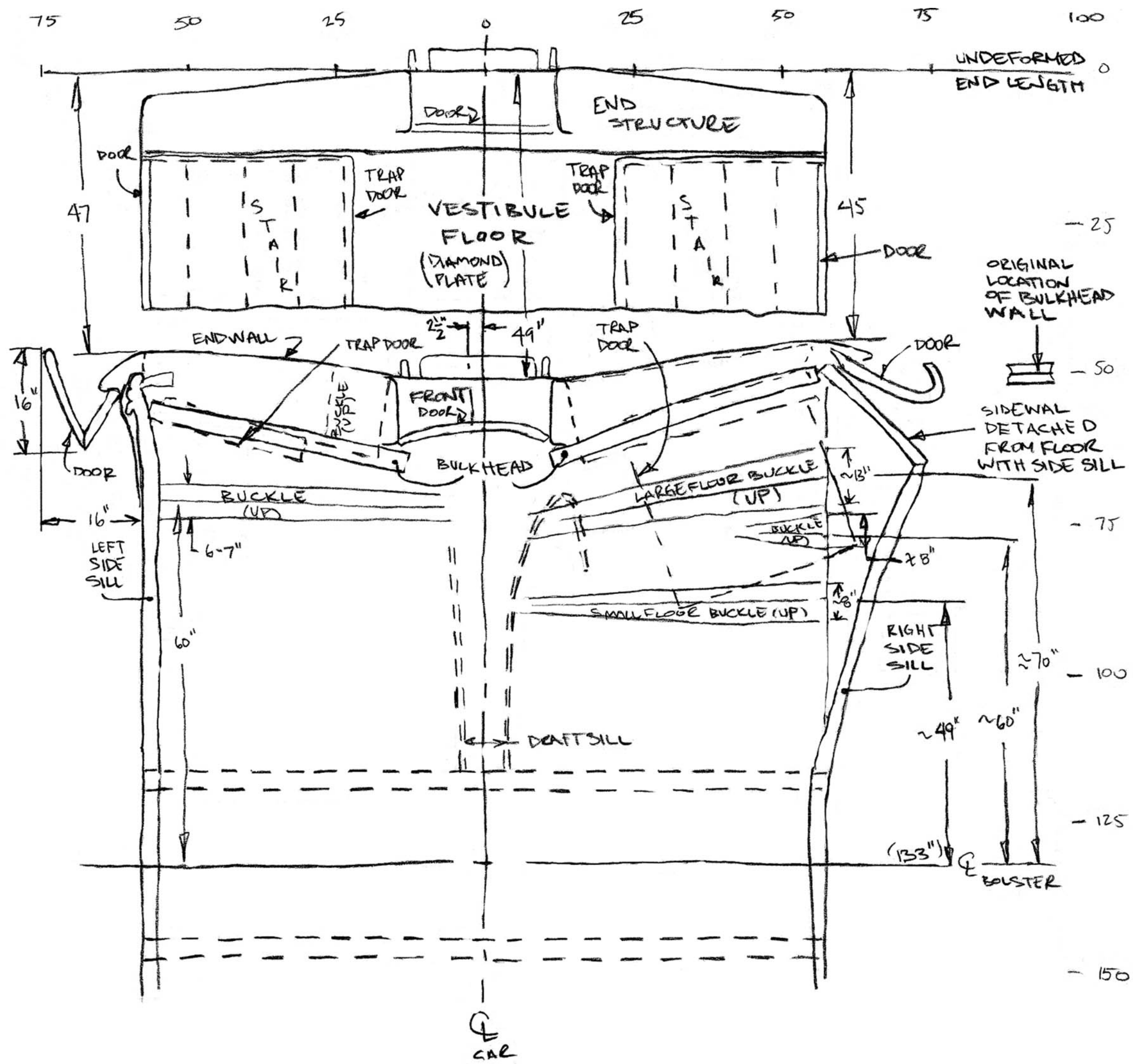

Figure 29. Sketch of Crush at Floorline, as Viewed from Above

Figure 30 shows the internal damage behind the bulkhead wall at the impacted end. The restroom closet on the left side of the car was pushed back past the leading edge of the first window. The closet, which is only weakly screwed into the surrounding paneling, moved back as a unit and would have impacted any seats installed between it and the window frame. Further occupant space was compromised on the right side where a bench is mounted along the right wall just aft of the bulkhead wall. The bench frame was seriously distorted and a major floor buckle occurred directly under the bench.

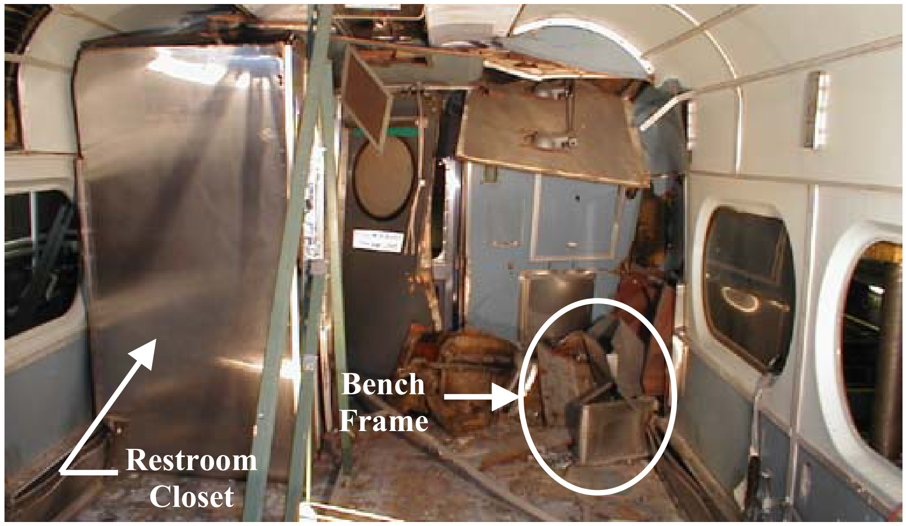

Figure 30. Internal View Looking Forward at Crush Zone

To gain better access to primary structural members and to assess overall structural damage, non-structural elements were removed inside the car between the first window frame and the bulkhead wall. Figure 31 shows the view from inside the impact end after the material was removed. One can see that the bulkhead wall remained mostly intact while the sidewalls aft of the bulkhead wall buckled outward.

Figure 31. Internal View Looking Forward of Crushed End After Material Removal

Figure 32 shows the buckled left and right sidewalls between the bulkhead wall and the first window frame. The position of the cant rails and belt rails are highlighted in the photographs. Also seen in the photographs are close-ups of floor buckling just aft of the bulkhead wall. The buckled diamond plate in the left-side photograph is the floor of the restroom closet. Like the closet, it was not well tied into the overall structure. The floor buckle in the right-side photograph involves deformations of the underframe structures.

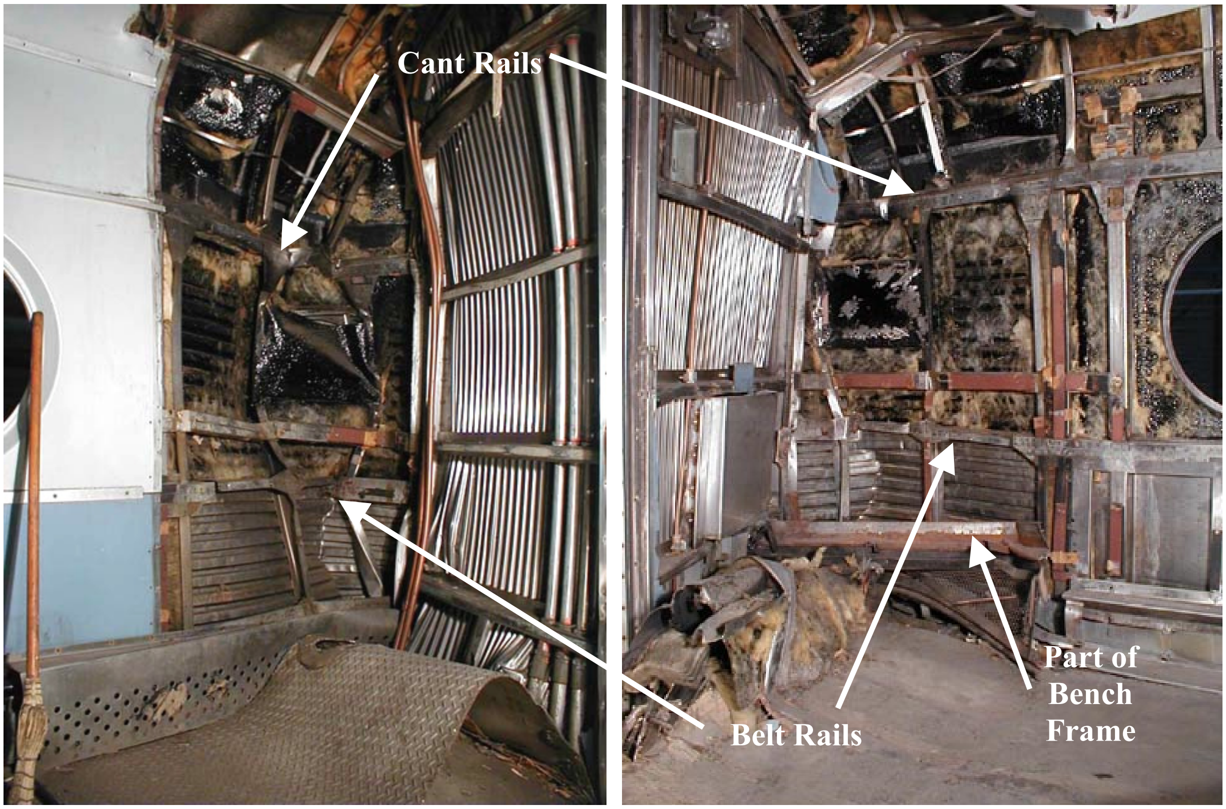

(a) Left Side **(b) Right Side**

Figure 32. Outward Buckling of Superstructure Between Bulkhead and Window Frame

3.3 OTHER STRUCTURAL DAMAGE AND DOCUMENTED ITEMS

3.3.1 B-End Damage

The non-impact, B-end of the lead test vehicle was inspected for test-induced damage. Figure 33 describes the major evidence of damage on the B-end of the vehicle found during the post-test inspection.

Some minor buckling was found on the right-side draft sill flange. From the nature of the damage, it appeared to have been induced prior to the test. Review of photographs taken of the draft sill before it was crash tested confirmed this observation.

The right-side vestibule door was also found to be stuck in its frame. There was evidence on the doorframe of some distortion, including a small buckle on the rain gutter above the doorframe. After applying a considerable amount of force, a person could open the door and shut it fully again in the doorframe. It is unclear whether this damage was a result of superstructure distortion induced during the crash test or if the damage was pre-existing. Review of the high-speed film showed some twisting of the carbody during the test but it is not clear if this impact response was sufficient to cause the door to jam in its frame.

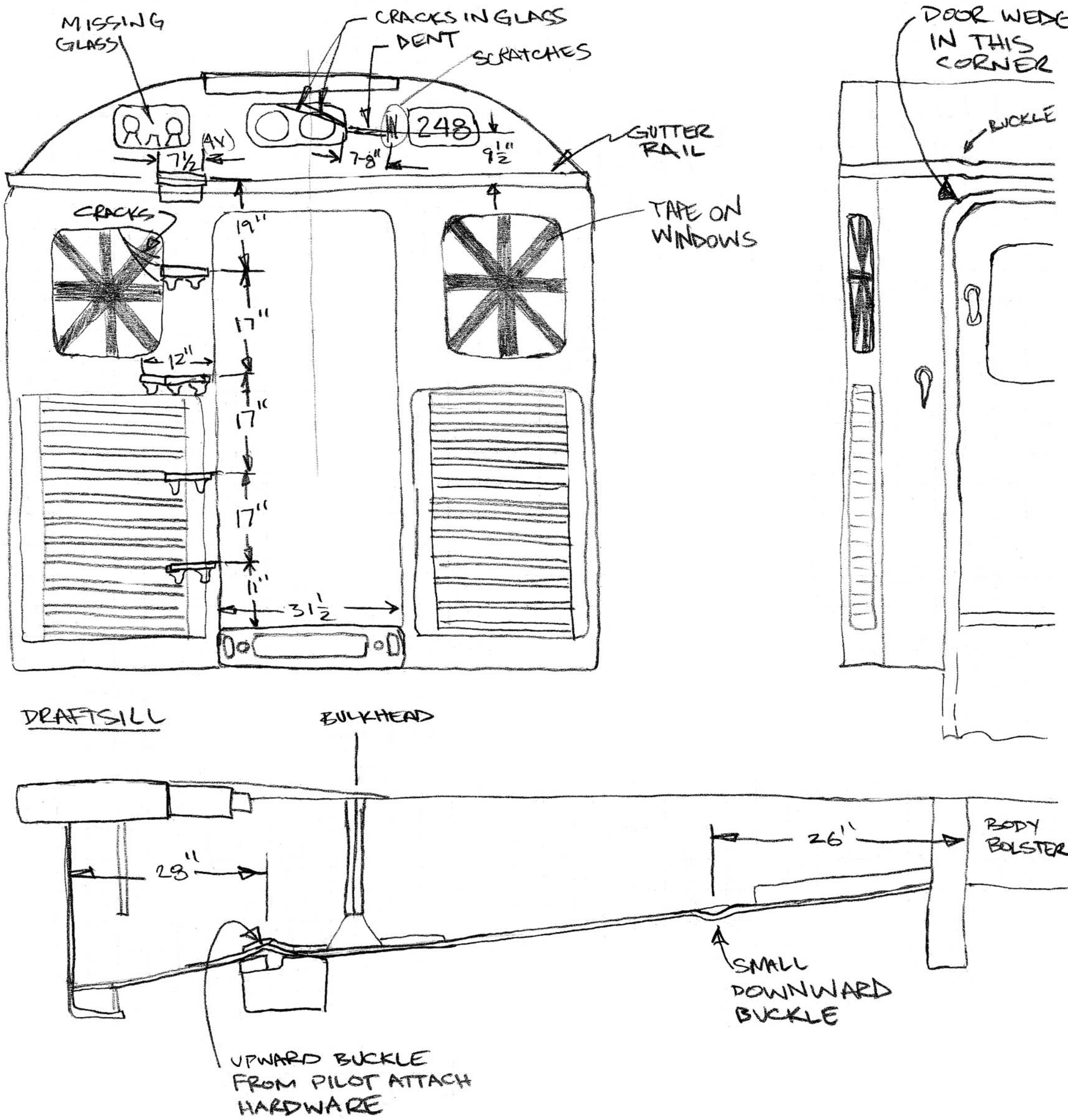

Figure 33. B-End Damage Documented During Post-test Inspection

Further evidence of damage was seen on the B-end face above the gutter rail, as shown in Figure 34. The mark in the steel seems to be from a step plate or some other horizontal surface. At first it was suspected that steps on the opposing face of the trailing car impacted the lead car. However, upon further investigation, this could not have been the case. First, the cars were coupled with the B-end of the lead car facing the A-end of the trailing car and the A-end of Pioneer cars do not have steps. Second, review of the high-speed film and video did not show evidence of contact at the top of the car bodies. For these reasons, it is believed that the damage was pre-existing or occurred subsequent to the test as the vehicles were re-railed and moved.

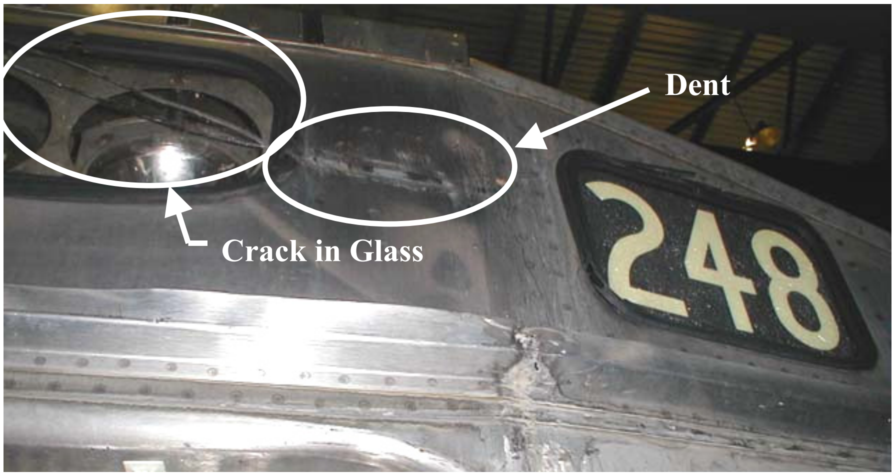

Figure 34. Evidence of B-End Impact Above Gutter Rail

Review of the high-speed video shows that the two cars did impact each other at the buffer beam. The buffer beam of the trailing car overrode the buffer beam of the lead car and slid off as the coupled connection rebounded. Figure 35 shows the resulting minor damage to the lead car buffer beam.

Figure 35. Evidence of B-End Impact on Buffer Beam

There is further evidence of some slight damage to the draft pocket of the B-end, as shown in Figure 36. This appears to have occurred during the collision as the coupler was driven back and impacted the front face of the draft pocket.

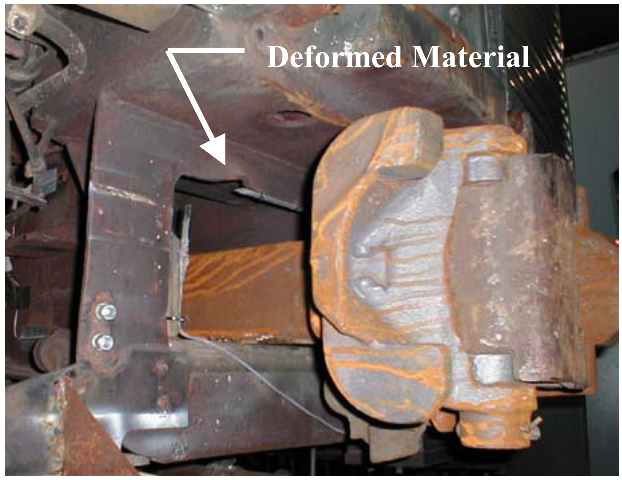

Figure 36. B-End Draft Pocket Damage

3.3.2 Concrete Distribution

Concrete was poured in various locations throughout the car to bring the vehicle up to its operational weight after all the seating and other internal equipment were removed. The location and dimensions of the concrete were documented for future reference. This information would be necessary to reproduce the correct mass distribution in a computer model of the test vehicle.

Concrete was primarily distributed under the floorboards and in the sidewalls below some window openings. Two closets on the B-end were also partially filled with concrete. Also, three of the four cast iron suspension bells above the air bladders were filled with concrete. The distribution and relevant dimensions are shown in Figure 37.

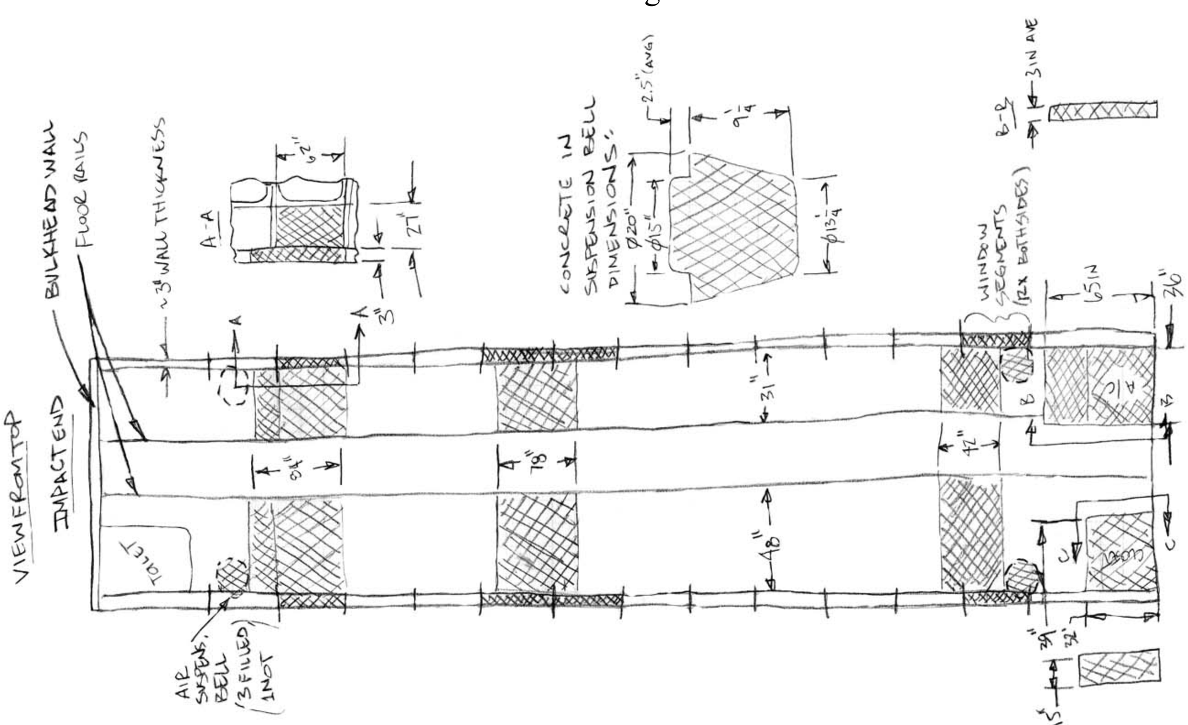

Figure 37. Concrete Distribution in Lead Car

Figure 38 below shows the detached front truck. Note that the left-side suspension bell was filled with concrete, as were both bells on the rear truck. A fracture in the right-side bell may also be seen in the figure. There was evidence of past repairs to the bell in the form of welds. It is not clear if this damage was a result of the collision test.

Figure 38. Forward Truck (Detached) from Left Side Looking Aft

3.3.3 Strain Gage Locations

Measurements were taken of the strain gauge locations distributed on the A-end and B-end draft sills as well as cant rails. This was done to aid in strain gage data post-processing.

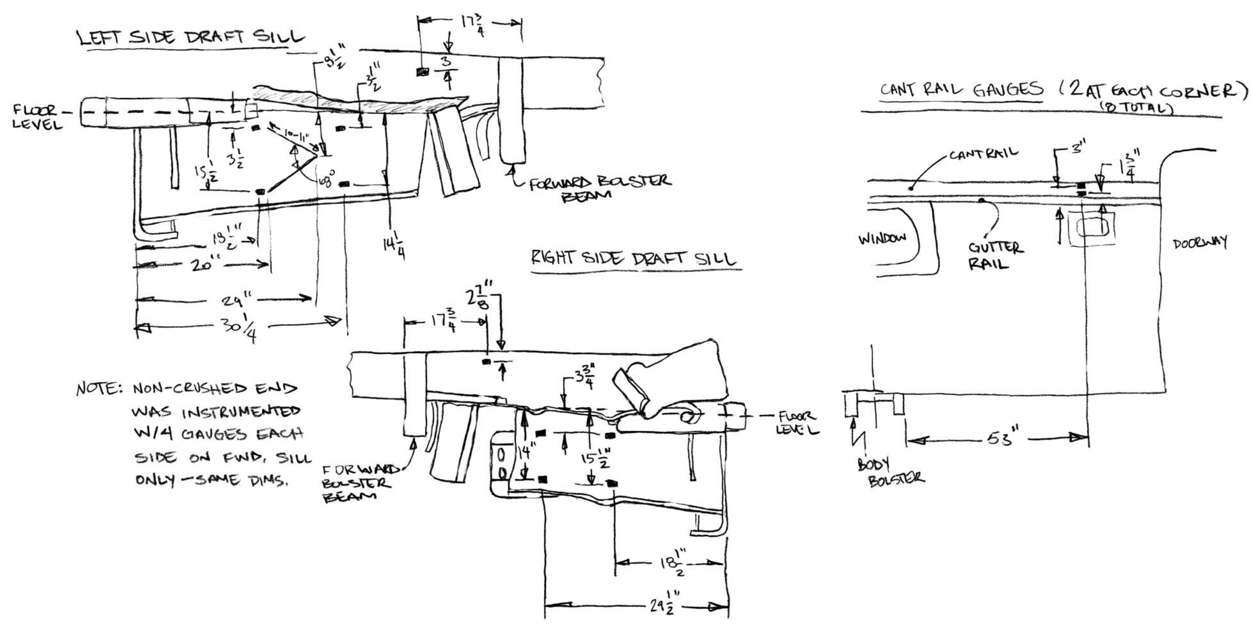

Figure 39. Strain Gage Locations on Vehicle Draft Sills and Cant Rails

4. SUMMARY AND CONCLUSIONS

A detailed post-test inspection and documentation was performed of the lead car from the two-car crash test performed on April 4, 2000, at TTC in Pueblo, Colorado. Damages to primary structural members including the draft sill, side sills, and cant rails were documented. Modes and magnitude of deformation are discussed. Other secondary structural components, such as the superstructure skin, belt rails, and floor in the vicinity of the impact, were also documented. B-end damage was documented also, even though the lack of knowledge of vehicle condition prior to testing made it difficult to determine whether some of the damage was a result of the crash test or was pre-existing. Other details such as concrete ballast distribution and strain gage location were documented for the benefit of future analysis.

Many similarities exist between the observed damage from the two-car and single car crash[*] tests. The collapse mode of the respective draft sills was largely the same, although the two-car test draft sill collapse was more extensive (64 5/8 inches (1.64 m) compared to 54 inches (1.37 m) of collapse between front of draft sill and body bolster) and slightly more symmetric. Like the single car test, the origination of the draft sill collapse was due to the failure of the welds surrounding the buff stop as the draft gear was driven back. This initiated the collapse of the draft sill between the buff stop and body bolster.

One major difference between results from the two-car test and the single-car test was caused by the absence of a pilot in the two-car test. In the single car test, the loads transmitted from the pilot weakened the connections of the attachment hardware mounted under the draft sill just forward of the buff stop. This allowed the forward part of the draft sill to collapse asymmetrically. Since a pilot was not mounted in the two-car test, the attachment hardware remained well connected to the draft sill, thus preventing the collapse of the forward draft sill.

Superstructure collapse was also similar for the two configurations, but again more symmetric for the two-car test than the one-car test. Due to the larger longitudinal collapse of the draft sill, the superstructure collapse behind the bulkhead wall was more extensive in the two-car test. As a result, other primary longitudinal structural members such as the side sills, cant rails, and belt rails experienced more crush than in the single car test.

Damage to the primary structural members is summarized as follows:

- The draft sill collapsed by a relaxed length of 64 5/8 inches (1.64 m). Peak crush was approximately 73 inches (1.85 m).
- The left-side sill collapsed straight back and was reduced in length by 14 3/8 inches (0.365 m). The right side buckled outward forming a single plastic hinge and was reduced in length by 11 1/8 inches (0.283 m).
- The left- and right-side belt rails both buckled outward, which reduced their longitudinal length by 14 inches (0.356 m) and 12½ inches (0.318 m), respectively. Fractures developed on both rails just forward of the first window frame. Overall, collapse was relatively symmetric.

[*] Similar post-test inspection and documentation were performed on the car used in the single car test.

- The left- and right-side cant rails both buckled outward, which reduced both of their lengths by 13 inches (0.330 m). Like the belt rails, the cant rails fractured just forward of the first window frame and collapsed relatively symmetrically.

5. REFERENCES

1. D. Tyrell, K. Severson, J. Zolock, and A.B. Perlman, "Passenger Rail Two-Car Impact Test Volume I: Overview and Selected Results," U.S. Department of Transportation, DOT/FRA/ORD-01/22.I, January 2002.
2. VanIngen-Dunn, C., "Passenger Rail Two-Car Impact Test Volume II: Summary of Occupant Protection Program," U.S. Department of Transportation, DOT/FRA/ORD-01/22.II, January 2002.
3. D. Tyrell, K. Severson, and A.B. Perlman, "Single Passenger Rail Car Impact Test Volume I: Overview and Selected Results," U.S. Department of Transportation, DOT/FRA/ORD-01/02.1, March 2000.

APPENDIX A: FULL-SIZE SKETCHES

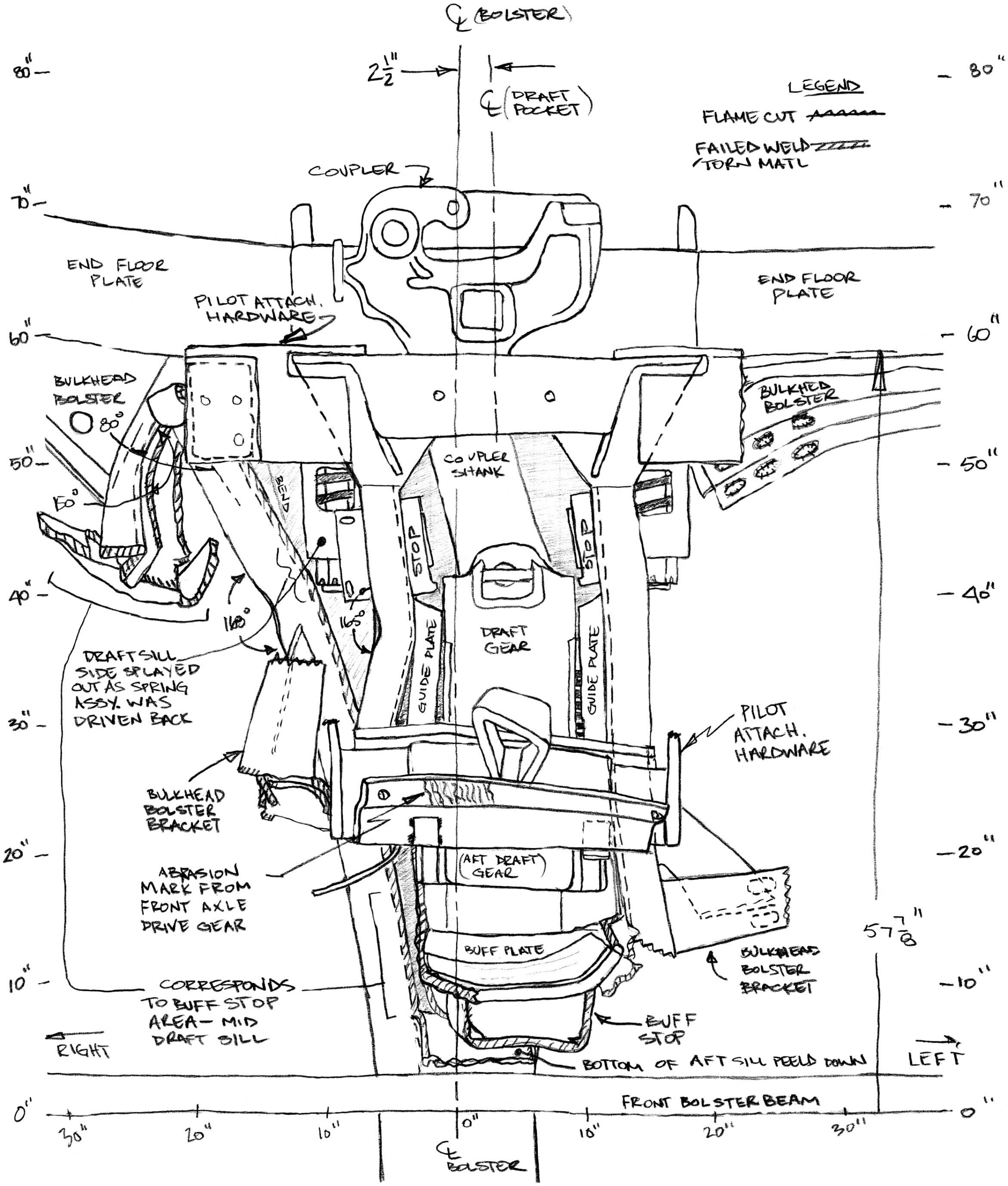

Figure A1. Draft Sill Collapse, Viewed From Below

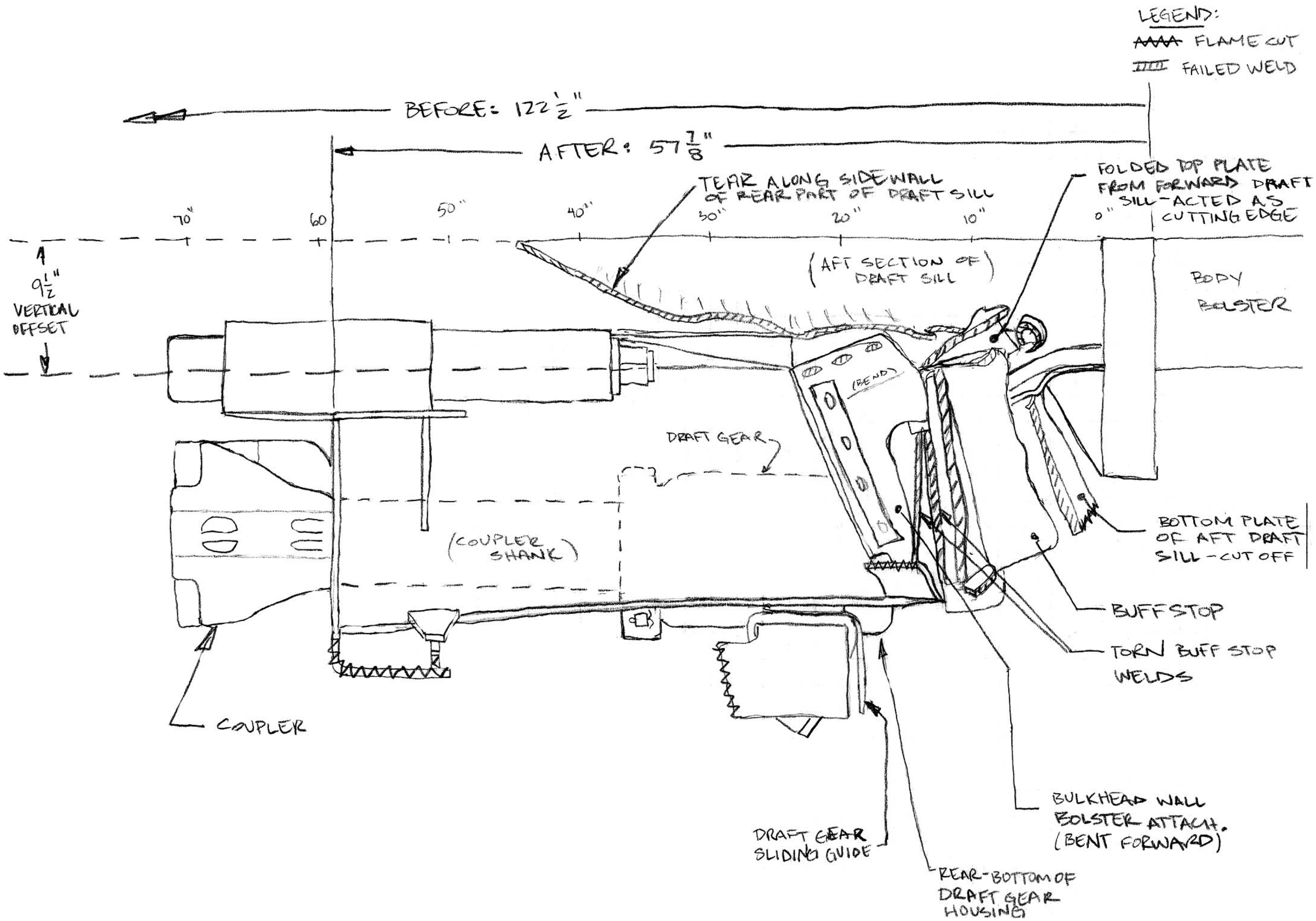

Figure A2. Draft Sill Collapse, as Viewed from Left Side

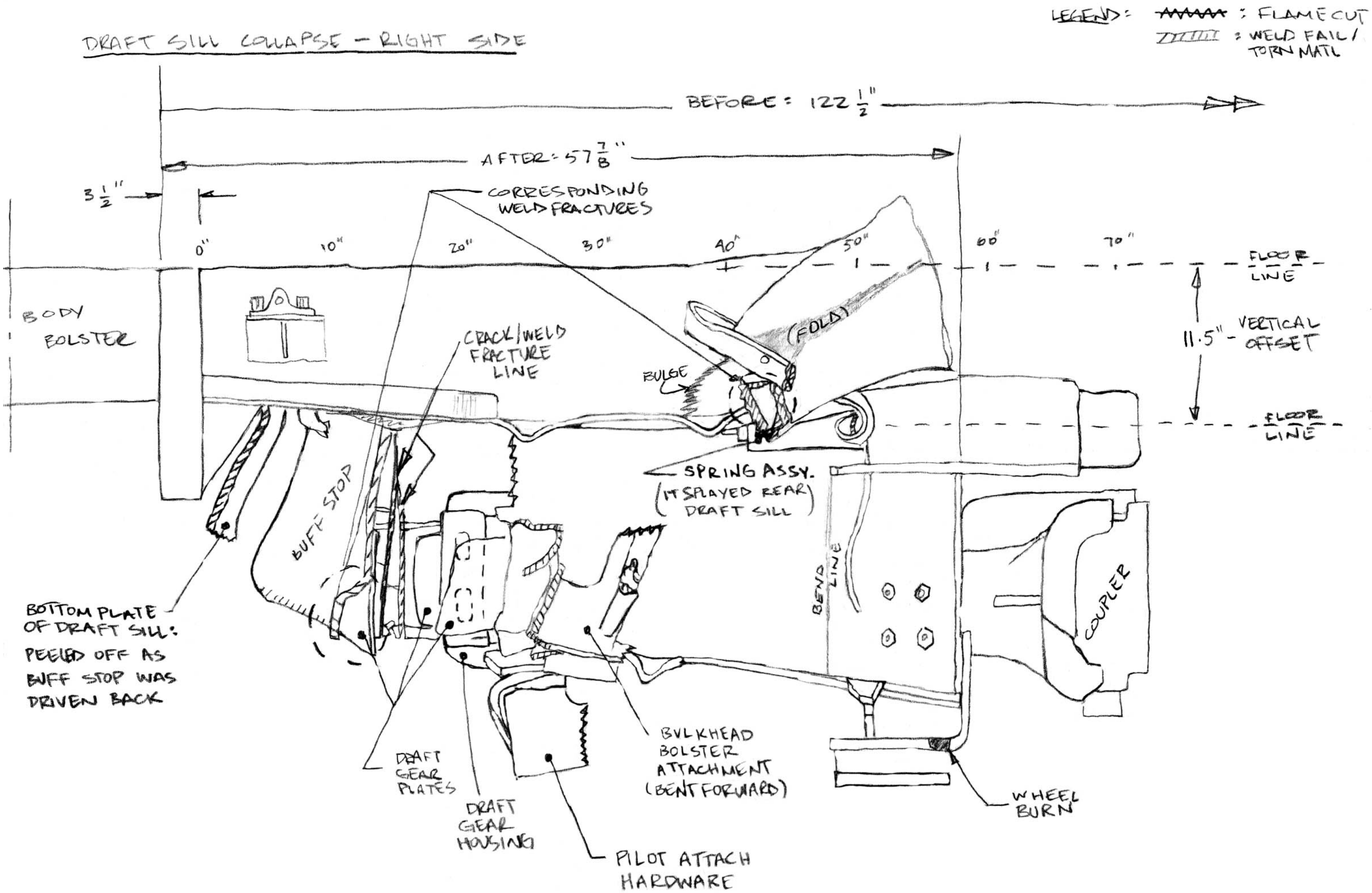

Figure A3. Draft Sill Collapse, as Viewed from Right Side

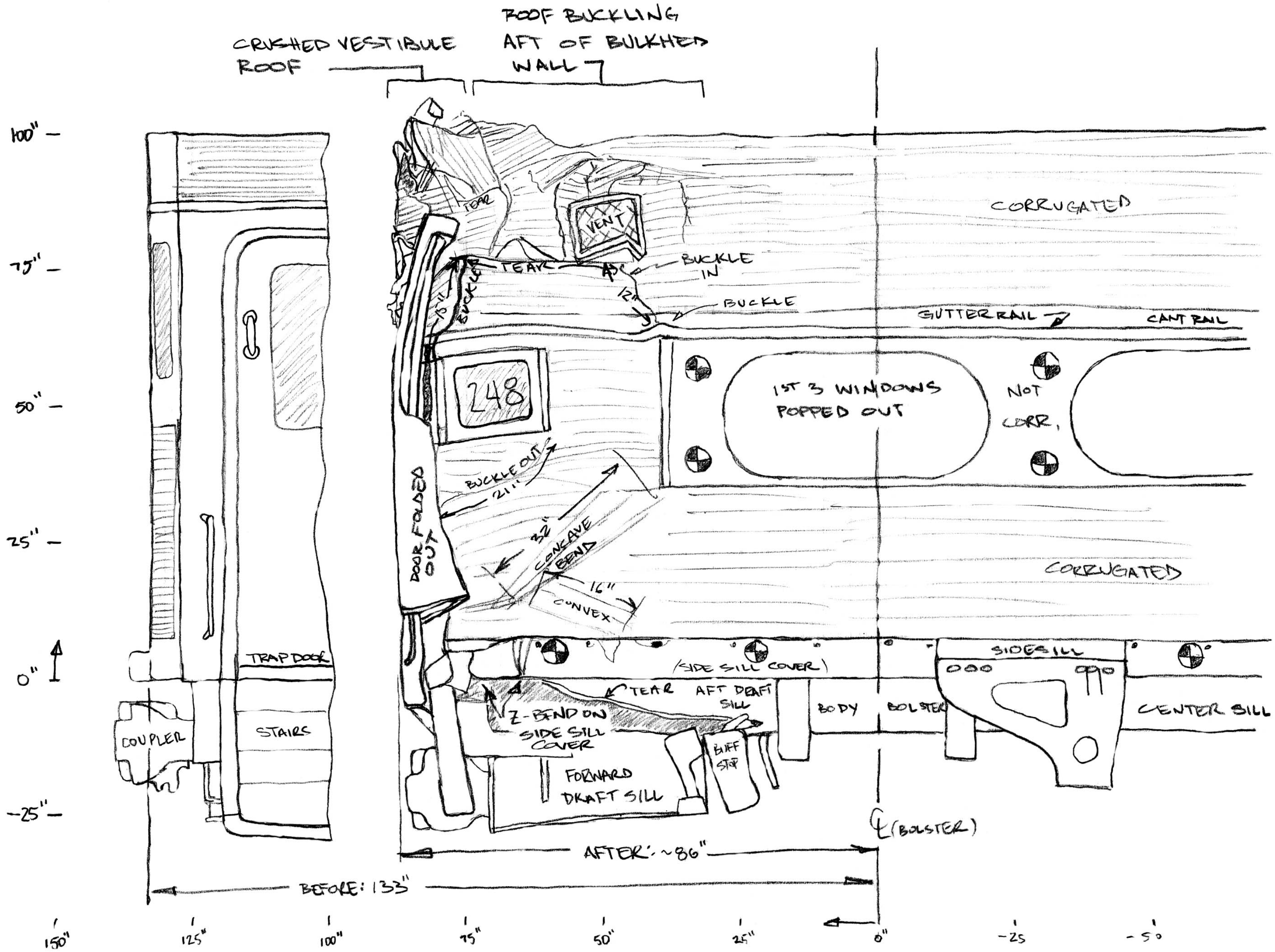

Figure A4. Superstructure Crush in Impact Zone—Left Side

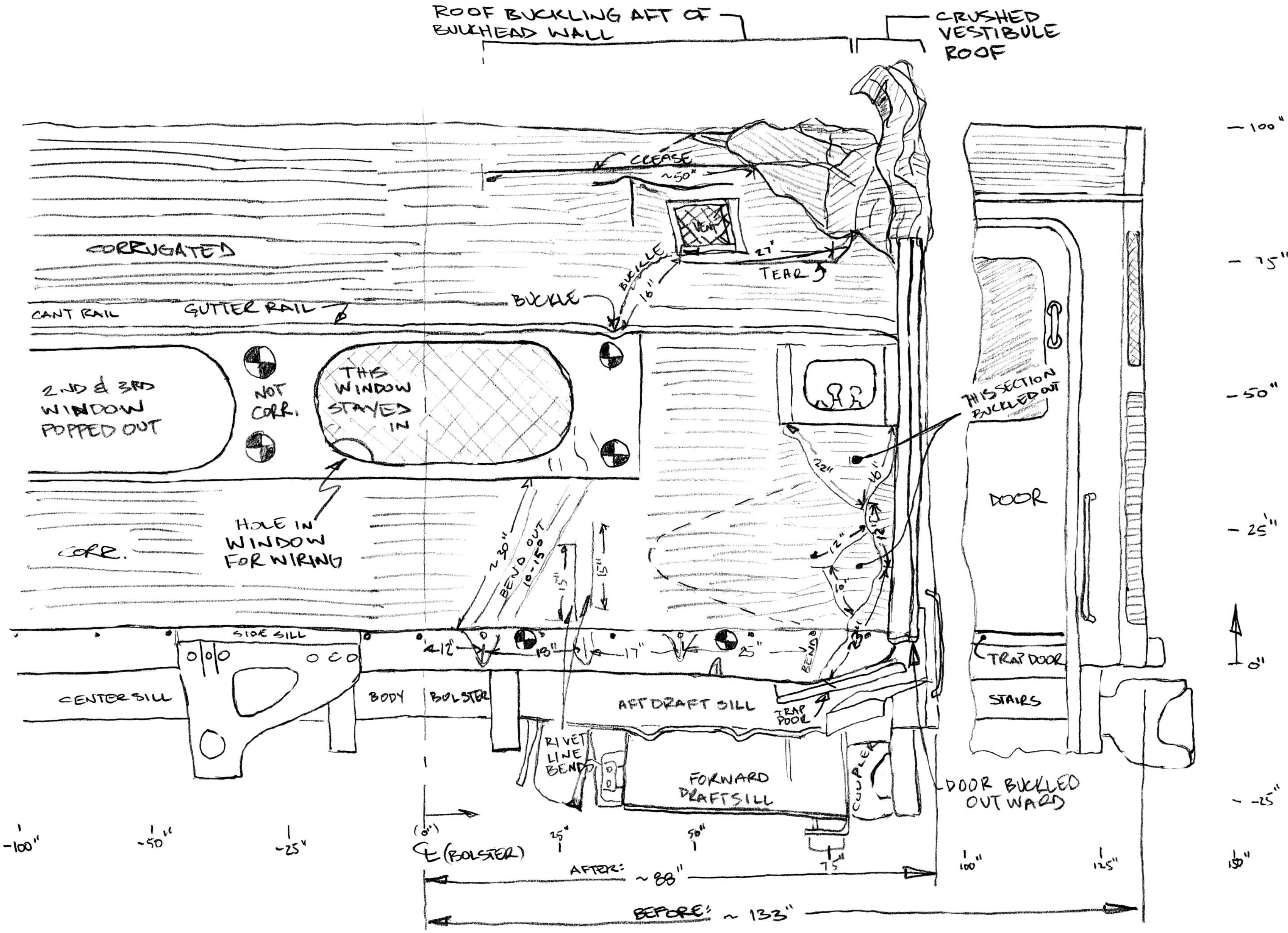

Figure A5. Superstructure Crush in Impact Zone—Right Side

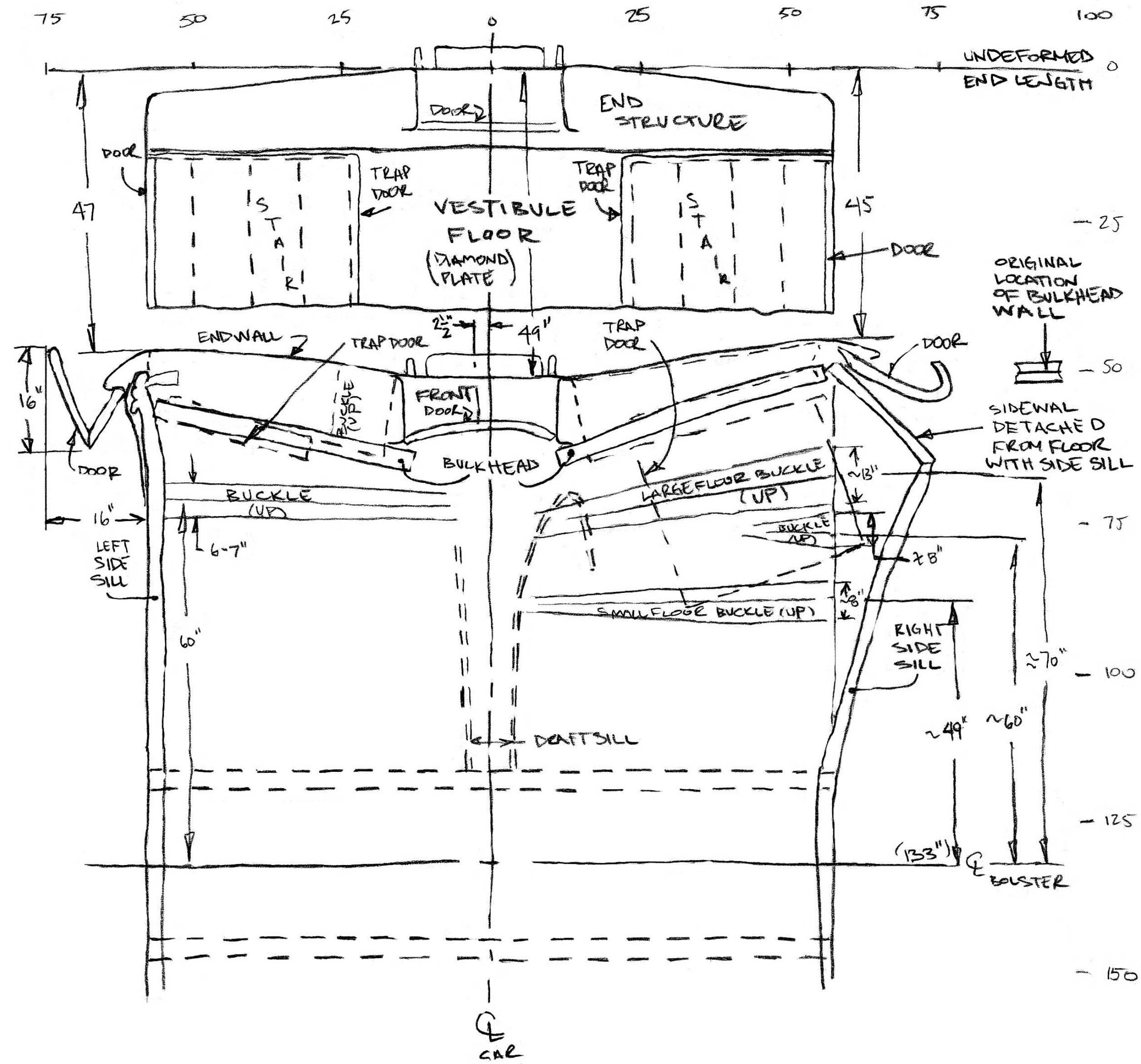

Figure A6. Crush at Floor Line, as Viewed from Above

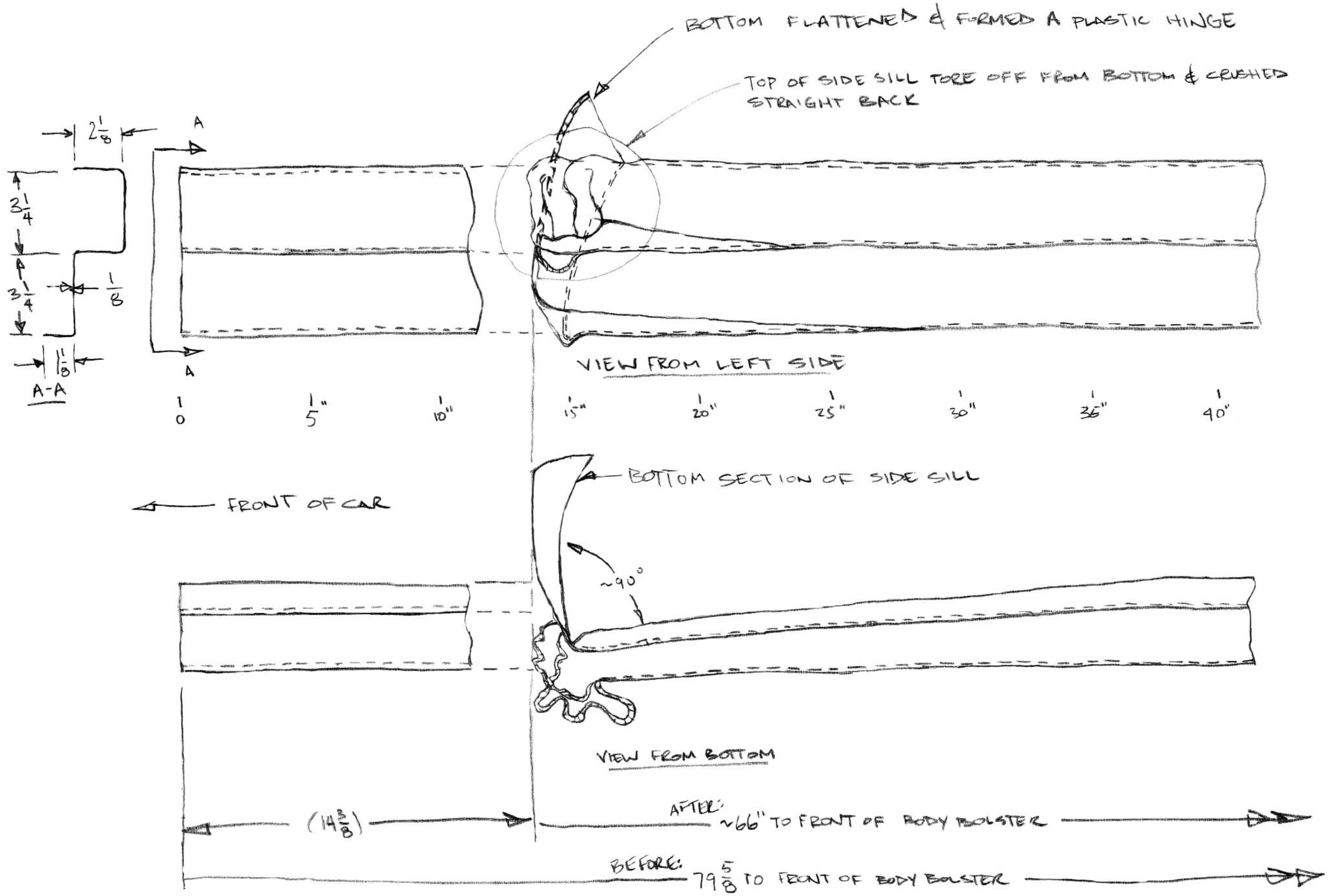

Figure A7. Left-side Sill Collapse

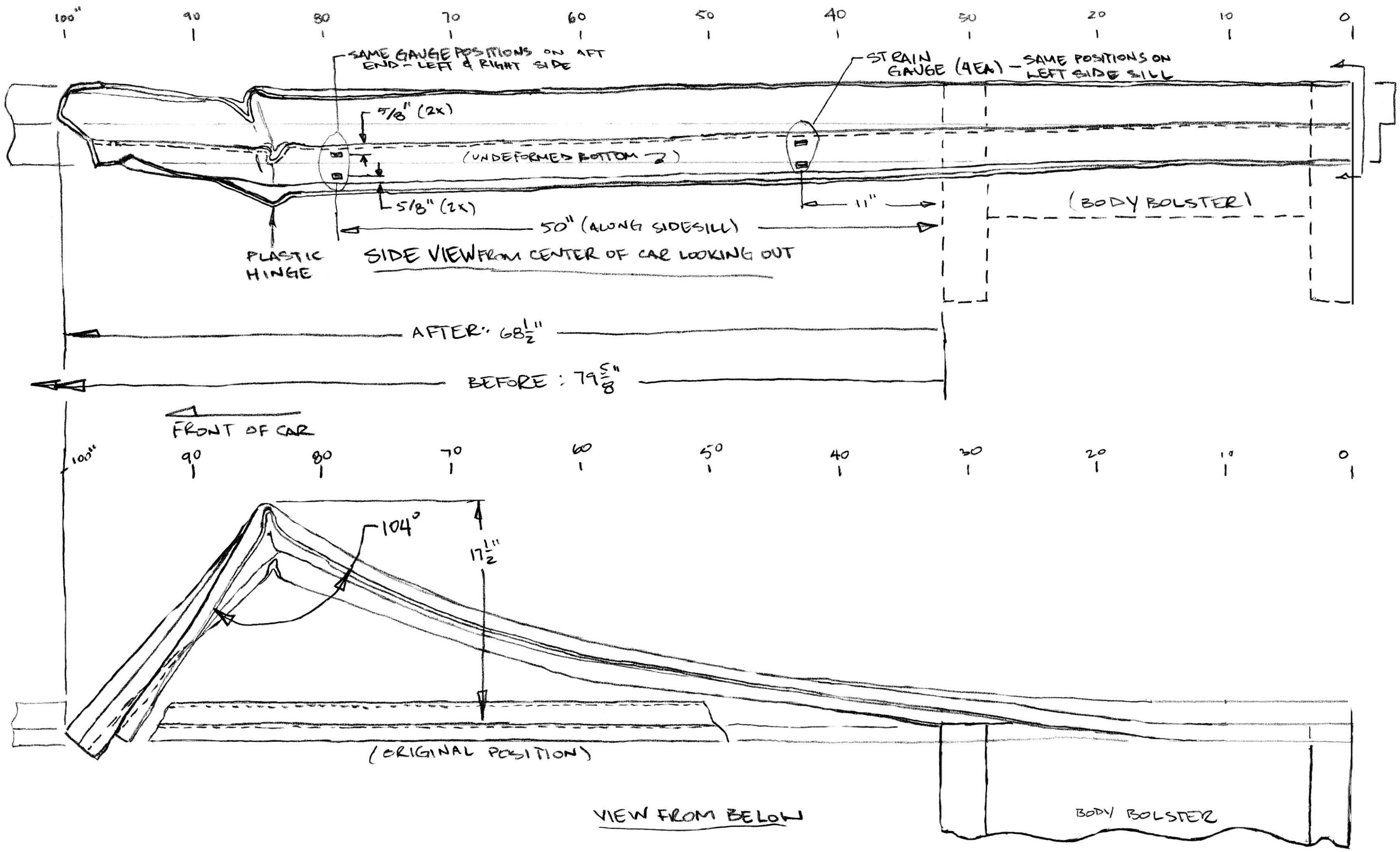

Figure A8. Right-side Sill Collapse (Note: view from below was mistakenly drawn as the mirror image of what it should be)

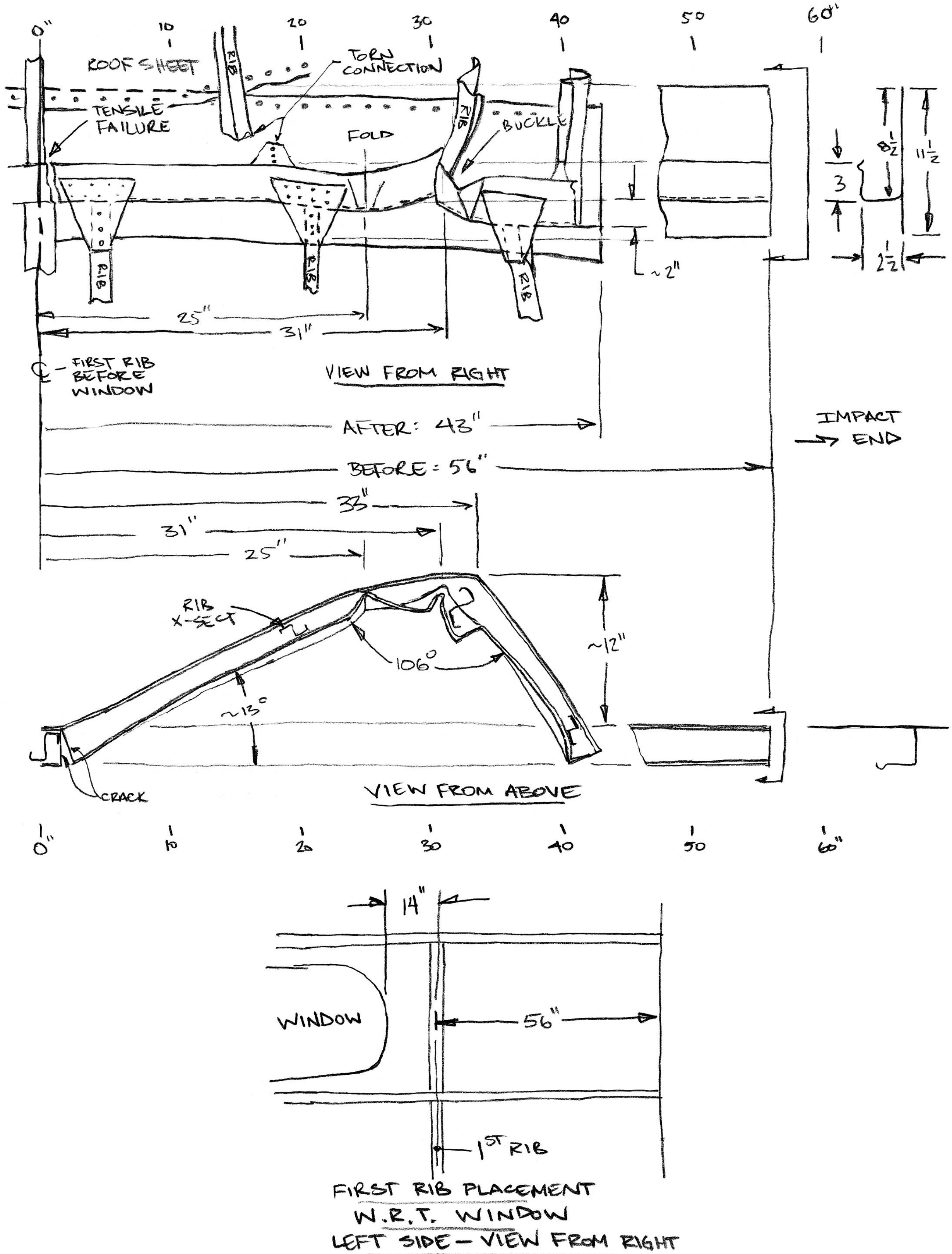

Figure A9. Left Cant Rail Damage

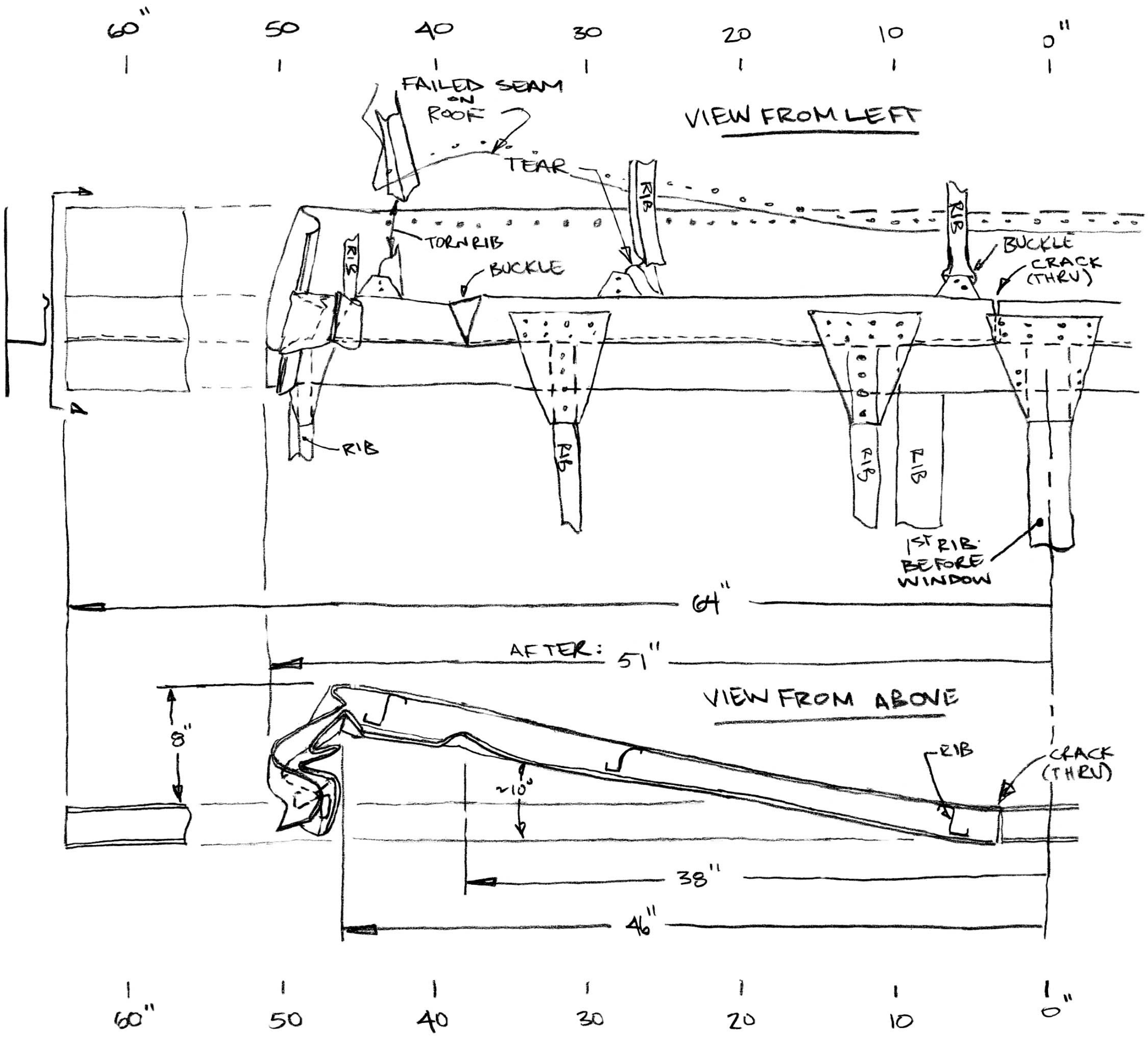

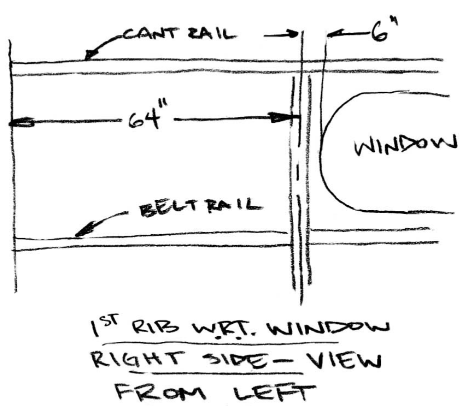

Figure A10. Right Cant Rail Damage

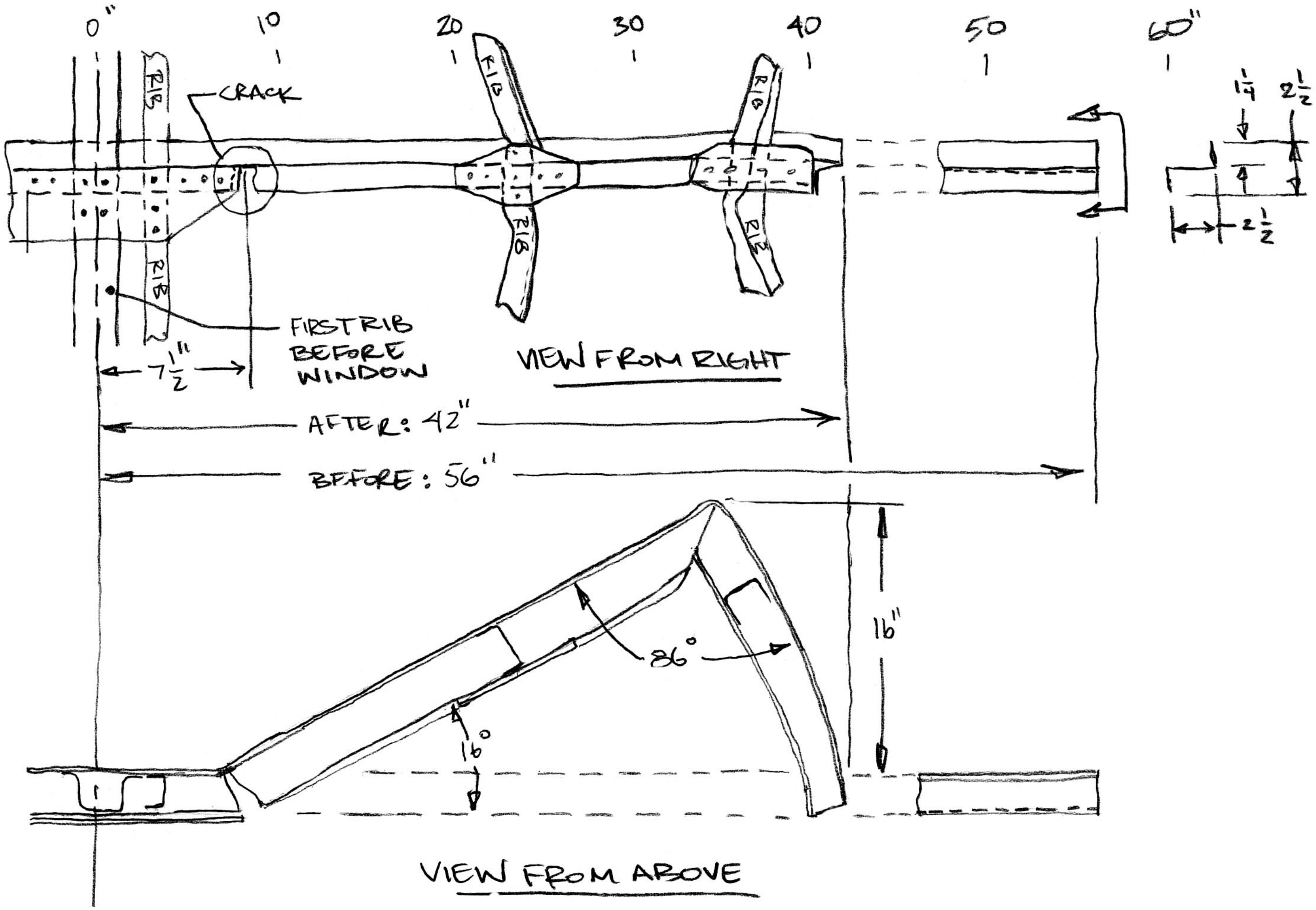

Figure A11. Left Belt Rail Deformation

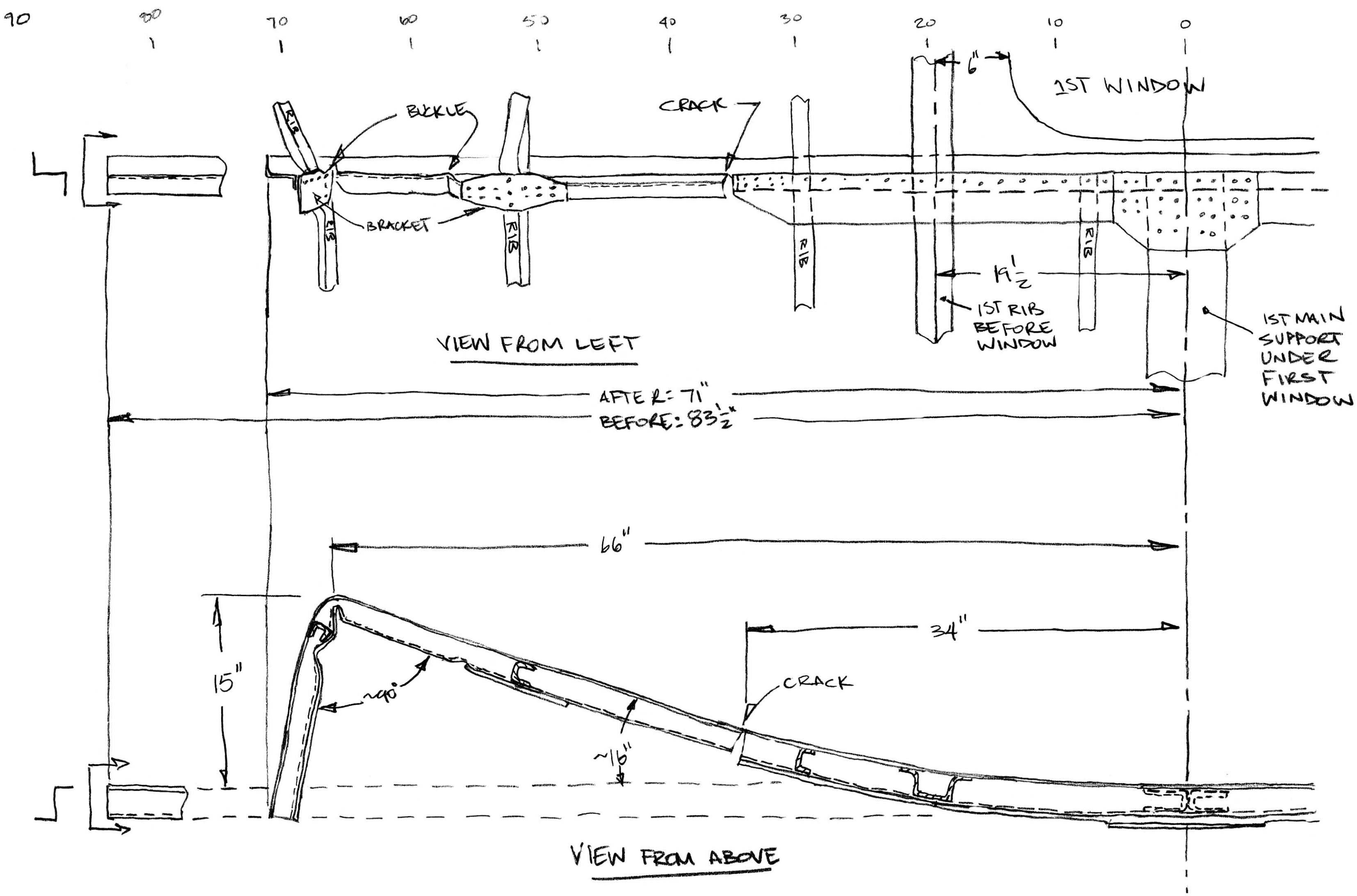

Figure A12. Right Belt Rail Deformation

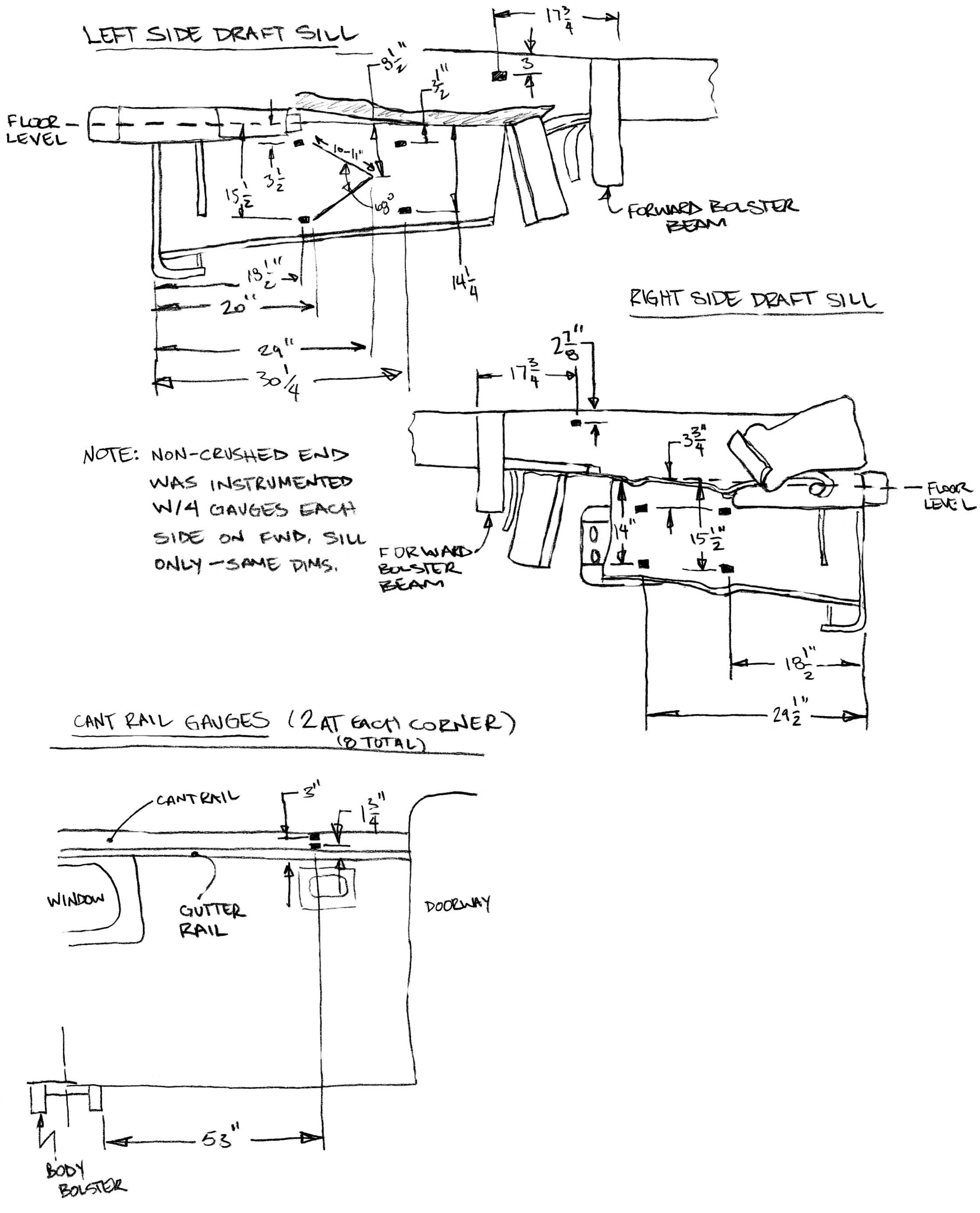

Figure A13. Strain Gauge Location Documentation

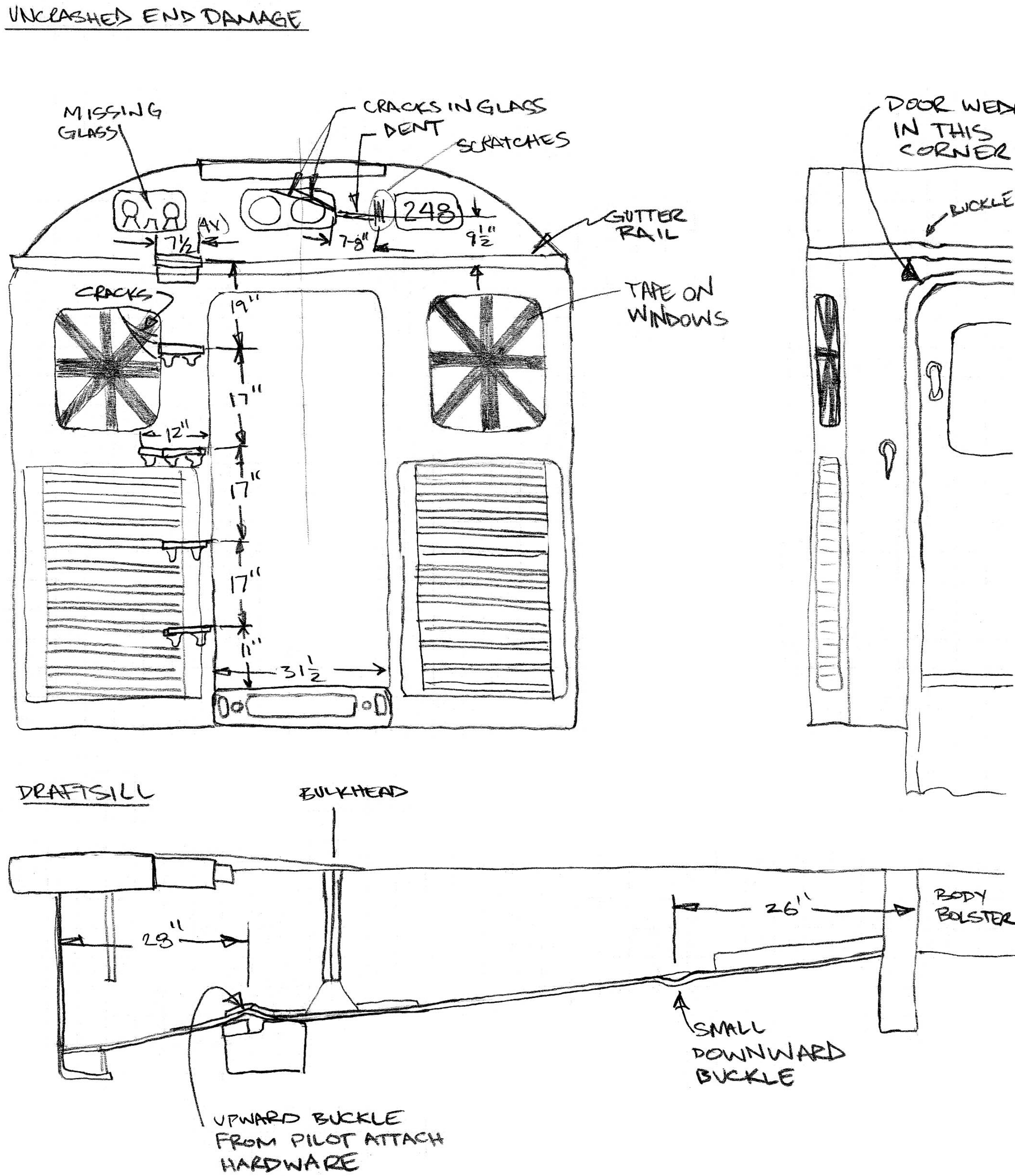

Figure A14. Documentation of Noted B-End Damage

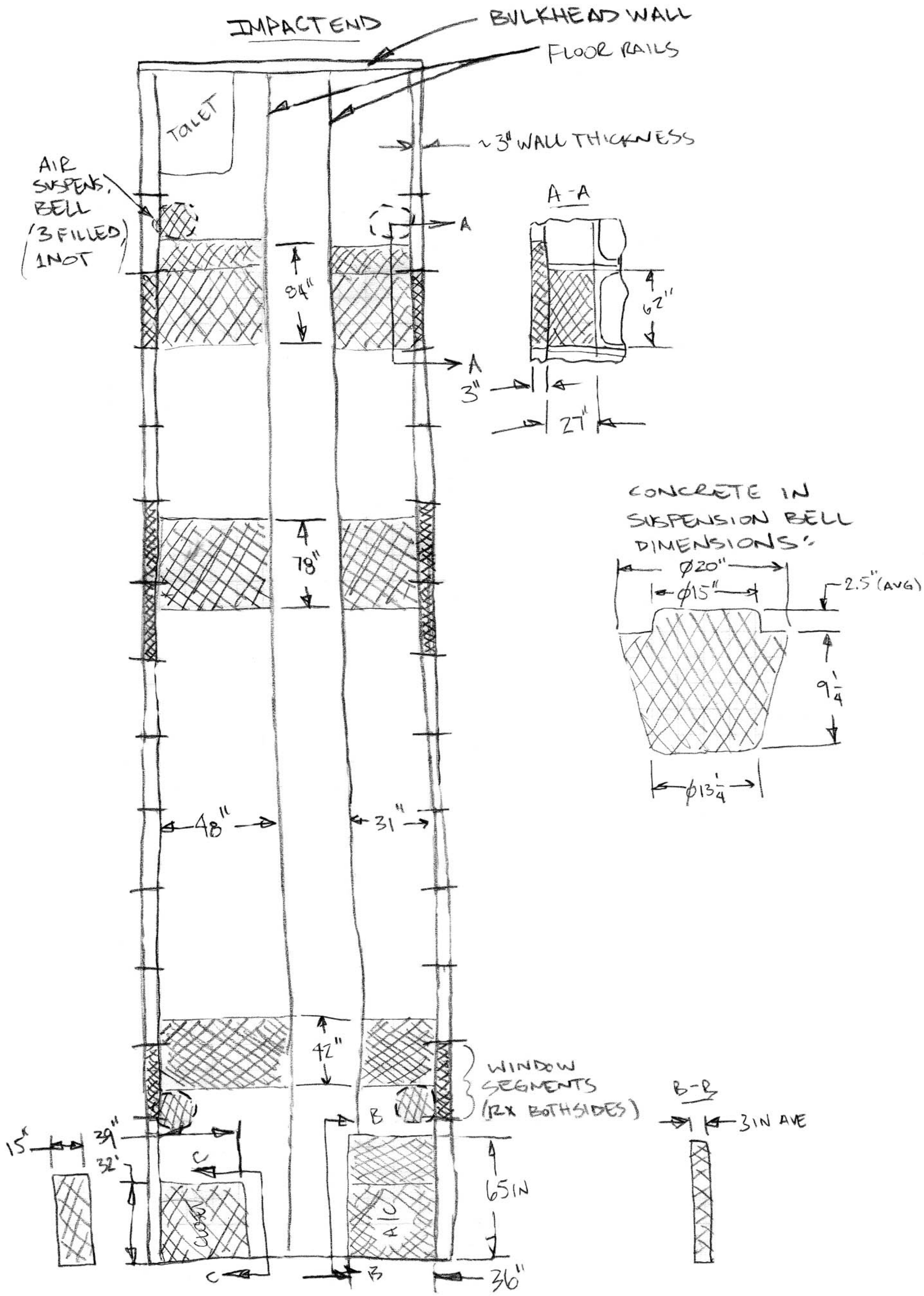

Figure A15. Concrete Distribution Throughout Car, Viewed from Top

APPENDIX B1: DRAFT SILL AND UNDERFRAME PHOTOGRAPHS

After Test (4 April 2000):

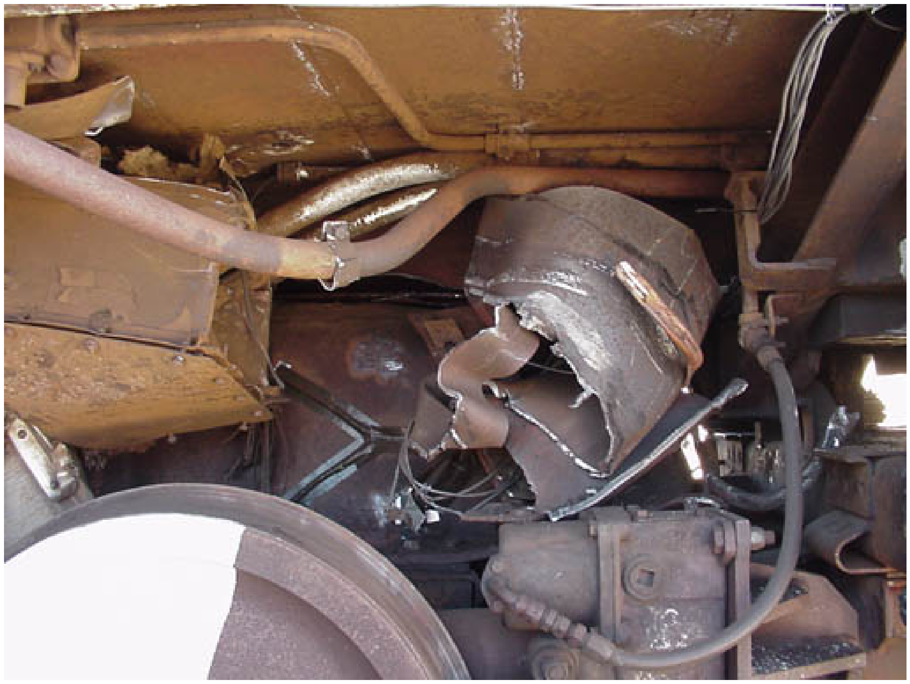

Figure B1-1. Left Side of Draft Sill Just After Test—Prior to Any Material Removal

Figure B1-2. Right Side of Draft Sill Just After Test—Prior to Any Material Removal

Before Truck Removal (29 Jan 2002):

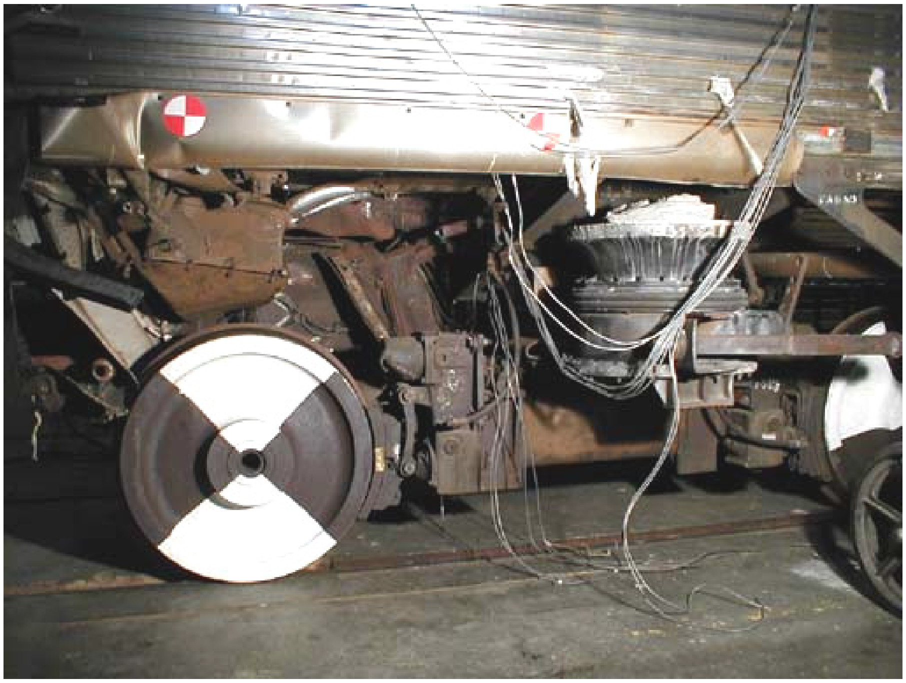

Figure B1-3. Draft Sill Collapse Zone with Truck from Left Side Looking Slightly Aft (note concrete on suspension bell)

Figure B1-4. Left-side Draft Sill Collapse Before Truck Removal

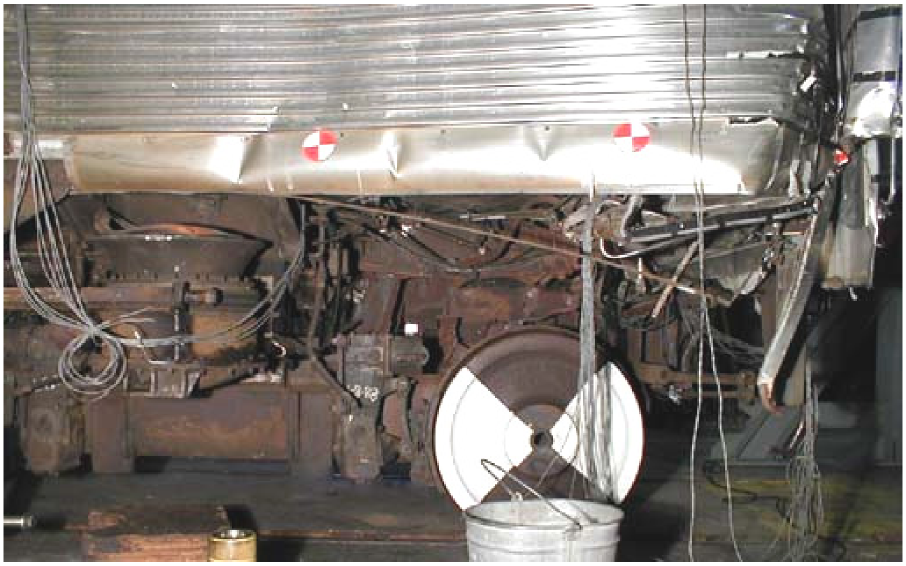

Figure B1-5. Draft Sill Collapse Zone with Truck from Right Side (note no concrete present on suspension bell—only one without it)

Figure B1-6. Right-side Draft Sill Collapse Before Truck Removal

Figure B1-7. Draft Sill Collapse Detail with Truck Attached, From Right Side (note pilot attachment hardware aft and below center line of front axle)

Figure B1-8. Draft Sill Collapse Detail with Truck Attached, From Left Side (note pilot attachment hardware aft and below center line of front axle)

After Truck Removal (30 Jan 2002):

Figure B1-9. Draft Sill without Truck, Right Side

Figure B1-10. Draft Sill, from Right Looking Forward

Figure B1-11. Forward Draft Sill, from Right Side Looking Slightly Upward

Figure B1-12. Aft Part of Draft Sill and Body Bolster Connection, from Right Looking Slightly Upward

Figure B1-13. Draft Sill Collapse from Behind, Slightly on Right Side, Aft Looking Forward

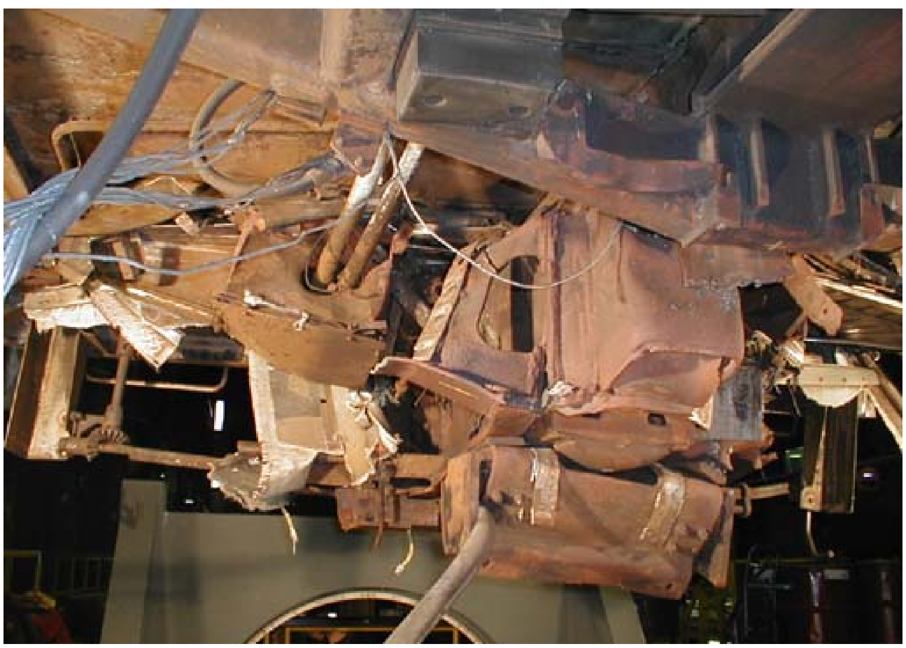

Figure B1-14. Draft Sill Collapse from Behind, Slightly on Left Side, Aft Looking Forward

Figure B1-15. Aft Part of Draft Sill and Body Bolster Connection, from Left Looking Slightly Upward

Figure B1-16. Left-side Draft Sill Between Body Bolster and Vestibule Wall Bolster

Figure B1-17. Front Draft Sill Collapse, Left Side

Figure B1-18. Detail of Body Bolster Without Bolster Beam. Aft Looking Forward from Left Side

Figure B1-19. Right-side Draft Sill Collapse and Forward Underframe Before Removing Trap Door, Aft Looking Forward

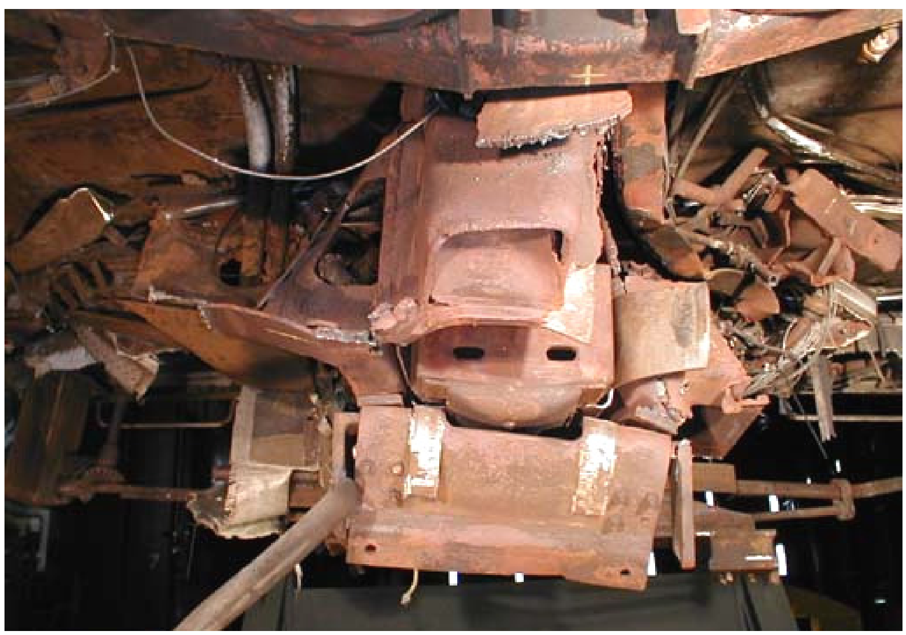

Figure B1-20. Draft Gear and Buff Stop Detail, Aft Looking Forward from Below

Figure B1-21. Right-side Forward Draft Sill and Underside of Floor Prior to Removing Trap Door

Figure B1-22. Draft Gear/Buff Stop Detail from Right Side

Figure B1-23. Right-side Bolster Beam Detail Showing Two Small Buckles, Forward Looking Aft

After Non-Structural Material Removal (31 Jan 02):

Figure B1-24. Left Side of Draft Sill After Material Removal

Figure B1-25. Left Side of Draft Sill - Impact of Buff Stop Against Body Bolster

Figure B1-26. Draft Sill - Right-side Deformations

Figure B1-27. Right-side Draft Sill, From Side, After Non-Structural Material Removal

Figure B1-28. Forward Draft Sill - Right-side Deformations

Figure B1-29. Forward Right-side Deformations - Buckling of the Floor Panels

Figure B1-30. Forward Draft Sill, Coupler Shank, and Pilot Attachment From Below

Figure B1-31. Forward Draft Sill Detail - Deformation of Pilot Connection Plate Under the Draft Gear

Figure B1-32. Forward Draft Sill Detail Showing Effects of Impact with the Front Axle

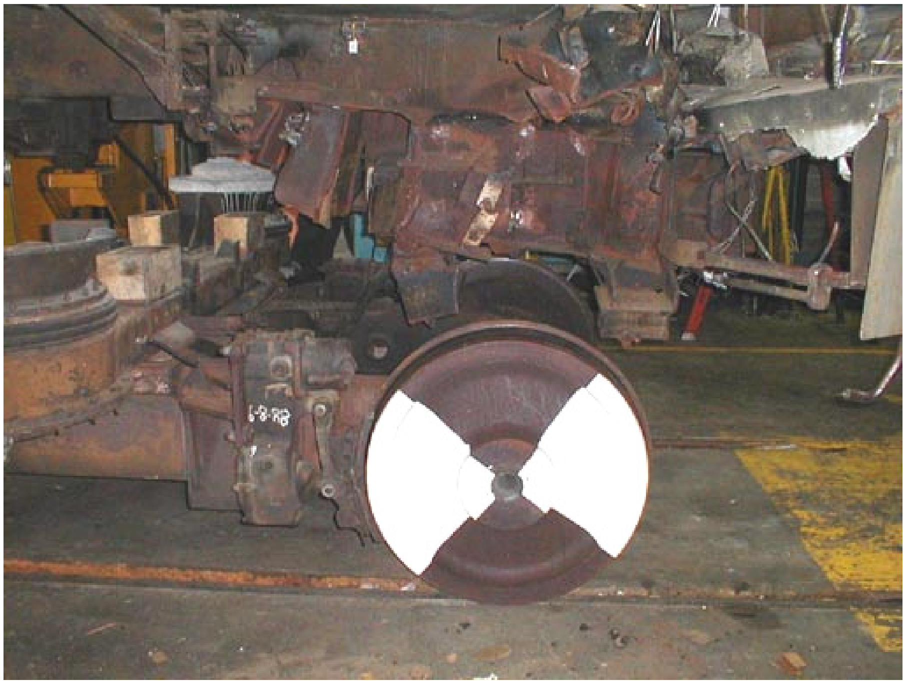

Figure B1-33. Draft Sill Position Relative to Truck—As Car was Being Lowered Back Onto Truck

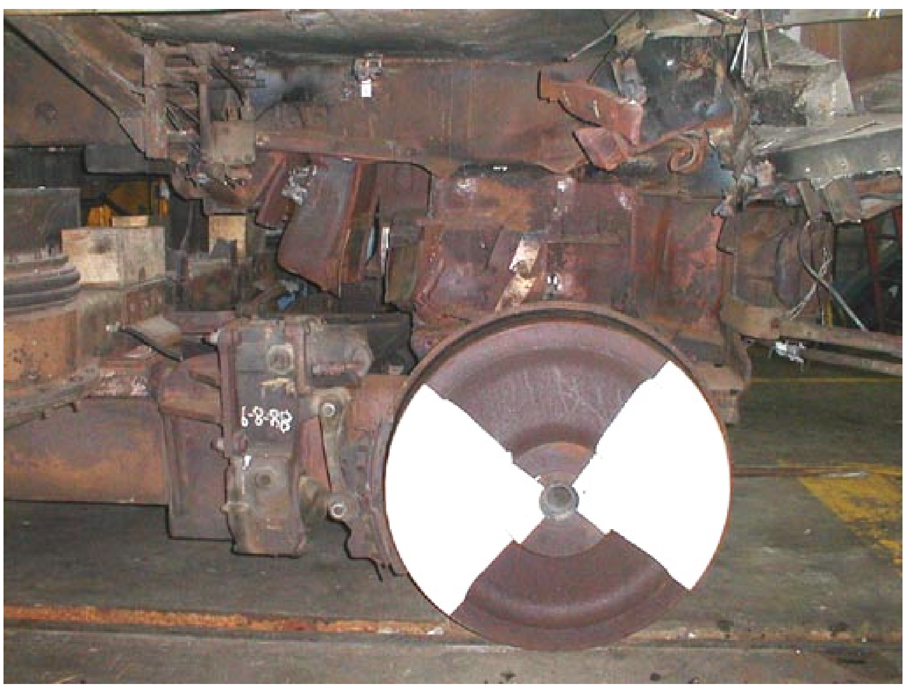

Figure B1-34. Draft Sill Position Relative to Truck—As Car Was Being Lowered Back Onto Truck

APPENDIX B2: SIDE SILL PHOTOGRAPHS

Figure B2-1. Detail of Deformed Side Sill Cover from Left Side Aft of Crushed Face (View of Side Sill is Obstructed by Cover)

Figure B2-2. Left-side Sill Collapse Detail, from Below Looking Forward

Figure B2-3. Right-side Sill Collapse Detail, from Below Looking Forward

Figure B2-4. Same as Above from Different Point of View

Figure B2-5. Detail - Side Sill Section and Accelerometer Mount

Figure B2-6. Forward Right-side Deformations - Buckling of the Side Sill and Floor Panels (Note Trap Door and Other Debris has been Removed)

APPENDIX B3: INSIDE DAMAGE PHOTOGRAPHS

Before Material Removal (30 Jan 2002)

Figure B3-1. Internal View Looking Forward at Crush Zone

Figure B3-2. Inside View, Detail of Water Closet Pushed Back Past First Window

Figure B3-4. Inside View of Water Closet

Figure B3-5. Inside Detail of Right Buckled Corner Aft of Bulkhead

Figure B3-6. Detail of Roof Structure Aft of Bulkhead

Figure B3-7. View From Inside of Vestibule Area Through Bulkhead Door

Figure B3-8. Cracks in Floor Sheathing Under Removed Floor Panels

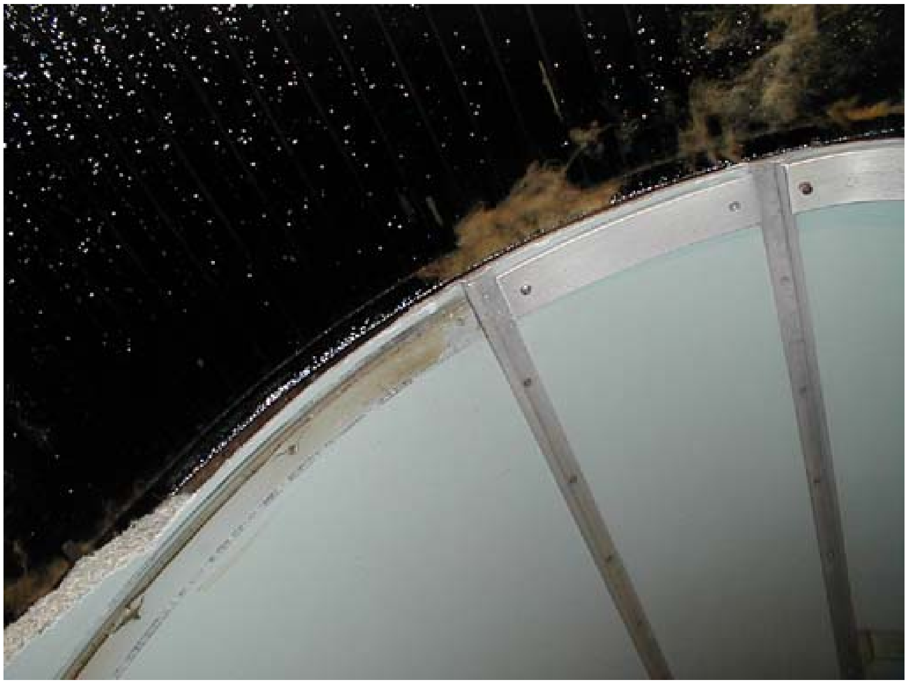

Figure B3-9. Coating in Inside Surface of Upper Sheathing in the Carbody

After Removal of Non-Structural Material Forward of First Window Frame (06 Feb 2002)

Figure B3-10. Composite Showing Forward Left-side Wall Between Bulkhead Wall and First Window Frame

Figure B3-11. Left-side Front Corner Aft of Bulkhead Wall

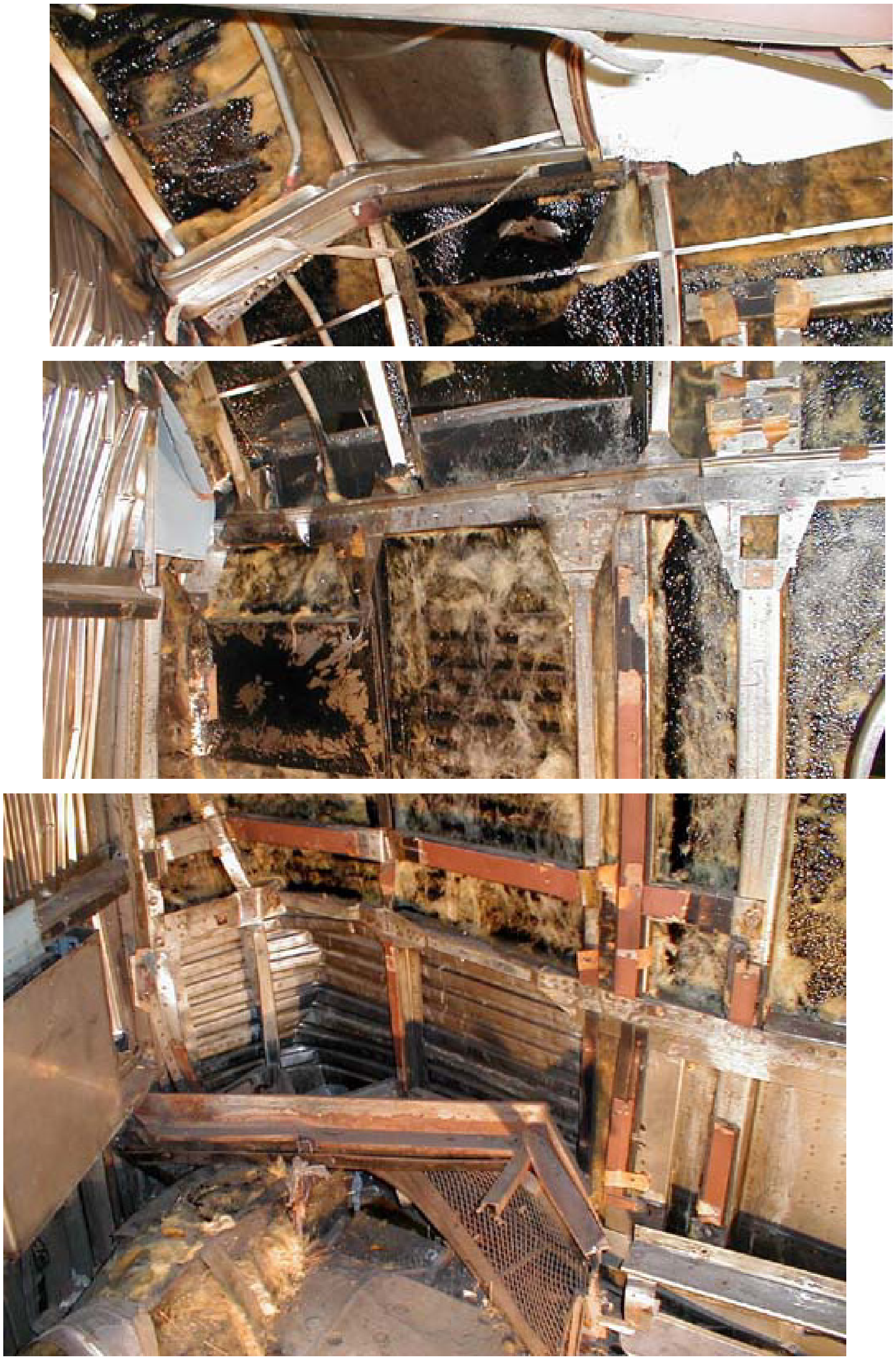

Figure B3-12. Composite Showing Forward Right-side Wall Between Bulkhead Wall and First Window Frame

Figure B3-13. Right-side Front Corner Aft of Bulkhead Wall

Figure B3-14. Left-side Cant Rail—Crack Detail Just Forward of Window Frame

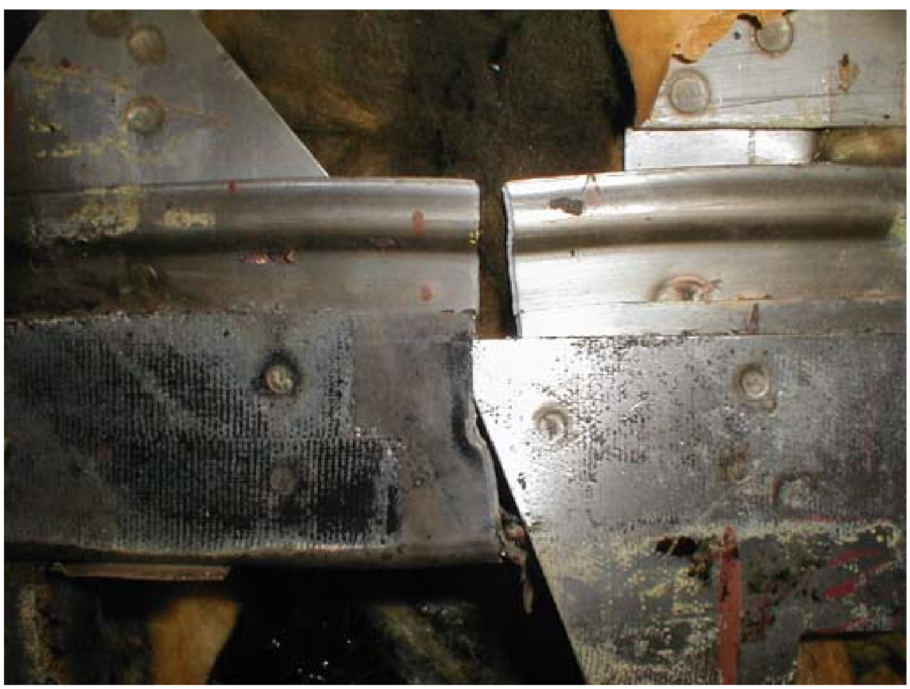

Figure B3-15. Right-side Cant Rail—Crack Detail Just Forward of Window Frame

Figure B3-16. Left-side Belt Rail—Crack Detail Just Forward of Window Frame

Figure B3-17. Right-side Belt Rail—Crack Detail Just Forward of Window Frame

Figure B3-18. Right-side Floor Buckling and Seat Frame Aft of Bulkhead Wall

Figure B3-19. Left-side Floor Buckling Aft of Bulkhead Wall

Figure B3-20. Internal View Looking Forward of Crushed End After Material Removal

Figure B3-21. Upper Damage aft of Bulkhead Wall—View After Material Removal

Figure B3-22. Skin Buckle on Upper Right-side of Bulkhead Wall—Typical Buckle Pattern of Superstructure Corrugated Skin

Figure B3-23. Same Buckle as Previous Picture from Slightly Different Point of View

Figure B3-24. Ceiling Damage Aft of Bulkhead Wall—View from Below

APPENDIX B4: SUPERSTRUCTURE PHOTOGRAPHS

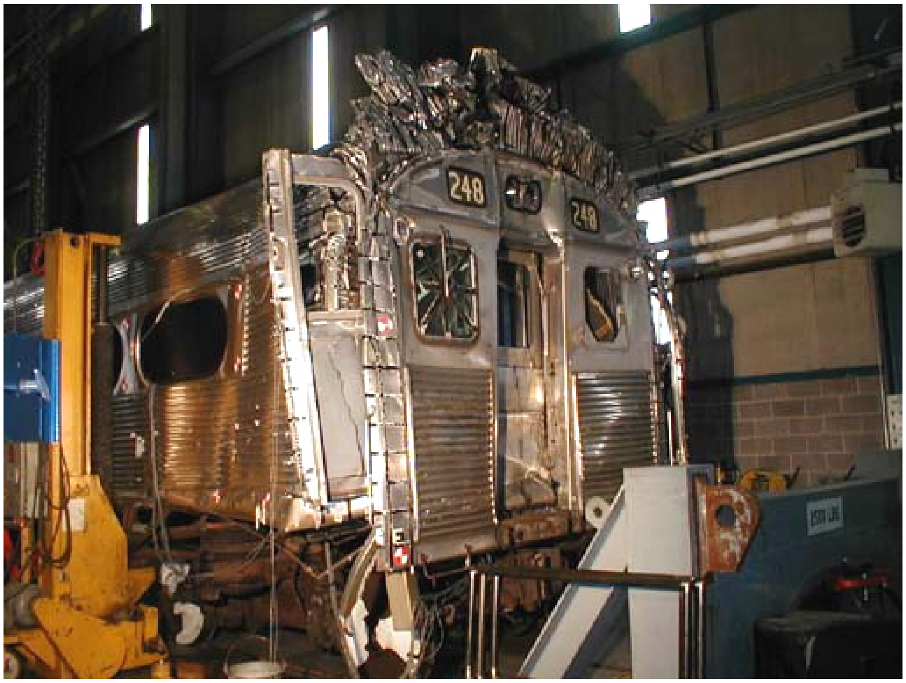

Figure B4-1. Right Front Corner of Crush Zone

Figure B4-2. Right Front Corner of Damaged End—Car Jacked in Air in TTC RDL Building

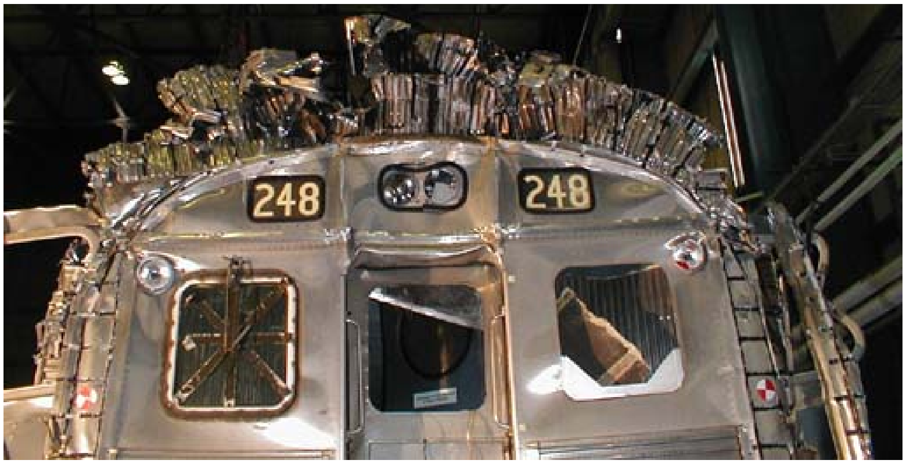

Figure B4-3. Front Top Face of Vestibule, Looking Up

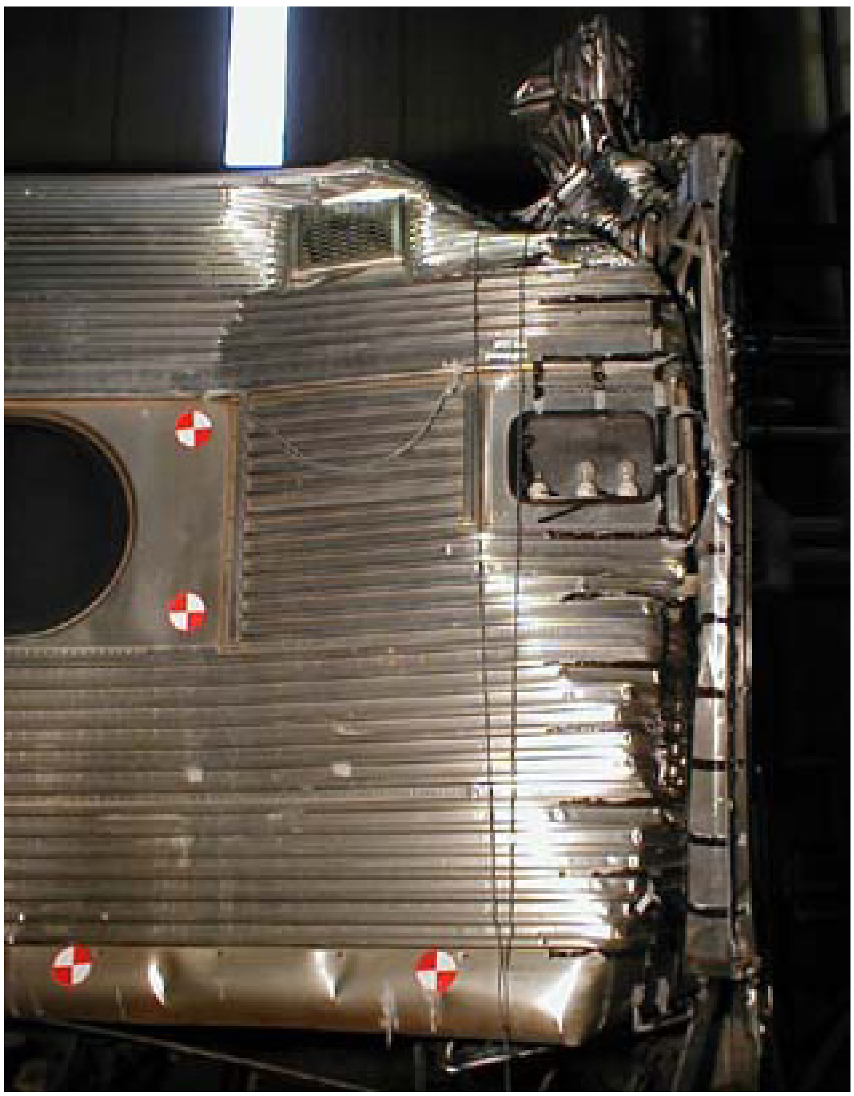

Figure B4-4. Superstructure Collapse Zone, from Right Side

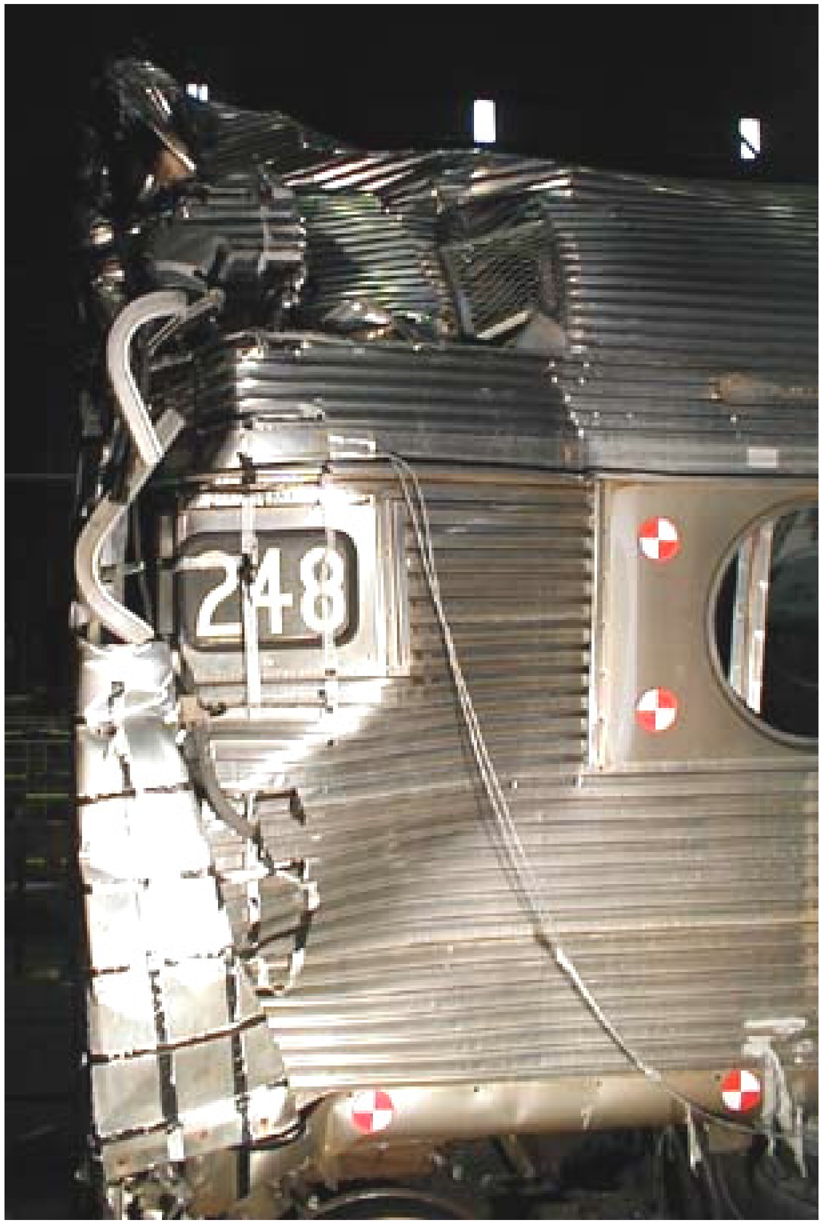

Figure B4-5. Superstructure Collapse Zone, from Left Side

Figure B4-6. Front Face and Left Corner of Crush Zone

Figure B4-7. Left-side Lower Superstructure Deformation, Looking Forward

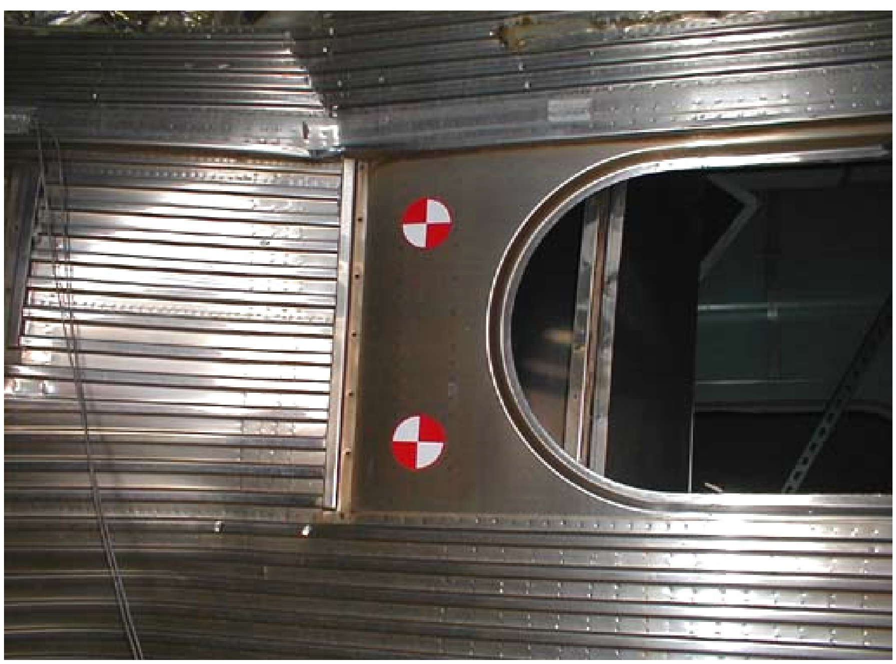

Figure B4-8. First Left-side Window - Showing Rear Wall of Toilet Enclosure Pushed Aft

Figure B4-9. View of Left-side Superstructure from First Side Window, Looking Forward

Figure B4-10. View of Right-side Superstructure from First Side Window, Looking Forward

Figure B4-11. View of Upper Left-side Superstructure in Crush Zone, Looking Forward

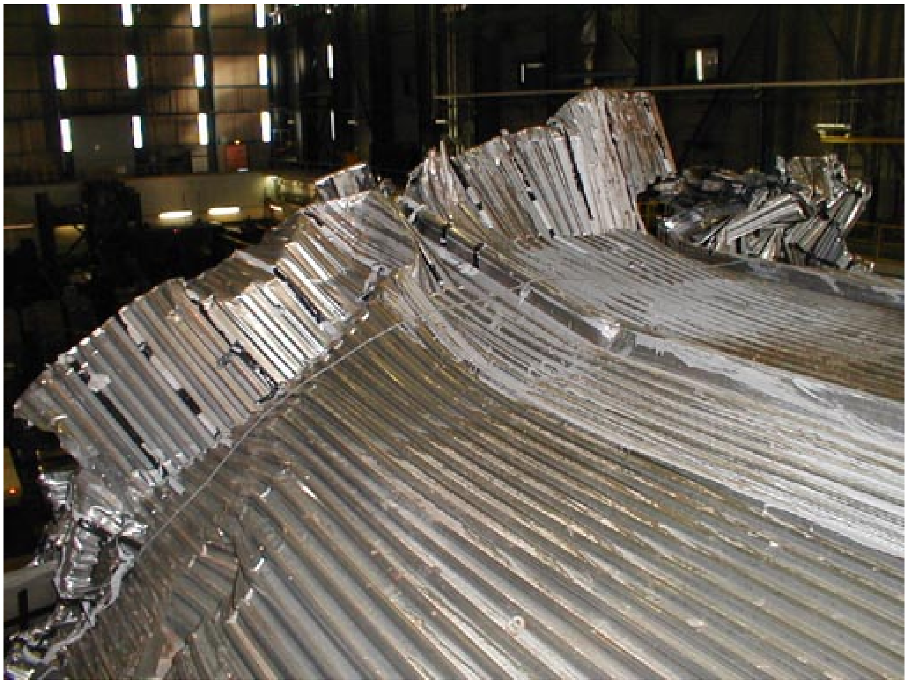

Figure B4-12. View of Upper Superstructure in Crush Zone, Looking Forward from Left

Figure B4-13. View of Upper Superstructure in Crush Zone, Looking Forward from Right

APPENDIX B5: B-END PHOTOGRAPHS

Figure B5-1. Damage above Rear Center Door - Impact of Rear Car Upper Step

Figure B5-2. Aft Draft Sill - Buckle of the Draft Sill Flange Above Pilot Connection Plate

Figure B5-3. Aft Draft Sill - Buckle of the Draft Sill Flange Above Pilot Connection Plate

Figure B5-4. Aft Draft Sill - Slight Buckling of the Draft Sill Flange

Figure B5-5. Detail - Door Frame Deformation in Right-Rear Door

Figure B5-6. Buckle in Rain Gutter Above Top Left Corner of Right-Rear Door Frame

Figure B5-7. Buckle in Rain Gutter Above Top Left Corner of Right-Rear Door Frame

Figure B5-8. Buckle in Top Right Corner of Right-Rear Door Frame – Outside

Figure B5-9. Step on B-End of Lead Car (From Below)

Figure B5-10. Detail – Step on B-End of Lead Car (From Above)

Figure B5-11. B-End Buff Stop—Collision Marks from Impact with Trailing Car

Figure B5-12. B-End Buff Stop—Collision Marks from Impact with Trailing Car

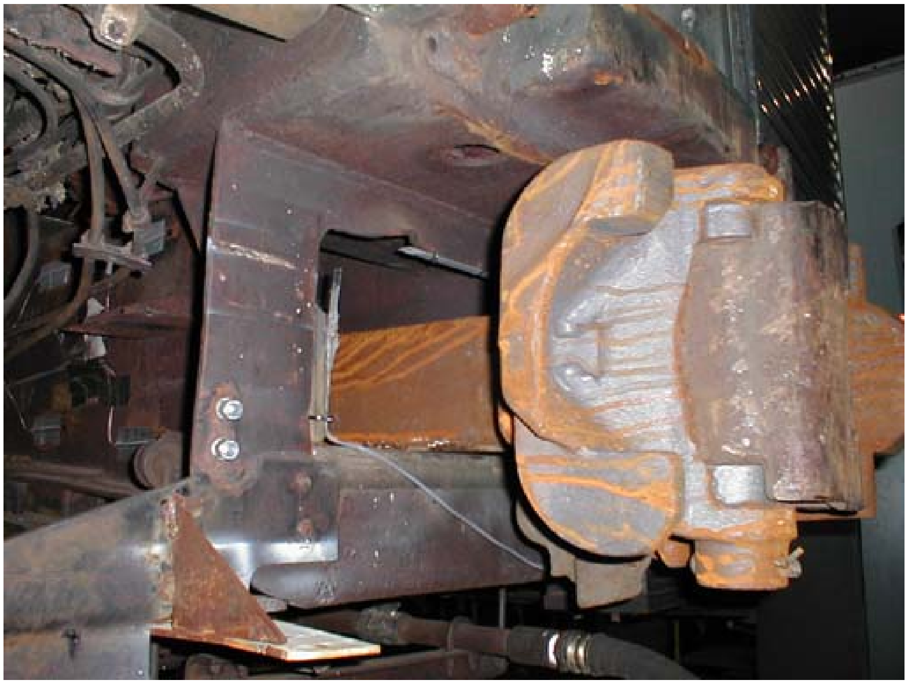

Figure B5-13. Aft Draft Gear and Sill - Damage at Edge of Coupler Pocket

APPENDIX B6: TRUCK PHOTOGRAPHS

Figure B6-1. Forward Left-side Bladder Suspension Detail—Before Truck Removal

Figure B6-2. Forward Truck (Detached) from Left Side Looking Aft

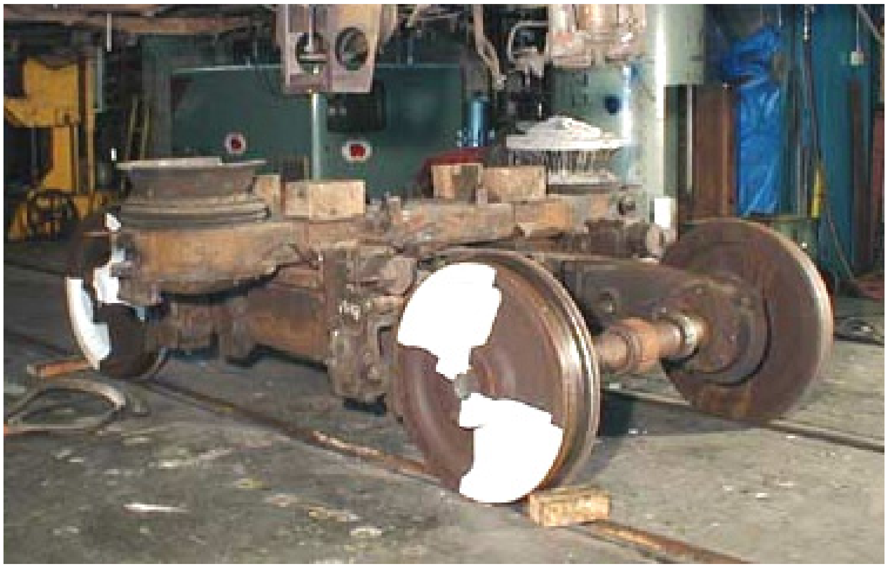

Figure B6-3. Forward Truck (Detached) from Right Side Looking Aft

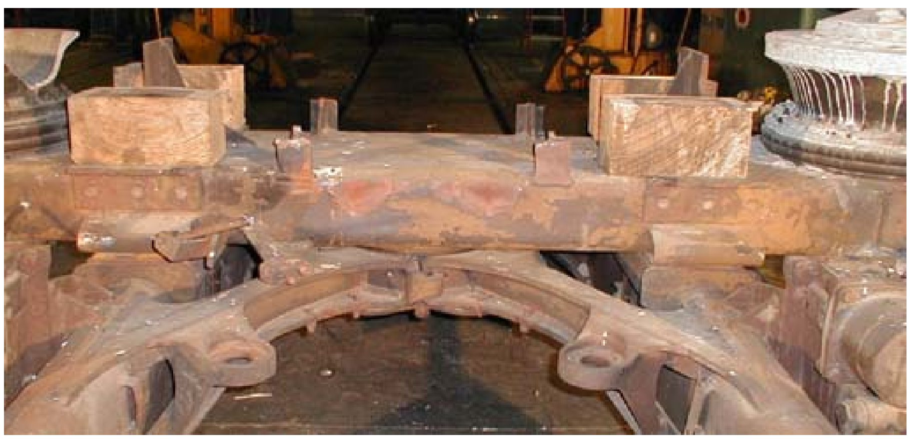

Figure B6-4. Forward Truck Detail Showing Indents from Bolster Beam Bracket Impact, Forward Looking Aft

Figure B6-5. Rear Truck from Right Side, Aft Looking Forward

Figure B6-6. Rear Truck - Bolster Beam, Viewed from Rear Right Side

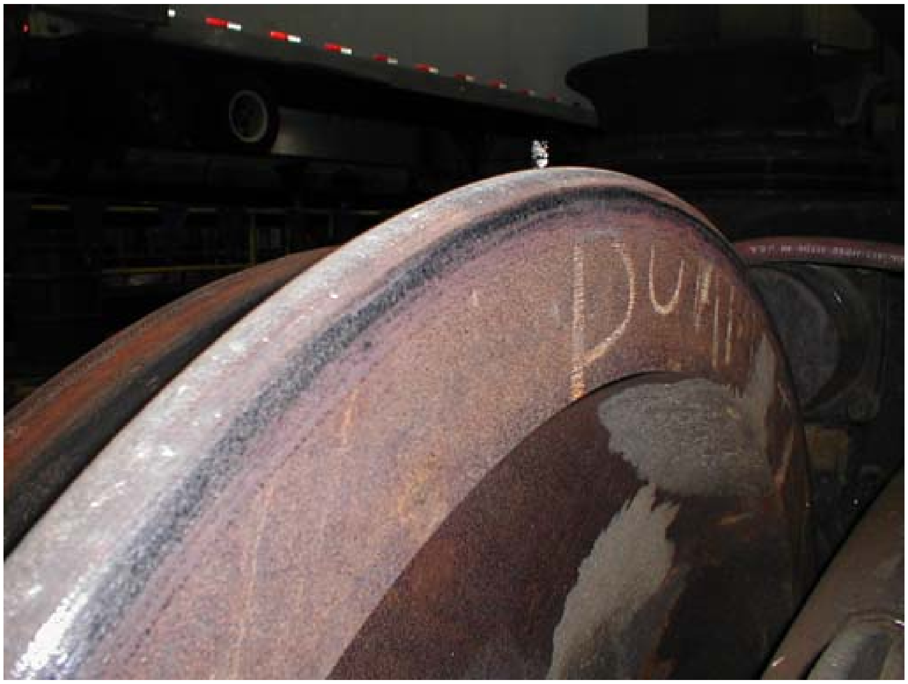

Figure B6-7. Wheel Burn - Polished Inside Surface on Right Front Wheel of the Forward Truck

Figure B6-8. Wheel Burn on Lower Forward Draft Sill - Right Side